Master's thesis

NTNU
Norwegian University of Science and Technology
Faculty of Information Technology and Electrical Engineering
Department of Electric Power Engineering

Matias Vistnes

Analysis of Interdependence in Electrical Distribution Power Systems and corresponding Information and Communications Technology Systems using Monte Carlo Simulations

Master's thesis in Electrical Power Engineering
Supervisor: Olav B. Fosso
Co-supervisor: Stine F. Myhre
June 2021

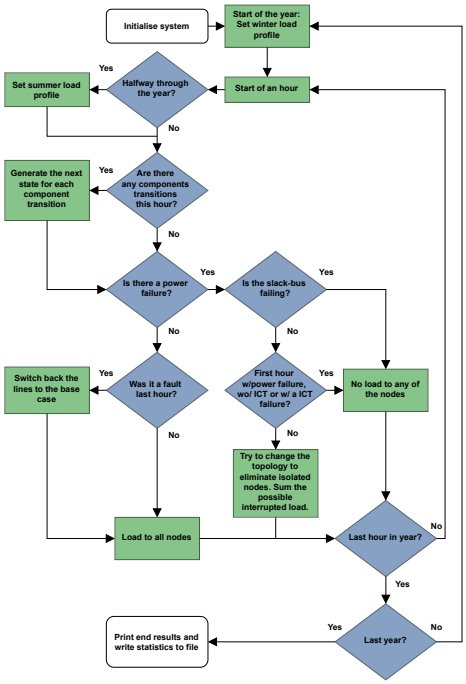

NTNU
Norwegian University of Science and Technology

Matias Vistnes

Analysis of Interdependence in Electrical Distribution Power Systems and corresponding Information and Communications Technology Systems using Monte Carlo Simulations

Master's thesis in Electrical Power Engineering
Supervisor: Olav B. Fosso
Co-supervisor: Stine F. Myhre
June 2021

Norwegian University of Science and Technology
Faculty of Information Technology and Electrical Engineering
Department of Electric Power Engineering

NTNU
Norwegian University of
Science and Technology

Abstract

Industrialised countries are experiencing an increased electrical consumption with the extensive electrification of, e.g., industry and transport and the changing consumption patterns at the end-users. Further increased electrification is also a response to climate challenges. This shift leads to a higher dependency on the continuous supply of electric power from the power systems, and in most cases, higher system utilisation and operation closer to the limits. Increased operation costs and significant investments in infrastructure development is needed to increase the power system‘s reliability in such a setting. New Information and Communications Technologies (ICTs) could help lower costs and improve the system‘s reliability through better monitoring and automated solutions. Since high reliability is the target, the behaviour and interdependencies with the existing power system need to be assessed. In this project, a Monte Carlo Simulation (MCS) tool was developed to increase the understanding of the consequences on the reliability of a distribution system when new ICT equipment is integrated into the power system.

Physical and cyber interdependencies, with cascading failures, were the focus when implementing the modelling tool. Several cases were simulated using the MCS on the IEEE 69 bus test system. Each case changes one or more essential factors in the simulation, including; ICT components in the system, backup lines as a remedial action after a failure, and changes in failure rate or repair time of a component. The cases were discussed using both basic[1] and aggregated[2] reliability indices.

In general, the power system with ICT was more reliable than the power system without ICT. The sectioning time until a system failure is isolated plays a crucial role in the system‘s reliability. The results may indicate that the reliability increases more with the introduction of ICT to have a quick sectioning time than having backup lines connected during failure in this power system. The scenario with ICT is sensitive towards line repair time, as well as transformer failure rate and repair time. In addition, the ICT components (i.e. Disconnector, Communication Hub, and Communication Line) show some impact on the model indices, but generally much less than the contribution of lines and transformers on system failure rate.

From simulations where different factors in the system were changed, it is reasonable to conclude that the power system model corresponds well with the predicted behaviour of a real-world power system. It is more difficult to conclude if the ICT system behaviour is realistic, as there is limited research on the topic. Nevertheless, one could predict that the general increase in reliability observed in the simulations using an ICT system could occur. The conclusion is still uncertain, as the failure rate for the ICT components is questionable. However, an increase in the failure rate of the communication hubs showed a decrease in the system reliability, thus indicating their importance to reliability.

[1] Failure rate λ, unavailability U, average failure duration r, and Energy Not Supplied (ENS)

[2] System Average Interruption Frequency index (SAIFI), System Average Interruption Duration index (SAIDI), Customer Average Interruption Frequency index (CAIFI), Customer Average Interruption Duration index (CAIDI), Average Service Availability Index (ASAI), Average Energy Not Supplied (AENS), and Average Customer Curtailment Index (ACCI)

Sammendrag

Industrialiserte land opplever i dag en økning i forbruk av strøm. Dette kommer i stor grad av den omfattende elektrifiseringen av blant annet industri og transport, og endringer i bruksmønster hos forbruker. Økt elektrifisering er også en reaksjon på klimaendringene. Dette skiftet fører til en økt avhengighet av kontinuerlig strømleveranse og, i de fleste tilfeller, bedre utnyttelse av systemet og en drift som ligger opp mot grensen for hva systemet kan klare. Behovet for store investeringer i infrastruktur og systemstyring er nødvendig for å få bedre pålitelighet i det elektriske kraftsystemet. Ny Informasjons- og Kommunikasjons-Teknologi (IKT) kan bidra til å holde investeringskostnadene nede og forbedre systemets pålitelighet gjennom bedre overvåkning og automatiske løsninger. Siden det er et mål at strømleveransen har høy pålitelighet, er det nødvendig å finne ut hvordan de nye IKT-komponentene fungerer i gjensidig avhengighet med gamle kraftsystemet. I dette prosjektet ble et Monte Carlo-simuleringsverktøy (MCS) laget for å øke forståelsen av konsekvensene ved integrering av nytt IKT-utstyr i et eksisterende strømnett.

Modellen ble laget med fokus på å implementere gjensidig avhengighet, både fysiske og digitale, som fører til kaskade-feil mellom systemene. Det ble gjort flere simuleringsforsøk ved bruk av MCS i IEEE 69 bus-testsystemet. I hvert forsøk ble det gjort endringer i en eller flere essensielle faktorer i simuleringen, inkludert; IKT-komponenter i systemet, reservelinjer som en avhjelpende handling etter en feil, og endringer i komponentens feilrate eller reparasjonstid. Forsøkene ble diskutert ved å bruke både enkle[3] og kombinerte[4] pålitelighetsindekser.

Overordnet kan man si at kraftsystemet med IKT-systemer var mer pålitelig enn det uten. Tiden det tar å seksjonere et system for å finne feilen ved strømbrudd spiller en avgjørende rolle i hvor pålitelig kraftsystemet er. Resultatene fra simuleringene kan indikere at påliteligheten øker mer ved introduksjonen av IKT-systemer sammenlignet med tilkobling av reservelinjer når feil oppstår. Scenarioene hvor IKT-systemer er i bruk ble påvirket av reparasjonstiden til strømlinjene og transformatorene, samt feilraten til transformatorene. Det kom også fram at IKT-komponentene (dvs. skillebrytere, kommunikasjonsknutepunkter og kommunikasjonslinjer) påvirker indeksene. Samtidig er effekten mye mindre enn bidraget fra feilraten til strømlinjer og transformatorer.

Ut i fra simuleringene for endring av ulike faktorer i systemet kan det konkluderes med at kraftsystemmodellen stemmer godt overens med hvordan kraftsystemer antas å fungere i den virkelige verden. Oppførselen til IKT-systemene er vanskeligere å dra en konklusjon for, ettersom det kun er en begrenset mengde forskning på området. Likevel kan det antas at den generelle forbedringen av pålitelighet som ble observert i simuleringene med IKT-systemer også vil skje i virkeligheten. En del usikkerhet er knyttet til denne konklusjonen, da feilraten til IKT-komponentene er diskuterbar. Samtidig viste en økning i feilraten for kommunikasjonsknutepunktene en nedgang i systemets pålitelighet, som kan indikere at disse knutepunktene har en effekt på påliteligheten.

[3]Feilrate λ, utilgjengelighet U, gjennomsnittlig feillengde r, og ikke-levert energi (eng: ENS)

[4]Gjennomsnittlig frekvens av systemavbrudd-indeks (eng: SAIFI), Gjennomsnittlig systemavbruddslengde-indeks (eng: SAIDI), Gjennomsnittlig frekvens av kundeavbrudd-indeks (eng: CAIFI), Gjennomsnittlig kundeavbruddslengde-indeks (eng: CAIDI), Gjennomsnittlig systemtilgjenelighet-indeks (eng: ASAI), Gjennomsnittlig ikke levert energi (eng: AENS), og Gjennomsnittlig energi i kundeavbrudd (eng: ACCI)

Acknowledgment

This project has been made successful through consistent advice and guidance by my supervisors. I would like to thank my main supervisor, Professor Olav B. Fosso, for his valuable guidance during the master thesis work. His engagement in a power system modelling course and as the creator of PyDSAL inspired me to work with this thesis. I would also like to extend my greatest appreciation to my co-supervisor, PhD candidate Stine F. Myhre, who supported and motivated me throughout the thesis work. She has been a great source of inspiration and knowledge.

Also, my appreciation goes to my family for their continuous support of my academic career. I would especially like to thank my wife for her endless support through all stages of the thesis work.

Trondheim, 11 June 2021
Matias Vistnes

Contents

List of Figures

List of Tables

List of Algorithms

Acronyms

ACCI Average Customer Curtailment Index.

AENS Average Energy Not Supplied.

ASAI Average Service Availability Index.

CAIDI Customer Average Interruption Duration index.

CAIFI Customer Average Interruption Frequency index.

DG Distributed Generation.

DSO Distribution System Operator.

ENS Energy Not Supplied.

FBS Forward-Backward Sweep.

HILP High Impact Low Probability.

HL Hierarchical Levels.

HV High Voltage.

ICT Information and Communications Technology.

IQR Interquartile-range.

LV Low Voltage.

MCS Monte Carlo Simulation.

MTTF Mean Time to Failure.

MTTR Mean Time to Repair.

MV Medium Voltage.

NERC North American Electric Reliability Council.

PV Photo Voltaic.

RMS Root mean square.

SAIDI System Average Interruption Duration index.

SAIFI System Average Interruption Frequency index.

SCADA Supervisory Control and Data Acquisition.

TSO Transmission System Operator.

1 Introduction

1.1 Background

The continuous supply of electric power is essential for the security and economy of society. People, together with public and private organisations are affected by even a short interruption of the supply. In the era of computers and internet, the productivity drops to a halt without electric power. Although most critical equipment and facilities have backup power for short interruptions, the consequences are more severe from prolonged interruptions of electric power. Potential effects after a few hours are; food in refrigerators and freezers defrosts and get stale, water pumping stops and the pressure drops as long as people use water, and mobile towers often only have backup for a few hours [1, 2]

As much of the society, the power systems delivering electric power to people are in a transition to a more digital nature. This brings dependency on digital Information and Communications Technology (ICT) equipment and programs for a smooth operation of the power systems. However, the ICT also depends on the continuous supply of electrical power. This is called interdependency and leads to a more complicated system and new possible paths of failure. To investigate how the interdependencies of the systems behave, without risking the continuous operation of the power system, it is possible to use mathematical models, as this thesis will present.

Why do we need to model the power system? (1) Only a few selected experiments can be conducted on the actual power system as interruptions cause enormous costs for both the system operators and their customers. Also, the loss of power could, in the worst case, be fatal for humans and farm animals. (2) New power system components, especially at higher voltages, are expensive and have a technical life of about 40 years. There is a potential of saving huge costs in protecting and implementing the components in such a way that they function for as long as possible. The extended life could also cause challenges with many generations of components from several manufacturers that need to operate interconnected. (3) The power system is critical to the well functioning of society and power outages should be minimised. Modelling and simulation of the system can give stakeholders and operators valuable information on how to further develop and operate it, preventing blackouts with great social and economic impacts. From a model, we can get an understanding of the function, operation, capacity, and limitation of the systems [3].

Reliability analysis can predict how the system is likely to behave in a longer timespan, often used for planning and prioritising months and years in advance of a project. There is a significant amount of research in the power system reliability field at the transmission level, but the sector is more immature at the distribution level. This is partly since, for a long time, the distribution system was passive and with little to no state monitoring. Currently, the distribution level is getting more dynamic with the inclusion of distributed generation,

smart meters, remotely operated breakers, and other intelligent components. This gives more opportunities for reliable operation and control of the system. People tend to be more satisfied with these changes, as the distribution system is the most significant individual contributor to the overall customer unavailability of electrical power [4]. Tøndel et al. [5] recognise a need for methods to identify and analyse the vulnerability of interdependencies between power systems and ICT systems. Reliability analysis of the combined system could use some of the vulnerabilities that are already are found in research [6–8].

One popular type of implementation of reliability analysis is a Monte Carlo Simulation (MCS). These types of analyses produce quantitative reliability indices that can provide relevant information about the expected system behaviour [9]. MCS is based on the statistical results from simulation of a large amount of random events.

1.2 Contribution

This thesis builds upon a specialisation project, by the author, on a literature review of possible methods and models suited for studying a power system with integrated ICT parts. In the conclusion and further work of the project, the most promising methods and models were highlighted. Some of these methods and models are further used for the problem formulation in this thesis.

The power system at the distribution level is changing rapidly from a passive system with little to no monitoring of its state to increasingly more distributed generation and monitoring. One promising method for simulation of the system is by MCS, using the Forward-Backward Sweep (FBS) method for the power flow calculation and an integrated ICT system model for the communication network between the nodes. The system model is in steady-state, where the system state is recalculated with time intervals of one hour. This work will implement and demonstrate a concept based on these techniques using a standardised test system. The implementation will be in the Python programming language.

The problem formulation follows.

> Develop a software tool in the Python programming language by using the Monte Carlo Simulation (MCS) methodology to examine if the introduction of Information and Communications Technology (ICT) components into a distribution power system increase the adequacy and resilience of the power system and if the model gives relevant information about their interactions.

The system performance is quantified by the following indices:

- System Average Interruption Frequency index (SAIFI),
- System Average Interruption Duration index (SAIDI),

- Customer Average Interruption Frequency index (CAIFI),
- Customer Average Interruption Duration index (CAIDI),
- Average Service Availability Index (ASAI),
- Average Energy Not Supplied (AENS), and
- Average Customer Curtailment Index (ACCI).

This thesis presents results from the following list of steps to answer the problem formulation.

- A MCS tool was developed in the Python programming language from the ground up with full transparency in every step of the process and code, from the component representation and the power flow equations to the simulation steps and the calculation of indices. It will be released to the public for further research. The tool could, in principle, be used to perform a MCS on any radial operated power system. However, the tool is only used on the test system in this thesis and optimised for its corner cases.
- A standardised test system, the *IEEE 69-bus* power system, was simulated with the MCS tool and indices of system performance are gathered.
- The indices were analysed with a focus on:
  - How representative is the model of the real-world behaviour of a distribution power system and an ICT-based system?
  - Do the simulation results give new insight into the interdependencies of the two systems in question?
  - How does the introduction of ICT components compare to other potential actions in a power system as reducing annual failures, decreased repair time, or addition of backup lines?
  - How sensitive are the results from the MCS to the input parameters?

The author has a background in power engineering with some experience with ICT engineering. The modelling, explored possibilities, and analysis are hence coloured by the background.

1.3 Structure

Chapter 1 — The background and motivation for the thesis are presented and the problem formulation is formulated.

Chapter 2 — Essential concepts and background theory are established for interdependent infrastructures, modernisation of power systems, reliability, and MCS.

The two first sections in the chapter are partially replicated from the specialisation project work by the author. The text is adjusted and extended for use in this thesis as the specialisation project is not publicly available.

Chapter 3 — Explanation of the MCS implemented for interdependent modelling of power systems and a corresponding ICT system. The model is written in the Python language from the ground up and important procedures are presented and explained.

Chapter 4 — The results from the model simulation cases of the test system, with and without ICT, and a small one-factor experiment of important model input parameters are presented and discussed.

Chapter 5 — Discussion of the model and method of analysis.

Chapter 6 — Concluding remarks and a summary of the most important discussions. Then, reflections on what could be further explored in the future regarding the model, method and problem formulation.

2 Conceptual background

This chapter introduces essential concepts to build a foundation for understanding and developing the formulas for the later chapters in this thesis. The chapter begins with an explanation of interdependent critical infrastructures in general, before the concept of resilience in a system is explained. Further on is a presentation of the reliability and power system analysis and the transition into a modern interdependent power system. After this, fundamental statistical concepts are introduced before they are used to explain the MCS method. The last section presents the power flow calculation method used.

2.1 On critical infrastructure and their interdependence

People are dependent on the correct functioning of many types of infrastructures that surrounds modern society. Some of them have a more critical function than others. This chapter discusses both this aspect as well as the essential definitions of interdependencies.

The literature has many definitions of a critical infrastructure [10–12]. This thesis defines critical infrastructure as the interdependent systems that provide essential services to critical societal functions and essential human needs. Without one of the critical infrastructures, one or more of the critical societal functions malfunction. This would most likely lead to a crisis. All critical infrastructures are dependent on at least one other critical infrastructure, for immediate and/or long-term operation. Critical infrastructures are telecommunications, electric power systems, natural gas and oil, banking and finance, transportation, water supply systems, government services, and emergency services [13]. Critical components in an infrastructure are the essential components for the system‘s reliable function. These components are on a gradient from not important to critical, and not all infrastructures have components at the extremities.

In this thesis, the electrical power infrastructure and the part of the communication infrastructure related to the electrical power infrastructure are discussed. They are both defined as critical infrastructures and are interdependent [12]. From now on the power system is used instead of the electrical power infrastructure, for brevity and in accordance with the literature used. The terms “power grid” and “power network” are also used in the literature, but this is avoided in this thesis to have consistent terminology.

2.1.1 Infrastructure interdependencies

Dependency is a linkage or connection, physical or other, between two systems, where the state of one influences the state of the other. Many systems are also *interdependent*, where system A depends on system B to function properly and system B depends on system A to function properly, also called a bidirectional relationship. One example is the power system and ICT system as interdependent systems, as seen in Figure 2.1. The last decades, the power system has been depending more and more on the ICT system

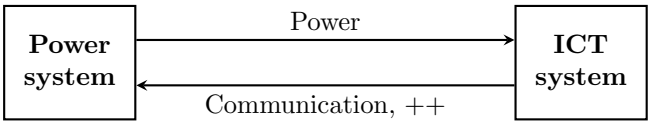

Figure 2.1: Interdependency between power systems and ICT systems.

for monitoring and control, while the ICT system depends on electricity from the power system to function. This relationship is the main focus of this thesis.

Using Perrow's extended taxonomy from Rinaldi et al. [12] of elements of increasing aggregation:

- **Part** A single identifiable component that can not be divided into smaller parts in the model.
- **Unit** A collection of parts with a functional relation. E.g. a turbine-generator set.
- **Subsystem** A set of units. E.g. the control system for the turbine-generator sets.
- **System** A collection of subsystems working together. E.g. a hydropower plant.
- **Infrastructure** A complete collection of similar systems. E.g. an electrical power system.
- **Interdependent infrastructures** The interconnected web of infrastructures and its environment.

This labelling of the elements gives some context to the severity of a fault, where a broken part has limited consequences, but fully broken interdependent infrastructures have huge economic and social consequences.

The complexity of an element can be divided into four categories based on the Cynefin framework [14]. The framework is built for crisis leadership, but brings forward interesting concepts that can be discussed.

- **Simple** An element with a clear relation between cause and effect in repeating patterns which is consistent over time. Analysed by: *Sense*, *categorise*, and *respond*
- **Complicated** An element with a relation between cause and effect, that is revealed during expert analysis and where more than one right answer is possible. Analysed by: *Sense*, *analyse*, and *respond*
- **Complex** An element with an unclear relationship between cause and effect with no right answers and many competing ideas. Analysed by: *Probe*, *sense*, and *respond*
- **Chaotic** An element with no clear relationship between cause and effect, so there is no point looking for them. Analysed by: *Act*, *sense*, and *respond*

Table 2.1: Selected dimensions for describing infrastructure interdependencies. Based on Rinaldi et al. [12]

Interdependencies	Type of failure	Coupling and response	State of operation
Physical	Cascading	Loose/Tight	Normal
Cyber	Escalating	Linear/Complex	Repair/Restoration
Geographic	Common cause	Adaptive	Stressed/Disrupted
Logical		Inflexible	

Applying the element taxonomy from above, a part, a unit and a subsystem are often, in the context of an electrical power system, simple and a best practice is easily built. In a system and infrastructure, the complexity increases leading to good practices, but there could be no ultimate solution on how to control it. The interdependent infrastructures are mostly complex, while they also have some chaotic characteristics. This is why an adaptive resilient strategy is important, which is discussed later. If the interdependent infrastructures are over the limit and inside the chaotic realm where they are impossible to analyse, the only way to proceed is by trial and error. An infrastructure with a high-reliability target should never be chaotic, and measures need to be taken to simplify it. With an even tighter interdependency between the electrical power system and other systems, and also internally from new ICT parts and subsystems, it is necessary to build the system so that it does not become chaotic from obscure interactions or functions of subsystems.

2.1.2 Dimensions of infrastructure interdependencies

Rinaldi et al. [12] gave an excellent overview of the dimensions for describing infrastructure interdependencies, shown in Table 2.1.

There are different types of interdependencies. Using Table 2.1, definitions for the categorisation of interdependencies are;

- **Physical Interdependency** — The material output from one system is used as input to another, and vice versa.
- **Cyber Interdependency** — Information transmission between the systems.
- **Geographic Interdependency** — A local environmental event changes the states in interdependent systems.
- **Logical Interdependency** — Other state-dependent connection between the systems.

Other taxonomies divide logical interdependency into more categories [10], but this is not needed for the discussions in this work. Cyber interdependency is the most emergent

interdependency, because of the recent digitalisation boom all over the world. This is happening through more censors and digital units being distributed throughout the systems, where there used to be only one system component located. Specifically, the cyber dependency of a physical system makes it a *cyber-physical* system with its implications discussed in later chapters.

Digitalisation promotes the coexistence of more infrastructures, which increases the geographic interdependencies. In addition, geographic interdependencies comes from an increase in natural hazards due to a changing environment. In a more globalised world, the physical interdependence between systems worldwide increase. Production chains are now often relying on the output from a system on the other side of the globe. The ever chase towards higher efficiency in corporations increases the use of the 'Just-in-Time'-principle of having small warehouses and relying upon the production chain always running. This last trend may be slowing down or reversing after the global pandemic of Covid-19, due to the stock shortages and delays in delivery time experienced the last year and a half.

The definition of a *failure* is the inability of a component or a system to provide the intended function. Relating this to the state of the infrastructure, the state is in the range from total failure via normal operation to peak loading where the system is stretched as far as it can go before it breaks down. The types of failures in interdependent systems are frequently defined as [12]:

- **Cascading failure** — Disruption in one infrastructure causes the failure of a component in a second infrastructure, and so on.
- **Escalating failure** — A cascading failure with a feedback loop, or at least an increase of the severity or the time until restoration.
- **Common cause failure** — Two or more infrastructure networks are disrupted at the same time because of a common cause.

In addition, the dependency between systems can be tight or loose, depending on the relative degree of dependencies the systems show when they are perturbed or stressed. If i is linked with j, j is linked with k, k is linked with i, then the linking is a feedback loop, which also shows Nth order effects (in general, in the same infrastructure or in others), where j is the first order of i and k is the second-order effect. Nth order effects are often difficult to find before they happen in systems with complex behaviour. Systems can also have a linear behaviour, which is easier to analyse. [12]

2.2 Resilience

Resilience is an expression of the ability of a system to maintain its function if a threat leads to an unwanted event and the ability of the system to resume its activities after the event occurred [11, 13, 15–17]. This includes important factors such as time, perturbations

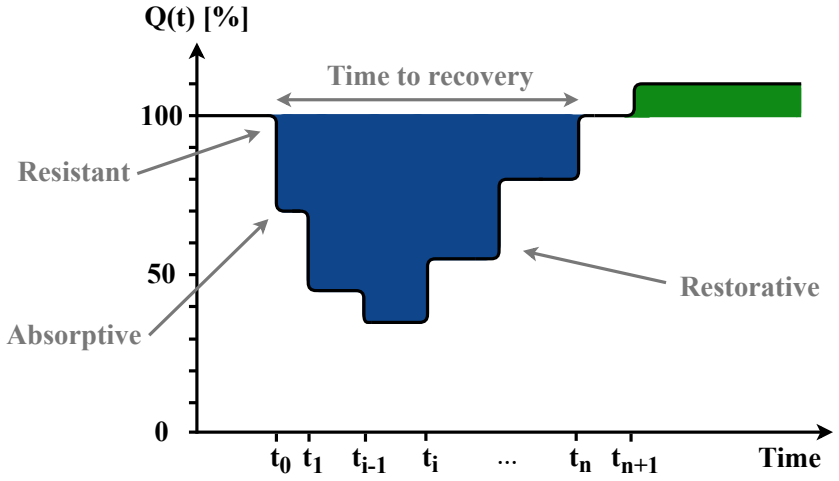

Figure 2.2: Resilience over time in an infrastructure modelled as the *Quality of Infrastructure*. Based on figure in Bruneau et al. [16].

and affected customers. Important aspects of the promotion of resilience are awareness, leadership, planning and resource allocation [11].

An event in the system could be divided into three phases where system resilience is important. According to Ouyang et al. [13], the three system capacities are the *resistant capacity* (before t_0), the *absorptive capacity* (t_0 to t_{i-1}), and the *restorative capacity* (t_i and onward), as seen in Figure 2.2. The initial response is the resistant capacity, where the system prevents or reduces the damage initially done by an event. The opposite of the resistant capacity is vulnerability, which is the inability of the system to withstand a perturbation. The absorptive capacity determines the consequences of the damage to minimise the escalating and cascading faults. In the end, the restorative capacity reinstates the system to normal function. After severe events, the system may take a long time to come back to the same level of operation as before the event. One related example for this thesis could be that the operators realise after an event that the system was operated too close to the physical limits of the system, and they increase the operating safety margin, enhancing the system's absorptive capacity. In a linear and simple system, the phases are easily identified and analysed, but in a complex system, the system would be juggling between the phases until the operators again have complete control and all systems are regenerated. The system could also be at a improved level of operation than before the event from upgrades or replacement of existing equipment or procedures.

Bruneau et al. [16] define a metric for resilience based on key characteristics of a resilient system, namely; reduced failure probabilities, reduced consequences from failures and reduced time to recovery. These key characteristics can in general terms be quantified by a *Quality of Infrastructure*-metric, Q. $Q(t)$ is a function of time and in percent. The resilience factor R is then the integral between normal operation 100 % and the actual

quality of the infrastructure, mathematically defined as

$$R = \int_{t_0}^{t_n} [1 - Q(t)]dt \tag{2.1}$$

A typical graph of R during a disturbance would look something like the blue area in Figure 2.2. The observant reader would also notice a green area in the figure. This area is a modelled enhancement of the infrastructure, a potential result of the restorative capacity. By learning from past events, it is possible to improve the *Quality of Infrastructure*.

2.3 Reliability analysis

The North American Electric Reliability Council (NERC) defines power system reliability as: "Reliability, in a bulk power electric system, is the degree to which the performance of the elements of that system results in power being delivered to consumers within accepted standards and in the amount desired. The degree of reliability may be measured by the frequency, duration, and magnitude of adverse effects on consumer service." [18] In many ways reliability and resilience are related. The types of resilience capacities also directly influence how reliable a power system is.

A division in the temporal range of the analysis is essential. *Security* is the short-term dynamic analysis of the power system‘s ability to deliver power to the customers. Especially the capability of the power system to withstand sudden disturbances in the system. *Adequacy* is the longer-term and steady-state analysis of the power system‘s ability to deliver power to the customers. When accounting for scheduled and unscheduled interruptions of system components, adequacy is the capacity of the power system to provide the total electric power demand at all times over a longer period. [18]

There are two aspects of security analysis; *static* and *dynamic*. The static security analysis is an analysis of the steady-state of the power system after a disturbance, where it verifies that no constraints are being violated. Dynamic security analysis is a time-variant analysis of stability in the power system and can be categorised into rotor angle stability, voltage stability and frequency stability [18].

Important elements in power system analysis were established before the 1960s, and without the widespread use of computers and communication networks. Today this becomes an increasingly interdependent part of the power system; from the planning, via normal control and optimisation, to fault detection and handling in the power system [19]. Central to the power system analysis is the stability of the power system. "Power system stability is the ability of an electric power system, for a given initial operating condition, to regain a state of operating equilibrium after being subjected to a physical disturbance, with most system variables bounded so the entire system essentially remains intact" [18].

A method typically used to categorise reliability studies into three different detail levels

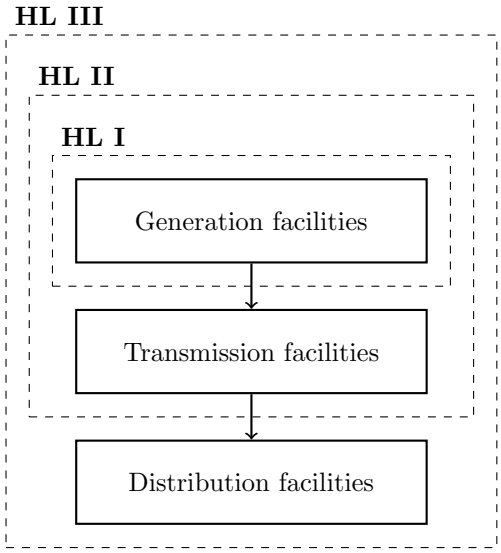

Figure 2.3: Hierarchical levels for reliability analysis [20]

is through the concept of Hierarchical Levels (HL). The first level, *HL I*, only assesses the generation facilities. The generation capacity's ability to supply the load requirement of the system is analysed. The limits of transmission capacity and transmission lines in the transmission sub-system are analysed in the second layer, *HL II*. In *HL III*, the distribution system is also included in the assessment [20]. The layers are shown in Figure 2.3.

This form of dividing the power system is useful and valid for a power system where the loads are passive and with bulk generation of power. Today, distributed generation becomes more and more prevalent in power systems. The past evident assumption of division between the reliability of the transmission level and the distribution level is no longer so distinct. Now, the layers are more connected and inseparable, with active customers and distributed generation. The behaviour mixes between the layers and levels can often not be analysed separately without losing some crucial interactions in the modelled system. However, the *HL III*, where the distribution system is in focus, is the best way to characterise the analysis in this thesis.

If the distribution system does not have adequate generation to run in island mode, it is possible to use a 100% reliable transmission system without losing much accuracy in the results. In the case of a distribution system that is able to behave like a microgrid for some limited time, the transmission system should be modelled as $< 100\%$ reliable to find the more realistic reliability of the limited supply of energy from the island operation. [21]

There are two main methods for analysing power system reliability, *analytical* and *simulation*. Analytical methods use mathematical models of component reliability to calculate how reliable a system is. *RELRAD* [22] and the *minimum cut set* method [20] are examples

of analytical methods, but are not explained further in this thesis. Simulation methods (like the Monte Carlo Simulation (MCS), described in detail in section 2.6) use component reliability as a probability of failure, and together with a model of the behaviour of the components, the system is simulated. After some amount of simulation time, the average reliability of the system can be found. More details often lead to increased computation time. For both methods, the assessment cannot be better than the model it originates from. A golden middle needs to be found where the model is of high enough fidelity but takes a reasonable time to calculate. A general rule of thumb is to use a simulation method if the system is extensive and/or have complex interactions. The output from the methods is organised as reliability indices, later introduced in subsection 2.7. This thesis uses a simulation method since the analysed system has complex interactions that are challenging to model with analytical methods. The complex interactions in power systems are explained in the next section.

2.4 Modernisation of the power system

As indicated in the last section, the power system is undergoing many changes. Customers want and are dependent on the continuous supply of power within quality parameters such as voltage, frequency, harmonics, and flicker. [23]. New technology in the production, control, and delivery stages could fulfil the demand within tight budgets. In the distribution system, this is particularly challenging as it generally consists of radial overhead lines prone to frequent and lengthy failures [23]. Rural areas have the lowest power demand, and thus few or none backup lines. One could assume that the inclusion of solar Photo Voltaic (PV), batteries, and other distributed generation would increase the reliability of the weak links, but there are several complicating factors that dilute the positive effects, as disconnection for the safety of the repair crew.

There are circuit breakers on the transformer(s) from the High Voltage (HV) transmission system to the Medium Voltage (MV) distribution system, but there are only fuses and disconnectors on the transformers to the Low Voltage (LV) side and at line endings most of the time. Circuit breakers are too expensive to be widely used in the MV distribution system, while they sometimes could be used to divide the system into sections. If a fault happens in the LV transformer, the fuse breaks the current, and the downstream customers are isolated from the main grid. There is no interruption to the customers connected to the same MV transformer if they are connected to LV transformers other than the one where the fuse breaks. If a fault happens between the low and MV transformer, i.e. a line or a disconnector fault, the circuit breaker in the MV transformer will isolate the nodes downstream.

The old method for the utilities to respond to a closed circuit breaker in a LV transformer often begins with a customer calling the operator to complain that they do not have any power. With communication to the LV transformer the repair time could decrease as the

Distribution System Operator (DSO) get immediate feedback that the breaker is closed.

Faults in a MV transformer is normally already automatically reported to the DSO. Next, the operator sends out a repair team to get the power back to the customer, physically turning breakers and disconnectors in the process. The repair team systematically tries to reconnect a section of the MV distribution system until the fault is located and isolated from the other part of the system. The time from the initial fault to when the fault is isolated is called the sectioning time and is often around one hour using this approach.

A modern (and in many places futuristic) approach has sensors in the system, closer to the connection point of customers, to monitor the voltage and current, or the lack thereof. When a fault is detected, an automatic system could try to reconnect the power if the fault is of a temporary type (lightning strike, small overload, and others). Further, or when the fault is not a transient type, remote-controlled disconnectors could help find the fault location. The resulting sectioning time is much shorter, which gives a strong increase in the restorative capacity of resilience for the system. Then, the DSO reconnect the system in another topology with the reserve lines. The operators send a repair team if there are still faulty components or customers without power.

When comparing the two methods of handling the fault, it is evident that the time before it is possible to get the power back varies considerably. However, if there is a need for a repair team to fix the fault, it takes almost the same time to fix the fault in both scenarios. ICT equipment could speed up the first process of finding the fault, but could also complicate the reparation process once found, since the ICT equipment makes the subsystem more complex. In the transition to a more digital substation, technicians could be experts on the electrical power part of the system, needing backup to fix faults or restarting the ICT equipment.

The difference in interruption time could significantly impact society, its economics, and individuals. In the era of computers and internet, the productivity drops to a halt without electric power. Although most critical equipment and facilities have backup power for short interruptions, the consequences are higher from prolonged interruptions to electric power. An effect is that after a few hours, food in refrigerators and freezers defrost and get stale, water pumping stops and the pressure drops as long as people use water, and mobile towers often only have backup power for a few hours [1, 2]

2.4.1 Information and Communications Technology in power systems

ICT can be defined as follows: “The technology involved acquiring, storing, processing and distributing information by electronic means (including radio, television, telephone, and computers)” [24]. ICTs monitor raw data, make higher-value information and control the electric power system in normal and abnormal conditions, both automatic and with manual intervention [25]. It creates a new layer to the power system, a cyber layer, making

the system a cyber-physical system. The two systems work in parallel but are also highly interdependent. Geographic interdependency is strong as ICT parts often need to be co-located with power equipment, and even more often, it is the most economical solution. A local environmental event could then knock out both systems leading to, among others, longer repair times.

Some of the many tasks of ICT parts in the power system are to aid in monitoring and control, optimise the use and increase the efficiency of maintenance and replacement of the power system components, detect and localise faults, enable self-healing and remote control for repair, and to give extensive amounts of data that could be aggregated to provide a new insight of the system behaviour. However, both active and passive failures, in the ICT reduce the possible improvement seen in the system [26]. There is an enormous potential, but also some significant challenges in the determination of the optimum type, mix, and placement of the ICT‘s sensing, communication, and control hardware [19]. Also, the decision on and implementation of software with the coordination of centralised or decentralised control are challenging [19]. In centralised control, one controlling hub receives measurements of the system‘s state and then sends out commands remotely to the distributed components. In a fully decentralised control, the distributed sub-systems coordinate between themselves how the system should be controlled, without the need of a central controller.

There are two distinct groups of ICT devices used. These are information devices and communication devices. The information devices measure, control, and analyse the power system. The Supervisory Control and Data Acquisition (SCADA) system is a system for control of the power system, and processes information coming from [24]

- Measurements of active and reactive power, voltage and frequency at nodes.
- Signals like breaker and transformer tap changer position.
- Event registration with timestamped registration of the state of all equipment at a substation under an event
- Analog registration of significant quantities, both in the instantaneous and the Root mean square (RMS) form.

The communication devices enable the transmission of information between the other parts. Different devices and the type of information have diverse requirements resulting in the use of a wide array of communication methods.

With the cyber-layer, there is a cyber interdependency, and because of that, new challenges arise. Generally, there are two types of concerns in the cyber-space; *safety* and *security*. Safety is about minimising latent faults in the equipment and systems, and faults triggered by nature and humans without intent. Security is, on the other hand, minimising attacks on the system from people with the intent of creating damage, and reducing the damage.

In addition, attacks of the information systems fall into two classes [27]:

- Deceptive attacks, provoking unperceived malfunctions, similar to latent errors. Divided into;
  - Passive, without any direct action on the power system.
  - Active, provoking configuration changes in the power system.
- Perceptible attacks, creating damage that could be detected.

An *error* or a *failure* are the effects when the safety or security are compromised. In computer and software engineering, an error is when the output of a system differs from the expected output, while a failure is the inability of a system to function as intended. They could both lead to cascading or escalating failures in the power system. An example a possible consequence is from the testing of a new under-sea cable between Norway and Germany. From a failure in the cable‘s control system, the power through the cable immediately went from 100 MW to 1400 MW. This resulted in a drop in the system frequency of 0.5 Hz, two inter-country connections had the power readjusted, a gas turbine power plant in Sweden started up, a big industrial gas producer disconnected itself from the main grid and was run in island mode, and a Finnish coal power plant shut-down the production [28].

2.4.2 Smart grids and microgrids

The term “smart grid” is today highly overused in scientific and popular literature, with many definitions and meanings. An attractive and broad definition is that the smart grid is the future power system, today‘s system but improved in many ways. With this definition, we acknowledge that, at least for the foreseeable future, the power system needs to be improved, being built and operated better. Examples of the changes power systems undergo are shown in Table 2.2. The smart grid is the notion of a connected and intelligent network that has new sensors and control mechanisms to enable improved operation and event handling than before. One of the essential and central concepts of the distribution level in the smart grid is the microgrid.

Originally the microgrid was defined as a cluster of loads and distributed generation, operating as a single controllable system that provided both electric power and heat to its area [30]. In this thesis, only the electric power distribution is discussed. The microgrid consists of basic components such as an energy manager, power flow controller, and a protection coordinator. Microgrids coordinate load, generation and the behaviour of all the components. The voltage is regulated through reactive power Q droop control and frequency is regulated though active power P droop control. This type of control is already implemented in *PyDSAL*, a power flow solver implemented in Python which uses voltage and power sensitivities in droop control of local active and reactive power regulation [31], explained later in subsection 2.8.1.

Table 2.2: The possibilities of the smart grid compared to the existing power system. Based on table by Farhangi [29].

Excisting power system	**Smart grid**
Electromechanical based	Digital based
One-way communication	Two-way communication
Centralised generation	Distributed generation
Hierarchical structure	Interdependent network structure
Few sensors, and none in the distribution system	Sensors throughout
No aggregation of sensor data	Self-monitoring
Manual restoration	Self-healing capability
Failures lead to blackouts	Adaptive and islanding behaviour
Manual check/test	Remote check/test
Limited control	Universal control
Few customer choices	Many customer choices

Microgrids are one of the alternatives to the challenge of the change in power flow production and power flow from distributed generation. Power systems are traditionally constructed for power flow from the transmission system to end consumers in the distribution system. Emerging power production in the distribution system, like solar PV, need some sort of control and coordination, or else it could degrade the quality and reliability of the local distribution system. This is generally also a challenge in all radial operated power systems. Important challenges here are related to behaviour in outages and voltage control. Microgrids try to solve these issues. They also give an opportunity of island operation of a subsystem, which further enhances reliability. This could be a good solution to smaller power systems connected to a larger power system through a weak or unreliable link.

In addition, a limited or expensive fast regulation in the central power system is a motivation for the implementation of microgrids. In Europe, many of the requirements for economic incentives are present. Norway is a special scenario with a substantial rapid regulation capacity from hydropower, and therefore it is little need in the near future for the extensive use of microgrids. However, some smaller islands in rural Norway with few inhabitants and weak and expensive power links to the central power system are potential candidates for these concepts.

Amin and Wollenberg [19] discuss "how to make an electric power transmission system smart", to enable a smart, self-healing power system that can cope with a broad array of destabilisers. They point towards distributed independent agents, where processors are placed in each component in the substation (and in the power system in general) to communicate with sensors in its part and other agents. In this context, and the rest of the thesis, an agent is defined as an entity with a location, capabilities and memory, with

metrics as input or output to other agents [12]. These agents should act fast and protect the system from unwanted events, not necessarily as fast as the protection system, but faster and better than a central control system can manage [19]. Amin [32] also points towards a future with distributed independent agents to make the power system adaptive and self-healing.

In practical implementations of a microgrid, one especially important factor for the resilience of the system is that the processing units are independent. This independence gives the substation an opportunity to be partly functioning even when one component in the substation fails. The research is now focusing on different opportunities to develop controllers for either centralised or decentralised control. The types of controllers have different compromises including, but not limited to, adaptive operation and robustness to a huge variety of disturbances [19]. In centralised control, it is easier to coordinate the behaviour of each sub-system, but they are vulnerable to faults in the communication interface. Decentralised control lessens the communication needs, and hence the vulnerability of that subsystem. It decreases the need for processing power at a central point, but increases the need for processing at all the distributed points of control. This results in higher redundancy from more units doing almost the same job, but also a coordination issue between the independent units.

The object-oriented approach of the Python tool developed makes the integration of such agents easily obtainable. The user can switch between different control strategies and agents without changing the underlying code for solving the power flow or the MCS.

2.5 Statistical background

MCS use random numbers to simulate the possible behaviour of a system from a time step to the next. The behaviour should be as close to the real system as possible. This can, at least on average, be the outcome from a MCS. The uncertainties in the simulation is important. Without knowing the probability of the correctness of the results, they are unsuitable for decision-making.

2.5.1 Random numbers

Random numbers generated by a mathematical method in a computer can only be pseudo-random, meaning that the numbers they generate will repeat and have some type of dependence between them. Good pseudo-random generators have three important characteristics;

1. highly uniform distribution on the interval chosen (often $[0, 1]$),
2. minimal correlation between the numbers generated, and
3. a long period between repeating patterns of numbers.

One should use a pseudo-random generator with these characteristics to avoid getting any bias in the results from a simulation.

2.5.2 Statistical distributions

Pseudo-random generators often output numbers as a uniform distribution, which is fundamental to computer simulations. In a uniform distribution, the probability of getting each number inside the interval chosen is the same.

$$f_{Unif}(x) = \begin{cases} \frac{1}{b-a} & \text{for } x \in [a, b] \\ 0 & \text{otherwise} \end{cases} \tag{2.2}$$

In an exponential distribution there is a higher probability of getting relatively small numbers compared to relatively larger numbers. The relative displacement is set according to the decay parameter β. The probability density function is

$$f_{Exp}(x) = \begin{cases} \frac{1}{\beta} e^{-x/\beta} & \text{for } x > 0 \\ 0 & \text{otherwise} \end{cases} \tag{2.3}$$

for $\beta > 0$. A variable X that has this distribution is mathematically written as $X \sim \text{Exp}(\beta)$. The cumulative exponential distribution function is

$$F_{Exp}(x) = P(0 \leq X \leq x) = \int_0^x \frac{1}{\beta} e^{-\alpha/\beta} \, d\alpha = 1 - e^{-x/\beta} \tag{2.4}$$

The exponential distribution has a relationship with the Poisson process. Using the Poisson distribution to find the probability of no events occurring in a Poisson process up to time t, we find that it is equal to the exponential distribution [33].

$$p(0; t/\beta) = \frac{e^{-t/\beta}(t/\beta)^0}{0!} = e^{-t/\beta} \tag{2.5}$$

is the same as the time before the first event, giving

$$P(X > x) = e^{-x/\beta} \tag{2.6}$$

A Poisson process is memoryless, meaning that future probabilities only depend on present information, and is independent of the past. Mathematically this is written as

$$P(X \geq t_0 + t | X \geq t_0) = P(X \geq t_0) \tag{2.7}$$

As such, the exponential distribution describes the time between Poisson events. [33]

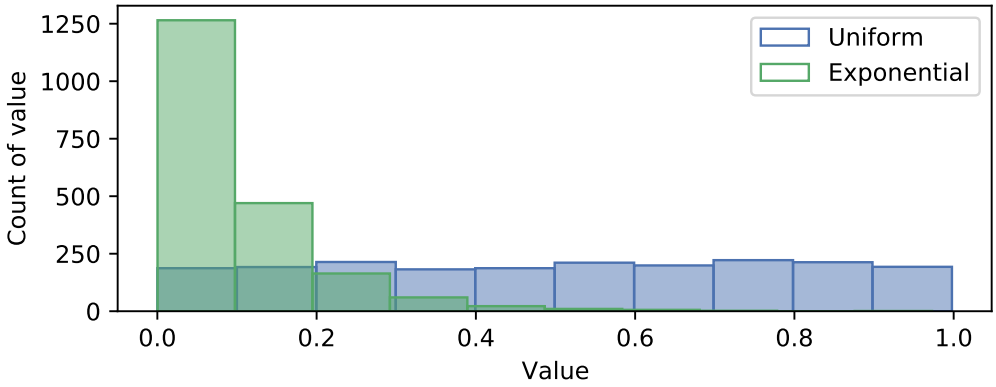

Figure 2.4: Visualisation of the inverse transform of random numbers from an uniform distribution to an exponential distribution. 2000 random numbers were generated and plotted as a histogram. The inverse transform used $\beta = 0.1$.

2.5.3 Inverse transform sampling

Inverse transform sampling solves the challenge of generating a random variable x described by a cumulative distribution function F_X [21]. In this thesis, the cumulative distribution function is the exponential distribution. This is not directly sampled on a computer, rather a number is sampled from a uniform distribution then, using the inverse transform, an exponential distribution is achieved.

The short deduction of the inverse transform sampling using an exponential distribution follows. Using equation 2.4 for an exponential cumulative distribution and solving for $y = F(x)$, the result is

$$F(x) = 1 - e^{-x/\beta} \quad \text{for } x \geq 0 \tag{2.8}$$

$$F^{-1}(y) = -\beta \ln 1 - y \tag{2.9}$$

This is the inverse transform sampling as $x = F^{-1}(y)$ where y is drawn from a uniform distribution ($Y \sim \text{Unif}(0, 1)$) such that x becomes exponentially distributed. The distribution for $1 - y$ and y are equal. Thus the equation can be simplified to

$$F^{-1}(y) = -\beta \ln y \tag{2.10}$$

Figure 2.4 shows the result after using the inverse transform sampling on random uniform numbers, to generate an exponential distribution.

2.5.4 Coefficient of variation

The coefficient of variation α is an expression of the accuracy level of the MCS. A short deduction is provided here, based on [21]. A component with two states, up and down, is

denoted by X_i where

$$X_i = \begin{cases} 0 & \text{for the component's up state} \\ 1 & \text{for the component's down state} \end{cases} \tag{2.11}$$

A set of N independent state samples is $X_1, \ldots, X_N$ has an estimated mean (unavailability) of

$$\overline{X} = \frac{1}{N} \sum_{i=1}^{N} X_i \tag{2.12}$$

with a sample variance of

$$\sigma_X^2 = \frac{1}{N-1} \sum_{i=1}^{N} (X_i - \overline{X})^2 \tag{2.13}$$

Using that X_i is either 0 or 1 and for large sample sizes the variance of the unavailability estimate is

$$\sigma_{\overline{X}}^2 = \frac{1}{N} \sigma_X^2 = \frac{1}{N} (\overline{X} - \overline{X}^2) \tag{2.14}$$

Thus, increasing the sample size and decreasing the sample variance are the two methods to be used to get a more accurate result. The coefficient of variation α is

$$\alpha = \frac{\sigma_{\overline{X}}}{\overline{X}} = \frac{\sigma_X}{\sqrt{N} \cdot \overline{X}} = \sqrt{\frac{1 - \overline{X}}{N \overline{X}}} \tag{2.15}$$

It follows that the accuracy depends on the unavailability of the system, but not the system's size. This is an advantage compared to analytical approaches that become impractically computation heavy, or even impossible to fully solve, for systems with many components.

2.5.5 Limit theorems

The following limit theorems lay the foundation of the MCS method. First, the law of large numbers states that with a large number of samples the estimated arithmetic mean tends towards the real mean with high probability. Mathematically

$$\lim_{N \to \infty} P\left[|\overline{X} - \mu| < \epsilon \right] = 1.0 \tag{2.16}$$

where μ is the real arithmetic mean of the N independent random variables $X_1, \ldots, X_N$ and ϵ is a sufficiently small positive number [21]. Second, the central limit theorem states that with a large number of samples the arithmetic mean follows a standard normal

distribution. Mathematically

$$\lim_{N\to\infty} \frac{\left|\overline{X} - \mu\right|}{\sigma/\sqrt{N}} \sim n(0,1) \tag{2.17}$$

where σ is the standard deviation [33].

2.5.6 Approximate Confidence Intervals

A confidence interval is an estimation of how statistically certain a number is. Here a confidence interval is deduced for an estimated mean when there is an unknown mean μ and an unknown variance σ of that given mean. Included for completeness, a full deduction is shown in [33]. The normal distributed random variable

$$T = \frac{\overline{X} - \mu}{\sqrt{S/N}} \tag{2.18}$$

had a t-distribution with $v = n - 1$ degrees of freedom, where S is the sample standard deviation. The probability of the sample being inside the limits should be $(1 - \alpha)$.

$$P\left(-t_{\alpha/2} <= T <= t_{\alpha/2}\right) = 1 - \alpha \tag{2.19}$$

Inserting eq. 2.18 and rearranging gives

$$P\left(\overline{X} - t_{\alpha/2}\frac{S}{\sqrt{N}}, \overline{X} + t_{\alpha/2}\frac{s}{\sqrt{N}}\right) = 1 - \alpha \tag{2.20}$$

With a large N, for any random variable with a distribution, the confidence interval can still be approximated by this equation. Using the fact that the critical value t from the t-distribution for a large v is the same as the critical value z from the normal distribution, this gives a $(1 - \alpha) \cdot 100\%$ confidence interval for μ

$$\left[\overline{X} - z_{\alpha/2}\frac{S}{\sqrt{N}}, \overline{X} + z_{\alpha/2}\frac{S}{\sqrt{N}}\right] \tag{2.21}$$

Table 2.3 presents selected critical values for a corresponding confidence level and Figure 2.5 presents a 95% confidence interval. As seen in the figure, with a 95% confidence interval the bulk of the samples is inside the interval, but importantly, not all. There is always a probability of the real mean being outside the interval.

2.5.7 Factorial experiment

Factorial experiment is a statistical method to determine how changes in factors impact the results of an experiment. A *factor* is any feature of the experiment such as parameters (failure rate, load, and others) or operational procedures (the use of backup lines, ICT

Table 2.3: Chosen critical values of the t-distribution for a two-sided confidence interval for a large v [33].

Confidence level	α	Critical value
95%	0.05	1.960
99%	0.01	2.576
99.9%	0.005	3.290

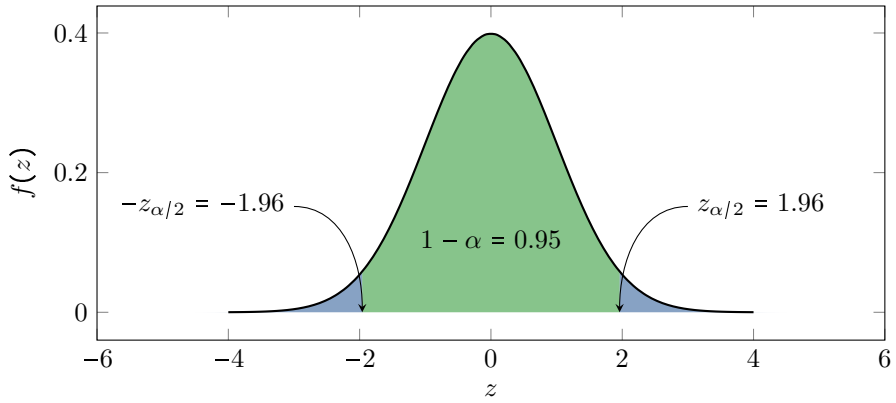

Figure 2.5: A 95% confidence interval. Inspired by [34].

components, and others) that may be varied from one case to the next. A *one-factor* experiment is conducted by running several experiments where only one factor is changed for each new case. The basic type of change is between *two levels*, but one could use as many levels of change in the factors as needed [33]. The results are compared to get an idea of the sensitivity in the model for different parameter changes. When changing at least two factors per case, it is called a *factorial experiment*.

2.6 The Monte Carlo method

The method is in general a stochastic simulation using random numbers. The name comes from Monte Carlo in Monaco, made famous by its gambling casino, and it has been used in many applications since the basic concept was established in the 18th century [21]. Since the method relies on random numbers, the estimated mean of a system index could increase its error compared to the true value with one additional sample. However, for each new sample, the error bound and the confidence interval are getting smaller, and, as stated in subsection 2.5.5, with a large sample pool, the mean is with high probability close to the real mean.

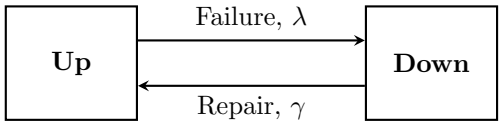

Figure 2.6: Two state figure

2.6.1 The state space method

The state space method builds upon the fact that a component or a system can be represented by a state. The state represents how well the object can do its function where there could be infinite states to choose from, but often only two states are sufficient. Then the two states are fully functional and fully dysfunctional, see Figure 2.6. For such a component there are two important numbers to consider; Mean Time to Failure (MTTF) with failure rate $\lambda = 1/m$ and Mean Time to Repair (MTTR) with repair rate $\gamma = 1/r$ [21]. They are equal for all load conditions as overload types of failures are relatively infrequent [35] and thus adds unnecessary complexity.

Exponential distributions are used to model the MTTF since the failures could be seen as a Poisson process, with a relationship explained in subsection 2.5.2. MTTR does not fit the Poisson process as well as the MTTF, but it is a good approximation to a challenge of high variance and many parameters. The time independence characteristic of the exponential function is useful when modelling the system, but since it cannot model ageing, an assumption that components are replaced and maintained before they have a considerably increased failure rate is needed.

2.6.2 The state duration method

There are several simulation approaches for MCS, and one of them is the state duration sampling [21]. The basic method is expanded for use in this thesis making the state of some components dependent on others. The basic method is found in [21]. In this approach, the system is simulated chronologically and it uses the component state duration distribution functions.

Step 1 Initially all components are assumed ok.

Step 2 Find the duration before each individual component changes its state. The inverse transform sampling is used to get the time using

$$T_i = -\beta_i \ln U_i \tag{2.22}$$

where β_i is the corresponding failure rate $\beta_i = 1/\lambda_i$ or repair rate $\beta_i = 1/\gamma_i$ for each component if the component is respectively up or down, and U_i is a uniformly distributed random number $\in [0, 1]$.

Step 3 After one time increment the components with the current time t switches state and get a new transition time according to

$$T_i = -\beta_i \ln U_i + t \tag{2.23}$$

Step 4 The system is analysed.

Step 5 If t equals the end time, the simulation ends. Otherwise, repeat from *Step 3*

The advantages with this approach (comparing to other approaches in [21]) is that

- The frequency index can be calculated
- The state duration distribution can be calculated
- The statistical probability distributions of the reliability indices can be calculated.

A big disadvantage is that this approach requires parameters for the state duration for all components. The parameters are sometimes hard to find and have an inherent uncertainty associated with them.

2.7 Reliability indices

Reliability indices are one possible quantification of the reliability performance of a system. Many indices are tailored to the part of reliability studied. In power system analysis, failure rate, failure duration, and energy not supplied are central in calculating the indices. These metrics can be converted into indices that make it easier to compare different power systems of various sizes, and are often used when evaluating the performance and future upgrade path of a power system. Indices are also used to report from the DSO to the Transmission System Operator (TSO), which uses a different set of indices compared to the intern indices for the TSO in the transmission system. The indices are often based on the same basic indices but altered to reflect essential aspects in that part of the system.

In general, the indices used for reflecting the state of interdependent infrastructures need to be [12]:

- Relevant to the effects they seek to measure.
- Suitable for use in developing data sets.
- Suitable for use in running and validating models.
- Helpful in prioritising threats and risks.
- Suitable for comparing and measuring alternative responses to interdependencies.

The basic reliability indices are failure rate λ, unavailability U, average failure duration r, and Energy Not Supplied (ENS). All these indices are averaged over a year and can be

calculated both for each separate node and for the system as a whole [20].

$$\lambda_s = \sum \lambda_i \text{ [interruptions/year]} \tag{2.24}$$

$$U_s = \sum \lambda_i r_i \text{ [hours/year]} \tag{2.25}$$

$$r_s = U_s/\lambda_s \text{ [hours/interruption]} \tag{2.26}$$

$$\text{ENS}_s = \sum L_{a,i} U_i \text{ [energy/year]} \tag{2.27}$$

where λ_i is the component failure rate, r_i is the component restoration time, and $L_{a,i}$ is the average load at the load point. The average load could be calculated as $L_a = L_p f$ where L_p is the peak load demand and f is the load factor. Or, from $L_a = E_d/t$ where E_d is the total energy demand in the period t.

From these the following widely used indices for distribution systems can be deduced [20]. The indices are tailored to get an understanding of what a customer at the endpoint should expect in terms of outages, frequency, and duration. N_i is the number of customers of load point i. They are categorised into two different groups 1) Customer-oriented indices and 2) Load-oriented indices.

Customer-oriented indices

- System Average Interruption Frequency index (SAIFI) is a measure on how often a customer should expect an interruption of power in a year. This can vary between load points in the system. The failure rate λ is the similar index for a single load point, while SAIFI is the weighted average for the whole system.

$$\text{SAIFI} = \frac{\text{Total number of customer interruptions}}{\text{Total number of customers}} = \frac{\sum \lambda_i N_i}{\sum N_i} \tag{2.28}$$

- System Average Interruption Duration index (SAIDI) is much the same as SAIFI but measures the *duration* of interruption rather than the *frequency*. Some systems could have many short interruptions and other systems few longer interruptions. This is an important distinction as mentioned in subsection 2.4.

$$\text{SAIDI} = \frac{\text{Sum of customer interruption durations}}{\text{Total number of customers}} = \frac{\sum U_i N_i}{\sum N_i} \tag{2.29}$$

  This index and the resilience factor R, in equation 2.1, measure a similar quantity. One could say that the SAIDI index is the average resilience factor calculated on a yearly basis, where the *Quality of Infrastructure*-metric is the percent of customers that have power.

- Customer Average Interruption Frequency index (CAIFI) is quite similar to SAIFI, but where SAIFI divide the interruptions by all customers, CAIFI only divides by

the customers that have experienced interruptions that year. As such, the index measures the average frequency of interruptions for a load point given that the load point has at least one interruption that year. A system with a difference between this index and SAIFI indicates that only parts of the system experience faults, and a big difference is that only a few load points experience interruptions per year.

$$\text{CAIFI} = \frac{\text{Total number of customer interruptions}}{\text{Total number of customers affected}} = \frac{\sum \lambda_i N_i}{\sum N_i(U_i > 0)} \tag{2.30}$$

- Customer Average Interruption Duration index (CAIDI) is the average duration of interruptions in the system when the interruption is counted on every load point. It has a relation to other indices in that it is the SAIDI index over the SAIFI index.

$$\text{CAIDI} = \frac{\text{Sum of customer interruption durations}}{\text{Total number of customer interruptions}} = \frac{\sum U_i N_i}{\sum \lambda_i N_i} = \frac{\text{SAIDI}}{\text{SAIFI}} \tag{2.31}$$

- Average Service Availability Index (ASAI) is a measure of how much of the time customers should expect to have power delivered (often given in percent). This is a scaled variant of the SAIDI index, measuring the availability instead of the unavailability.

$$\begin{aligned}\text{ASAI} &= \frac{\text{Customer hours of available service}}{\text{Customer hours demanded}} = \frac{8760 \cdot \sum N_i - \sum U_i N_i}{8760 \cdot \sum N_i} \\ &= 1 - \frac{\sum U_i N_i}{8760 \cdot \sum N_i} = 1 - \frac{1}{8760} \cdot \text{SAIDI}\end{aligned} \tag{2.32}$$

where 8760 is the number of hours in a year.

Load-oriented indices

- Average Energy Not Supplied (AENS) is similar to the SAIDI index, but while SAIDI measures the time (h), AENS measure the energy (kWh). For the power utility company this is an important index as they get paid for the delivery of energy. With that said, the time aspect is also important, both for the reputation of the company and the size of fines from interruptions.

$$\text{AENS} = \frac{\text{Total energy not supplied}}{\text{Total number of customers served}} = \frac{\sum L_i U_i}{\sum N_i} \tag{2.33}$$

- Average Customer Curtailment Index (ACCI) and *AENS* have the same difference as CAIFI for SAIFI, the first is divided on only customers that have experienced interruptions that year.

$$\text{ACCI} = \frac{\text{Total energy not supplied}}{\text{Total number of customers affected}} = \frac{\sum L_i U_i}{\sum N_i(U_i > 0)} \tag{2.34}$$

Generally, for all indices, a lower value is better, except for ASAI where a high value (availability) is preferred. However, an increase or decrease in one of the indices do not necessarily have the same value to all customers, and will be discussed later in this thesis.

2.8 Power flow calculation

Physical flow models use, in the context of transmission power systems, either the linearised DC power flow model or the higher-order AC power flow model to accurately model the real flow of power in the system in steady-state. For distribution power systems the FBS is also an option.

2.8.1 Forward-Backward Sweep

FBS is used for radial operated power systems [31, 36]. Each iteration consists of a backward and a forward iteration, with convergence to a result. First, the backward iteration estimates and summates the load at each node beginning from the nodes furthest from the root node, where the root node is the node connected to the external grid. Then the forward iteration estimates the voltage based on the load current at each bus.

The opportunities using FBS are great for extended control over the power system, as seen in the demonstration using *PyDSAL* [31]. These opportunities are not used in this thesis, but would be a natural next step in the direction of a model using the modern opportunities of Distributed Generation (DG), advanced voltage control, and ultimately microgrid operation (explained in subsection 2.4.2). To make an extension of the tool developed more easily achievable the tool is already integrated with FBS.

Below are some equations based on Haque [37]. In the first iteration backward through the nodes, beginning at the node furthest away from the root node, the load current is calculated using the latest voltage vector. A flat start of nominal voltage or an estimation of the voltage is used. The load is assumed to be of constant power type. For a distribution line from node k to node m the current is estimated using

$$I_i = \frac{P_i'^2 + Q_i'^2}{V_m^2} \tag{2.35}$$

where $P_i^{'}$ and $Q_i^{'}$ is respectively the active and reactive power at node m flowing through line i and V_m is the voltage magnitude at node m. Then losses are estimated using the load current with the help of

$$P_i^{loss} = R_i I_i \tag{2.36}$$

$$Q_i^{loss} = X_i I_i \tag{2.37}$$

where R_i is the line resistance and X_i is the line reactance. The inflow power at node k is

updated using

$$P_i = P_i^{'} + P_i^{loss} \tag{2.38}$$

$$Q_i = Q_i^{'} + Q_i^{loss} - V_k^2 y_k \tag{2.39}$$

where $y_k = 1/z_k = 1/(R_i + X_i)$ is the admittance of line i. In the forward iteration the node voltages are calculated forward from the root-node through the network using the previously calculated currents at each node. The complex voltage is

$$\mathbf{V}_m = \mathbf{V}_k - I_i(R_i j X_i) = \left(\mathbf{V}_k - \frac{P_i R_i + Q_i^{''} X_i}{V_k}\right) + j\left(\frac{Q_i^{''} R_i - P_i X_i}{V_k}\right) \tag{2.40}$$

where $Q_i^{''} = Q_i + V_k^2 y_k$. By setting the voltage angle at the root node to zero, the voltage angle δ_m and the voltage magnitude V_m are

$$\delta_m = \delta_k + \arctan\frac{\Im(V_m)}{\Re(V_m)} \tag{2.41}$$

$$V_m = \sqrt{V_k^2 - 2(P_i R_i + Q_i^{''} X_i) + (P_i^2 + Q_i^{''2})\frac{R_i^2 + X_i^2}{V_k^2}} \tag{2.42}$$

The voltage angle is not directly used in the FBS in this thesis, but could be useful for understanding the system better and is included for completeness of the system state. The change of voltage at the nodes is used for the convergence determination using the convergence criteria of

$$\max(|V_m(t-1) - V_m(t)|) < \epsilon \tag{2.43}$$

where ϵ is a low value convergence limit.

Using partial derivatives of the voltage with respect to the active or reactive power, it is possible to find the approximate voltage change from a change in the active or reactive power injection [31]. By using these sensitivities, active components could easily be implemented in the system, without needing to go through lots of iterations to close in on the value of compensation needed for a new load profile.

3 Methodological approach

The focus of this thesis is to investigate the adequacy aspect of power systems. A quantitative system analysis tool was built from the ground up, relying on mathematical models and computing power. Such tools will always rely on the quality of the input data, which is also the case here. As strong security laws make widely available statistical data on components complex to get hands-on, it is essential to consider the input data.

3.1 The Monte Carlo simulation tool

Power systems are connected to communication ICT systems. The interdependency between the systems is integrated through the codebase. In the integration of ICTs, there is an option to turn off all ICTs for the following simulation. The differences this gives for the behaviour of the system are explained in this chapter.

The system boundary is set upstream at a step-down transformer from HV to MV to a distribution power system, downstream to the next step-down, from MV to LV, where the consumers are connected. Modelling detail level and choice of the analysis method to be able to study the correct phenomena is loads at each bus point calculated by using the FBS. Outage or isolation of one node/step-down transformer is the smallest failures in the system, and total failure of the system is when none of the nodes/step-down transformers can deliver power to the customers.

In the developed tool, *PyDSAL* software [31] is used as a basis. *PyDSAL* is used for the component class structure (Bus-class and Line-Class) and the FBS method to solve the power flow problem in a radial operated power system. Some modifications were done in the code to get all scenarios with topology changes to end up correctly without manual intervention — also, some modification were done to decrease the computation time for the specific application in this thesis.

3.1.1 Component classes

An object-oriented approach is used to take advantage of the Python programming language. In addition, Python has a good readability. This is important in complex models. The tool developed uses the *PyDSAL* software by extending the software‘s existing classes.

State-class is used for good readability of each component. It has the state-values of *ok*, *isolated*, *failed* and *disabled* with the corresponding numbers of 0–3, see Figure 3.1 and parts of Figure 3.2.

The Component-class is used as a common (parent) class for all types of components in the system. The class structure is shown in Figure 3.2. It has common variables that are used for all components;

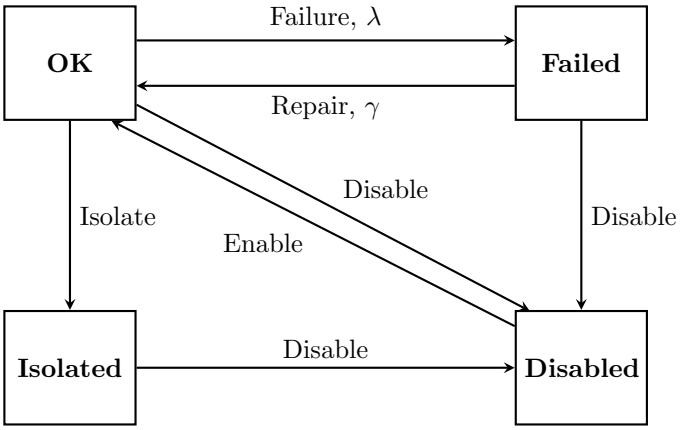

Figure 3.1: Illustration of the four states of a component with the possible transitions between them

- *state* of type State,
- *betaF* is the inverse MTTF, $\beta_F = 1/\lambda$, for the component,
- *betaR* is the invers MTTR, $\beta_R = 1/\gamma$, for the component and
- *transition* is the hour, counting from the start of the simulation, when the transition to the next state happens.

Child classes inherit all variables and functions of the parent class. The child classes of the Component-class are; Bus, Line, Disconnector, Communication Hub, and Communication Line. For each component, there is made an object of the correct class. That object is filled with the correct information and is connected to the other components, according to Figure 3.3. In addition, the objects of all components are placed into a list corresponding to the component type, giving five lists of components.

Figure 3.3 shows, with arrows, which component each component type is connected to. As an example, the Bus-class has variables for the previous line, the next line, the next bus, and the connected communication hub. In addition, the Bus-class has active load requirement P and reactive load requirement Q, and the Line-class has the resistance R and the reactance X of the line, as seen in Figure 3.2.

The Component-class also has a function, *tostring*, to return a string of important details for identification and the state of the component. This function is overloaded (rewritten to include some of the extra information provided by the child class) for all sub-classes of components to have an easy method for reporting what changes each hour in the simulation and easy debugging of the code logic.

Transitions for all components are calculated using the inverse transform sampling, equation 2.10, where $\beta = 1/\lambda$ if time until the next fault should be calculated, and $\beta = 1/\gamma$ if

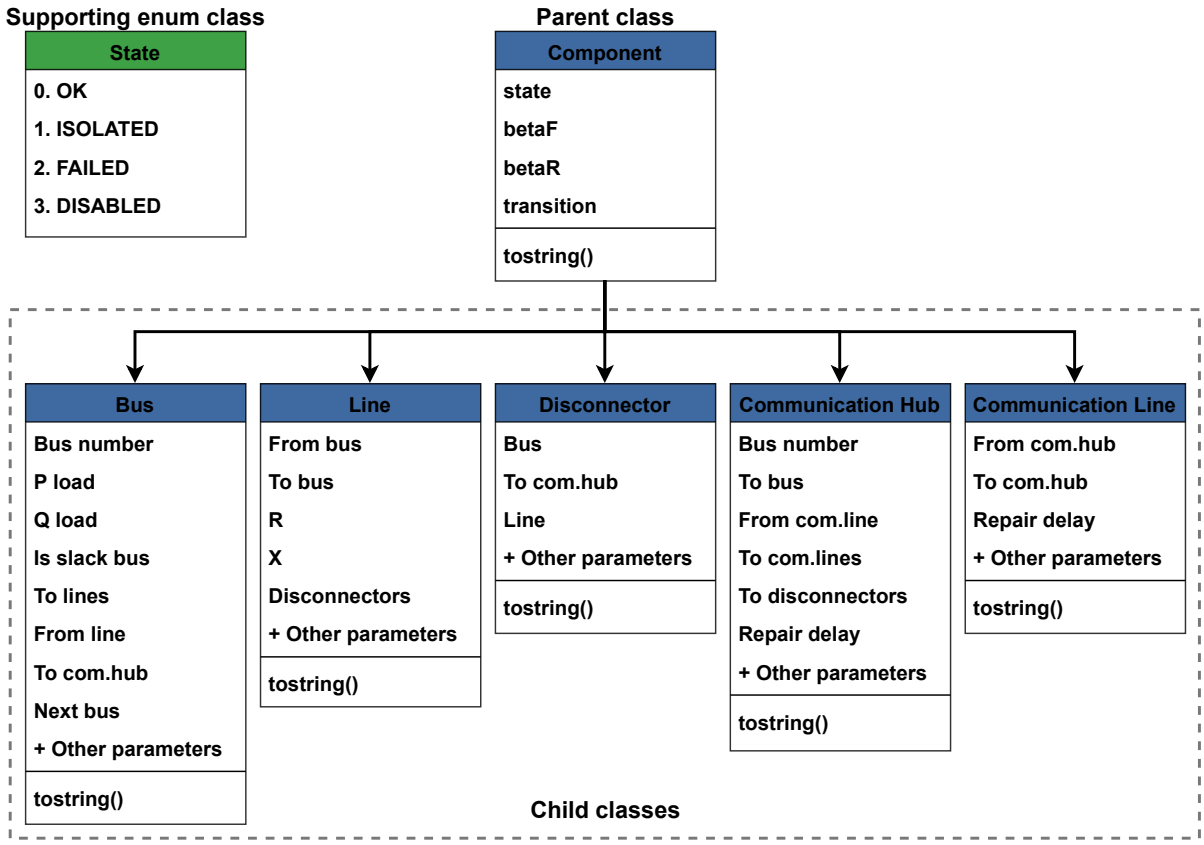

Figure 3.2: Class structure of the MCS tool. A supporting enum class State used by the other classes. The parent class Component with variables and a function. Child classes which inherits Components variables and function.

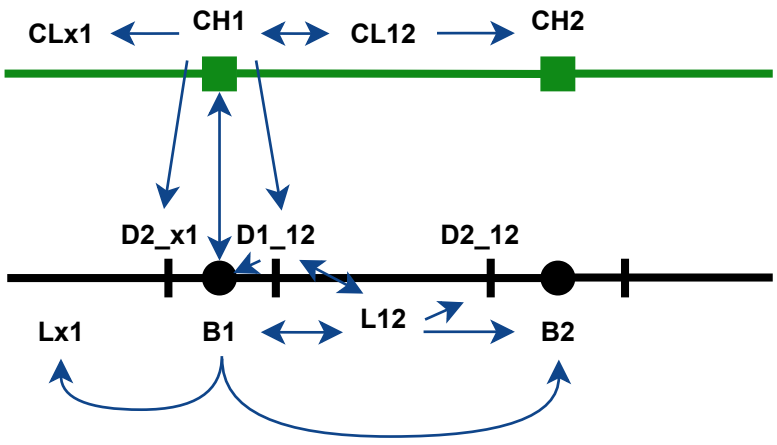

Figure 3.3: Component structure with connections. For one of each component type, the arrows show what components it have variables for. Bus (B), line (L), disconnector (D), communication hub (CH), and communication line (CL).

time until the component is repaired should be calculated. The bus has an additional MTTR variable for when it is connected to the communication system, and the system is functioning, then the MTTR for the bus is reduced with 25%. The reduction is calculated based on the different MTTRs for transformers in the source material [8, 35, 38], $(1 - 6/8) \cdot 100\% = 25\%$, and has a high associated uncertainty.

It is assumed that the communication components cannot be repaired when the power is out, and the power first needs to be repaired. The transition to repair of a communication component is delayed the same amount of time that the power is out at that particular node. This is added as an extra variable on the ComHub-class and the ComLine-class, "Repair delay" in Figure 3.2.

The topology of the system is especially important in a radial operated system, since without any intervention, a fault cutting power upstream of a node will lead to a power outage. The structure data is built in two steps; (1) finding and correcting the direction of lines such that the system is connected with all its nodes (based on similar behaviour in *PyDSAL*) and (2) making a topology list that has an easily iterative structure. Then the topology list is built using the Bus-class as the centre for iteration.

As mentioned before, there is a possibility of running the simulation without any ICTs. The scenario with ICT uses all components available, while the scenario without ICT neither include Disconnectors, Communication hubs, or Communication lines, nor their functions. Removal of Disconnectors means that the remote control switching of disconnectors in the system model is also removed, but not the manual disconnector switching.

3.1.2 Monte Carlo Simulation

The state duration method of MCS is used where the functional flow of the main program is shown in Figure 3.4. In the initialisation phase, the nodes and lines need to be loaded into the program. With the core electrical power components loaded, and if the case should include ICT, communication hubs and lines are connected to and mirroring the existing structure.

Disconnectors are added on each line explicitly if there are ICT parts in the system. Even though it is not explicit in the code, there are still disconnectors in the modelled system when there are no ICT parts. It follows from an assumption that the amount of mechanical faults in the disconnector is negligible compared to faults in the communication parts, thus they do not need to be included for cases without ICT.

Next in the initialisation phase is the generation of failure transitions for each component. The next transition for each component should be sorted throughout the simulation to have easy access to the components that have a transition in each simulated hour. Most components use the time from start of simulation, incremented each new simulated hour, to determine the transition. However, the disconnectors only increment their own failure

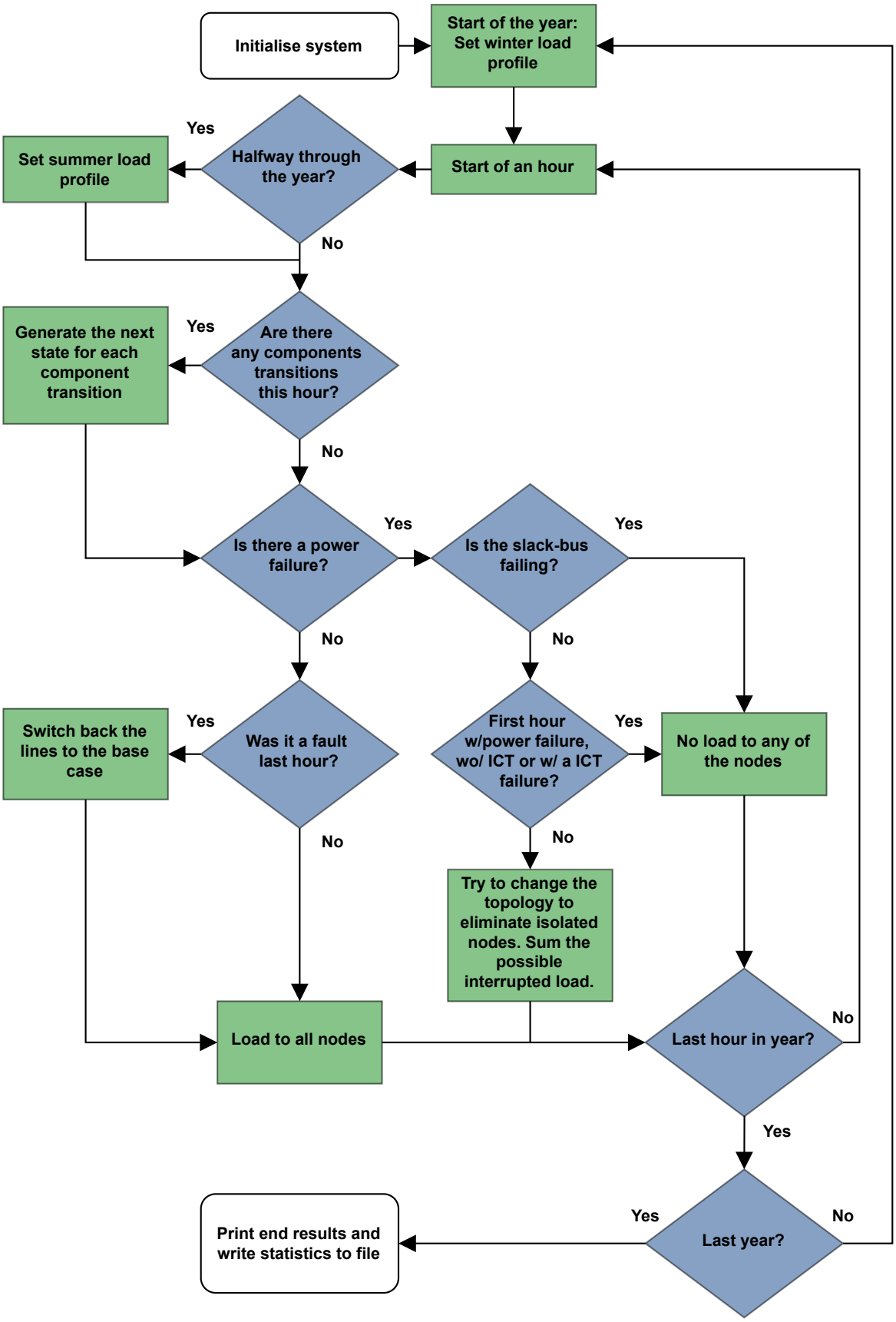

Figure 3.4: Flow of the Monte Carlo simulation

Algorithm 3.1 Check dependencies in the system in the correct order.

```
if there is a line upstream then
  check the line
  if there are ICTs in the network then
    check the communication line upstream.
  end if
  check the lines disconnectors.
end if
check the node.
if there are ICTs in the network then
  check the communication hub.
end if
```

time when they are used. This happens when there is a failure in one of the current carrying components (unless it is the root node) and the communication components are running. The disconnector increments its repair time as all the other components.

To capture the behaviour of the system the following two variables are used; ENS and unavailability for each node. The unavailability is recorded as two numbers for each node, the frequency of faults and the total duration of faults. Also, a third number is included in the code, and it is only used to temporarily indicate that there is an ongoing fault at the node. With these two variables all of the indices in subsection 2.7 can be calculated straight forward.

3.1.3 Isolation of nodes

If there is at least one failure in the system Line or Disconnector, the code should run the isolation procedure. Isolation/islanding rules for the nodes follow

1. For line faults on the radials all downstream nodes from this line are isolated.
2. A failed bus only blocks the local load, and the downstream system is unaffected, except the slack bus where all downstream load is lost.
3. Check connected nodes after a line failure. If an isolated bus is found, check for alternative paths with open disconnectors.

The algorithm for finding and correcting the state of the components follows the topology structure of the system. The structure is easy to iterate by using the nodes, so each component is relative to the current node in the topology. For each node the Algorithm 3.1 is used.

Affected components of a fault in a specific component are explained.

- Power interrupting components, isolate all components downstream.
  - Line: On the current node, the node and the communication hub are isolated.

  - Disconnector: Same as line, but can be isolated by an ICT fault.
  - Root-node: Isolate all components downstream. *All other nodes only isolate the LV-side, leaving the power system in scope unchanged.
- Communication line and hub: ICT components/non-power interrupting components, only isolate ICT components downstream.

3.1.4 Reconfiguration of topology

The following procedure aims to simulate how the system operator would respond to a fault in the system. The procedure for fault handling is explained in section 2.4 for ICT, where the "new" method is used, and without ICT, where the "old" method is used. A fault that enables this algorithm is either on the slack-bus/root node, a line or a disconnector. Either all load is shed due to the sectioning time, or the algorithm tries to switch lines to get power to all nodes. All load is shed if the communication system has at least a fault or if the "old" method is used in the scenario without ICT. The assumption is that the fault is located and switched out in much less time than an hour with remote-controlled disconnectors and breakers.

Algorithm 3.2 is used to change the topology of the system when a node or several nodes are isolated from the root nodes. It uses a naive method to determine which line to connect, the first line in the disabled-lines-list where one node connected is isolated from the root node and where one is functioning. Between each line switch, the network is updated to ensure that only one backup line is used per fault area and to ensure radial operation. The procedure is repeated as many times as necessary or until no lines that satisfy the criteria exist.

When all faults in the system are fixed the topology is changed back to the base topology, as seen in Algorithm 3.3. Importantly, the procedure is only run when all faults in the system are fixed. There is a related alternative method to solve the same problem, try to switch back the lines that one fault caused after that particular fault is cleared. Such a method could be more in line with the real operation of the power system for longer faults in different parts of the system. This has not been implemented in this thesis, as it adds complexity and gives no benefits to the indices in question. It could, however, in a model that focuses on it, give lower power losses in the system using all lines more actively.

Along the simulation it is written to file when a component fails or is repaired and when a line is connected or disconnected. The simulation continues until the set years of simulation are reached. As the AENS is the slowest index to converge [21], this could also be used as a method to determine the end of the simulation.

Algorithm 3.2 This algorithm tries to find possible lines to connect such that fewer nodes are isolated. It also disconnects the correct line such that the system always is operated in radial.

```
for all DISABLED lines do
  if the line is not FAILED and (one of the end-nodes are OK and the other end node
  is ISOLATED) then
    for all connected lines on the ISOLATED node do
      while there are more lines further out do
        if the line is FAILED or disconnector is FAILED then
          Disconnect the FAILED line with its disconnectors
          Connect the DISABLED line with its disconnectors
          Reconfigure the topology structure to reflect the lines now connected
          Rerun the algorithm to check for (still) ISOLATED nodes
          return
        end if
      end while
    end for
  end if
end for
```

Algorithm 3.3 Clean-up and switch back of lines after all faults are cleared.

```
for lines in switched lines do
  Enable the disconnected line with its disconnectors
  Disable the previously enabled line with its disconnectors
end for
Set all the lines from- and to-nodes to base topology
```

3.1.5 Load profile

The load profile is generated to have an individual winter high load and summer low load at each load. In a cold climate, as in the Nordic countries, this is a typical seasonal variation of the electric power consumption as many buildings are heated with electricity. The high load $load_H$ is chosen to be between 0.5 and 1.1 pu, as this is a typical high loading for distribution transformers. And the low load $load_L$ is calculated using

$$load_H = x_1 \cdot (1.1 - 0.5) + 0.5 \tag{3.1}$$

$$load_L = load_H(x_2 \cdot 0.2 + 0.4) \tag{3.2}$$

where x is a random number in the range $[0, 1]$. It is calculated using this method to have a correspondence between the winter load and the summer load at the nodes, while still having differences between the nodes. Reactive power consumption is calculated as 70% of the active power consumption. This value is close to the relationship between active and reactive power originally found in the *IEEE 69-bus* system (70.9%). Such a high power factor ($P/(P+Q)$ is not the norm in many systems, and are often compensated for with

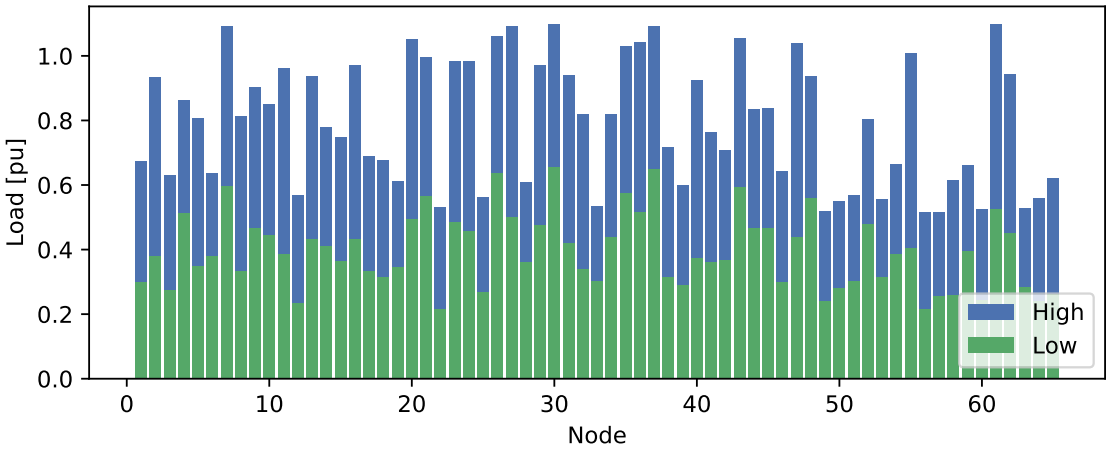

Figure 3.5: High (blue) and low (green) loads for all nodes.

shunt capacitor banks, but results depending on Q is not discussed in this thesis. The load for each bus is visualised in Figure 3.5 and the numerical values are found in the appendix in Table B.1.

3.1.6 Number generator

The Mersenne Twister random number generator with 53-bit precision floats [39] is implemented to generate random numbers. In this generator there is a period of $2^{19937} - 1$ and it has been extensively tested with statistical tests for randomness, with high uniformity and minimal correlation between the numbers generated [40]. Thus it has all the important characteristics of a good pseudo-random number generator. As for all mathematical pseudo-random number generators, it is deterministic given a starting seed for the generator, which is appropriate to get reproducible results. Another important factor is the fast execution time of the generation of uniform numbers on the interval $[0, 1]$, a consequence of the generator being mainly written in the C programming language.

3.1.7 Reduction of computation time

Possible methods for reduction of the computation time.

- The fact that the Python tool is developed from the ground up and only for this purpose, with only a few superfluous calculations and no redundant options, gives an inherent speed increase.
- Manually assigning threads made the code more complex and gave no benefit to the execution time beyond the automatic multi-threading by Python.
- With the most popular power flow solvers, like the Newton-Raphson and FBS methods, start-values for voltage and angle are needed. In contingency analysis and simulation over a period of time one typically either uses a *flat start* or a *warm start*.

With a *flat start*, all voltages are set to nominal, 1.0 pu, and all voltage angles are set to 0 rad. However, a *warm start* is just using values found as a result from the previous power flow as the start values. Here a *warm start* is used when a new power flow calculation is needed.

- It is possible to select the number of iterations for the FBS-method; more iterations give a more accurate answer but longer computation time. A number of iterations where the results are satisfying is chosen.
- When the load is changing, a higher memory usage could be traded for lower computation time by pre-calculating and saving the results from each load profile.

Below follows the optimisations which are implemented specifically for the Python programming language:

- Usage of well established and optimised libraries (*pandas* and *numpy*) for data storage.
- Limit the use of functions that are repeated (as a function call use a small amount of extra time, without sacrificing much readability, this is a balance).
- Using functions written in the C programming language from the standard Python library instead of extended Python-functions.
- Calculate indices in less demanding ways (storing the sums of lists and add to that sum instead of calculating the whole list each time).
- Keep lists of switched lines and faulty components instead of searching through all components to find the correct ones.
- The function for finding isolated nodes is divided in two, one for the scenario with ICT and one for the scenario without ICT. The function is frequently used and the reduction of if-statements increase the run time.

3.2 Test system

The test system used to verify the functionality and further to analyse the general behaviour of the interdependencies between a power and an ICT system is the *IEEE 69-bus*. Specification of the buses/nodes in the system is found in Table B.1 and for the lines Table B.2 [41]. Figure 3.6 shows the topology of the power system. The system originally has buses 1–4 in very close proximity (estimated to be within a few meters, compared to other lines in the system of a few km) and without any load. Therefore, buses 1–4 where merged into bus 1 instead and the lines associated merged into line 1–2. All other buses have changed their numbering accordingly. The Python tool imports the system description (in per unit) from an xlsx-file of the format:

- For each bus/node: Bus number, High active power P (pu), High reactive power

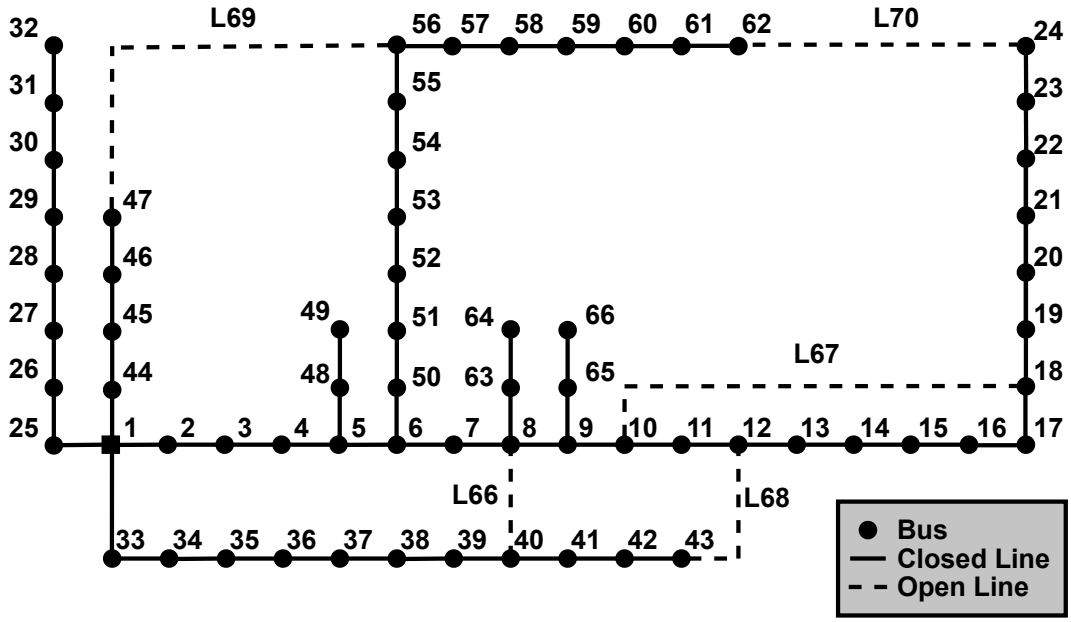

Figure 3.6: Single line diagram of the IEEE 69 bus test power system.

(pu), Low active power P (pu), Low reactive power (pu)

- For each line: From bus, To bus, Resistance (pu), Reactance (pu), betaF, and state (normally open or normally closed)

Although the system has three phases, it is assumed to have a balanced load and the system is therefore modelled as a single phase system. The *per unit* values are calculated using a $U_{ref} = 12.66\,\text{kV}$ and $S_{ref} = 100\,\text{kVA}$, giving an impedance reference of

$$Z_{ref} = \frac{U_{ref}^2}{S_{ref}} = \frac{(12.66 \cdot 10^3)^2}{100 \cdot 10^3} = 1602.756\,\Omega \tag{3.3}$$

The MTTF for the lines is calculated from the line‘s resistance and assumed area of the conductor A.

$$\begin{aligned} mttf_{line} &= l(\text{km}) \cdot 0.07(\text{failures/km}) \cdot (\text{per year}) \\ &= \frac{R(\Omega) \cdot A(\text{mm}^2) \cdot 0.00007(\text{failures/km})}{\rho(\Omega/\text{mm}^2)} \cdot (\text{per year}) \end{aligned} \tag{3.4}$$

Table 3.1 presents the MTTF and MTTR used for the individual component. The only time MTTF and MTTR are used is when an inverse transform is calculated using Equation 2.10. The equation uses the inverse of the MTTF or MTTR value, thus the values are stored as β to save the inverse computation for each inverse transform calculation.

It is assumed that there is 1 customer per node in the system investigated for simplicity when calculating the aggregated indices. A typical LV transformer have 1–150 customers

Table 3.1: MTTF and MTTR for all types of components used in the MCS. Based on [8,35,38]. *$8 \cdot 0.75 = 6$ with a functioning communication hub.

Component	MTTF		MTTR	
Bus	7.295	(hours per 100 per year)	8*	(h)
Line	7	(hours per 100 km per year)	6	(h)
Disconnector	0.03	(hours per 100 per year)	2	(h)
Com. hub	0.2	(hours per year)	2.5	(h)
Com. line	0.068	(hours per year)	3	(h)

connected. This could be easily implemented, but doing so would hide some of the fundamental differences between the placement of nodes and backup lines, making it harder to analyse. In addition, the transformers in this thesis only have two states affecting power, full available power transfer or no available power transfer. Thus they cannot only deliver power to parts of the customers at one instant, leaving the sectioning of the number of customers per node unnecessary. In an analysis of a system to determine where upgrades are needed and are economically suitable, it could be necessary to differentiate the number of customers per node.

3.3 Case definitions

The test system is run for 3 different cases in order to investigate the impact of changes in input parameters or the elimination of backup lines. For all the cases the test system is run with ICT and without ICT, where the ICT components are Disconnectors, Communication hubs, and Communication lines. The case definitions follow:

0. Base case: The system is simulated with backup lines for one scenario with ICT and one scenario without ICT.
1. Unchanged topology: The system is simulated without backup lines (lines L66–L70) for one scenario with ICT and one scenario without ICT.
2. Factorial experiment cases: One case is run for each factor change;
   - an increase ($\times 2$) or a decrease($/2$),
   - of MTTF (failure rate) or MTTR (repair time),
   - for each component type.

   All cases are summarised in Table 3.2. A failure rate or repair time change in disconnectors, communication hubs, and communication lines is only possible in the scenario with ICT. The cases are enumerated to reflect how changes in failure rate and repair time on the system components impacts the system reliability. This gives 28 different sub-cases.

Table 3.2: All sub-cases run for Case 2. Each cell on the format "B:incF" is one sub-case that modifies one component's MTTF (F) or MTTR (R). Some sub-cases are run with ICT (yes) and some are run without ICT (no).

Component	Modified parameter	ICT case	Increase (x2)	Decrease (/2)
Bus	MTTF	yes	B:incF	B:decF
		no	B:incF	B:decF
	MTTR	yes	B:incR	B:decR
		no	B:incR	B:decR
Line	MTTF	yes	L:incF	L:decF
		no	L:incF	L:decF
	MTTR	yes	L:incR	L:decR
		no	L:incR	L:decR
Disconnector	MTTF	yes	D:incF	D:decF
	MTTR	yes	D:incR	D:decR
Com. Hub	MTTF	yes	CH:incF	CH:decF
	MTTR	yes	CH:incR	CH:decR
Com. Line	MTTF	yes	CL:incF	CL:decF
	MTTR	yes	CL:incR	CL:decR

4 Case results, comparison and discussion

In this part of the thesis, the test system is simulated with each of the cases described in the previous chapter, and the results are presented and discussed for each case. Only a few important figures and tables with results are included in this chapter, while the rest of the results are presented in appendix C. All energy indices are calculated in per unit (pu). The influence of starting seed, together with the different cases "Base case", "Unchanged topology", and "Factorial experiment", will present different aspects, opportunities, and disadvantages with this specific implementation of interdependencies between the power system and the ICT.

4.1 The influence of starting seed

Box plot is a great visualisation tool to show the variation of data. The plot consists of five elements; a solid line representing the median of the data, a dashed line representing the mean of the data, a box representing the middle 50% of the data (Interquartile-range (IQR)), whiskers representing the IQR extended range, and outlier circles representing data not in the IQR extended range, as shown in Figure 4.1. The whiskers are calculated using $[q1 - 1.5 \cdot (q3 - q1), q3 + 1.5 \cdot (q3 - q1)]$, where the first quartile $q1$ and the third quartile $q3$ are the threshold in which 25% and 75% of the data points are below, respectively. The IQR is $IQR = q3 - q1$.

The test system was simulated with Case 0, the base case, for 10000 years with ICT components enabled using three different seeds. Then the AENS index was calculated for each year. Further the index was plotted as a box plot for the first 100 years, the first 1000 years, and all 10000 years, presented in Figure 4.2. The outliers (circles) are not essential, as only the likely and average behaviour, the mean value and the IQR extended range of the system are analysed in this thesis. At 100 years of simulation, there is a noticeable difference between the different seeds. At so few iterations, the MCS has not managed to converge to a reasonable level. The seed 67505 has two years with abnormally high AENS in the first 100 years, but the other seeds have not the same high values of AENS. As more years are simulated, the irregular years are averaged out by many "normal" years, leading to a consistent average regardless of the seed used to start the simulation. Still using 1000 years of simulation, the difference for the IQR extended range is noticeable, but at 10000

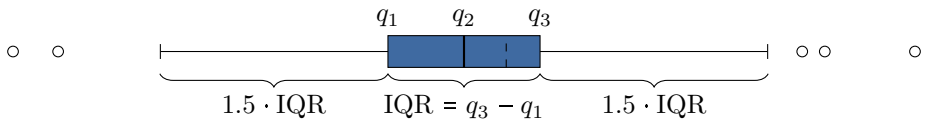

Figure 4.1: Box plot explanation with the mean, the median, quartiles, whiskers, and outliers. Inspired by [34].

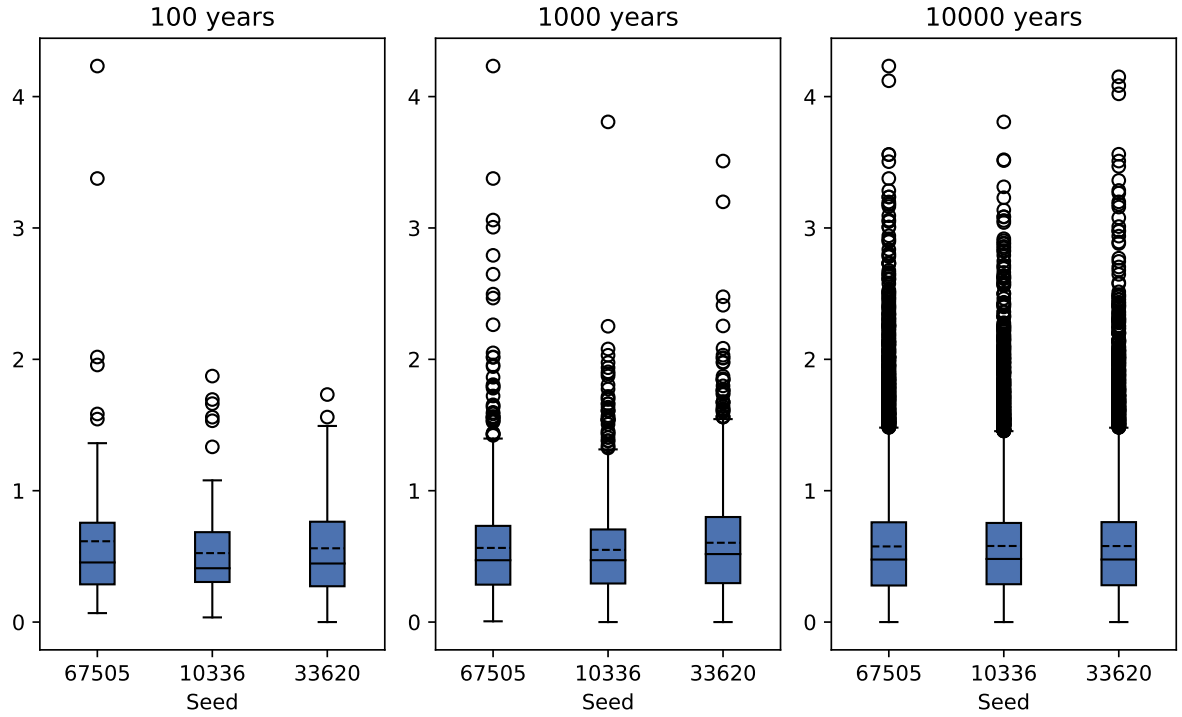

Figure 4.2: Comparison of boxplots of the AENS index using different starting seeds and various simulation durations. The system is run with ICT components. Inside each box there are two lines; the continuous line is the median of the data, and the dashed line is the mean of the data.

years the IQR extended range and mean are very close to each other. If investigating the system's vulnerability through analysis of chosen hours with lots of interrupted power, the assortment can be improved by increasing the number of simulation years.

Results presented in Table 4.1 indicate that the simulation method is accurate, as the mean with two different seeds for SAIFI give $\overline{X} = 0.170289$ and $\overline{X} = 0.175753$. The α value was calculated by

$$\alpha_{SAIFI,ICT,67505} = \frac{\sigma_X}{\sqrt{N} \cdot \overline{X}} = \frac{0.201804}{\sqrt{10000} \cdot 0.170289} = 0.011851 \tag{4.1}$$

The complete table for all indices is presented in the appendix in Table C.1. It shows the evidence of the similarity of all the indices for a 10000 year simulation. Not all indices are within the estimated values plus or minus the α value between all seeds. The indices that are outside the α-range are for the scenario with ICT; CAIDI, ACCI, and for the scenario without ICT; SAIFI, SAIDI, CAIFI, AENS, and ACCI. Still the differences are small and the standard deviation σ_X is much larger than the differences of the mean. The indices not overlapping could be caused by a biased pseudo-random number generator or that the α value is not a good measure for the convergance in this MCS. Despite that, the

Table 4.1: The SAIFI and AENS indices mean $\overline{X}$, standard deviation σ_X and the convergence parameter α for different starting seeds. 10000 years of simulation.

Seed	ICT			No ICT		
	$\overline{X}$	σ_X	α	$\overline{X}$	σ_X	α
SAIFI						
67505	0.170289	0.201804	0.011851	6.188600	2.487509	0.004020
10336	0.175753	0.212603	0.012097	6.218100	2.466566	0.003967
33620	0.173488	0.207920	0.011985	6.214700	2.489423	0.004006
AENS						
67505	0.575678	0.424585	0.007375	4.210712	1.682630	0.003996
10336	0.579127	0.419085	0.007236	4.226545	1.666662	0.003943
33620	0.578578	0.423827	0.007325	4.230165	1.684620	0.003982

difference between the scenario with ICT and without ICT is much greater than within a σ_X of the mean $\overline{X}$ (except for the ACCI index, which will be discussed later). If the results later show that an index is relatively similar between different cases, one cannot be certain if there are any real difference between them. Assuming that the converging properties of the system does not change significantly with the different cases, it is thus sufficient to only use a single starting seed for further comparisons of cases in this thesis when the simulation is run for 10000 years.

4.2 Base case — Case 0

This section presents and analyse Case 0, as previously defined in section 3.3. Since the focus of this thesis is to examine the power system dependency on the different ICT parts, two cases are compared within this case; one with ICT parts and one without.

The AENS index (or its unscaled equivalent, ENS) usually is the slowest index to converge [21]. Figure 4.3 shows that both with and without ICT, the AENS converges relatively quickly toward the mean value. Stopping the MCS after 1000 years gives a higher uncertainty than after 10000 years since the MCS have not fully converged yet. One option is to use 5000 years of simulation. Doing so will cut the simulation time in half while still achieving almost the same accuracy as 10000 years of simulation. However, the differences between the two cases are much more significant than the uncertainty in the index itself for most indices. For cases where the differences between indices are smaller, other parameters and model choices impact the indices significantly more than the index uncertainty.

The seasonal changes in power consumption give only small variations between the seasons, as seen in Figure C.2 in the appendix, and the sectioning of the results into seasons does

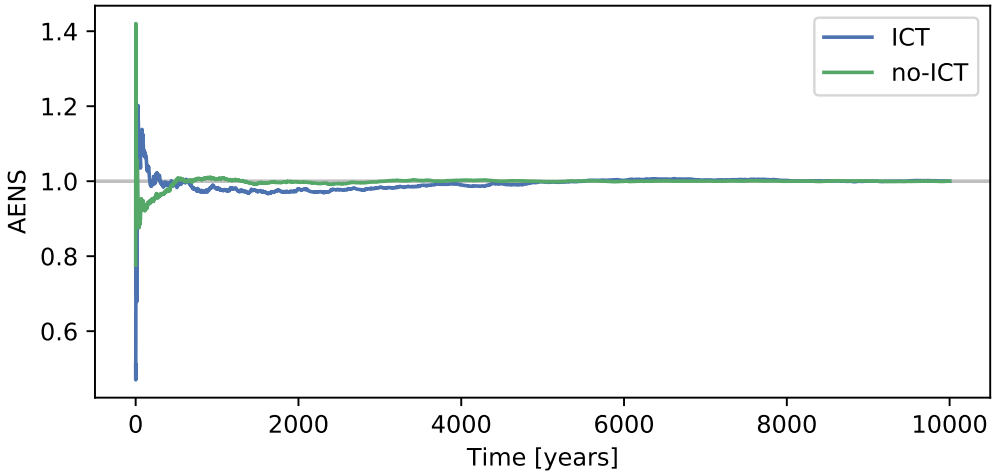

Figure 4.3: AENS index divided by the mean of the index. Simulation for 10000 years.

not show anything of particular interest. Therefore all results will be presented on a yearly basis. A change in the probability of failure of an overhead line for a season could move these further apart. External fault triggers are more typical in the distribution system and many of the external triggers have seasonal variations [35].

Figure 4.4 presents separate histograms for each of the indices in focus, and the following paragraphs include the corresponding discussions. The ASAI index is not shown because of the linear relationship with the SAIFI index, see equation 2.32. The distributions for all indices, except ACCI, are strikingly different between the scenario with and without ICT components.

When comparing the SAIFI and the CAIFI indices, for the scenario without ICT ("no-ICT" in Figure 4.4a and 4.4c respectively), it is evident that they are quite similar. This is because the indices are based on the total amount of faults in the system on a per node basis, where the only difference is that SAIFI is divided by all customers and CAIFI is only divided by the customers that experienced faults that year. However, since the system is modelled to shed the load for at least one hour for many faults in the scenario without ICT, all or none of the customers experience faults most years. The same argumentation and conclusions can be drawn when comparing the AENS and the ACCI (Figure 4.4e and 4.4f, respectively).

Comparing the SAIDI and AENS indices, both with and without ICT parts, they correlate well. SAIDI measures the average outage durability in hours and AENS measures much the same, but in energy. The similarity comes from the modelling choice of having the same probability of component failures for both the high and low load scenarios and thus for all seasons. In addition, using the load-oriented indices, it is important to consider the modelling choice having a random load distribution with a low variance. A higher variance could have decreased the similarities to the customer-oriented indices. The same

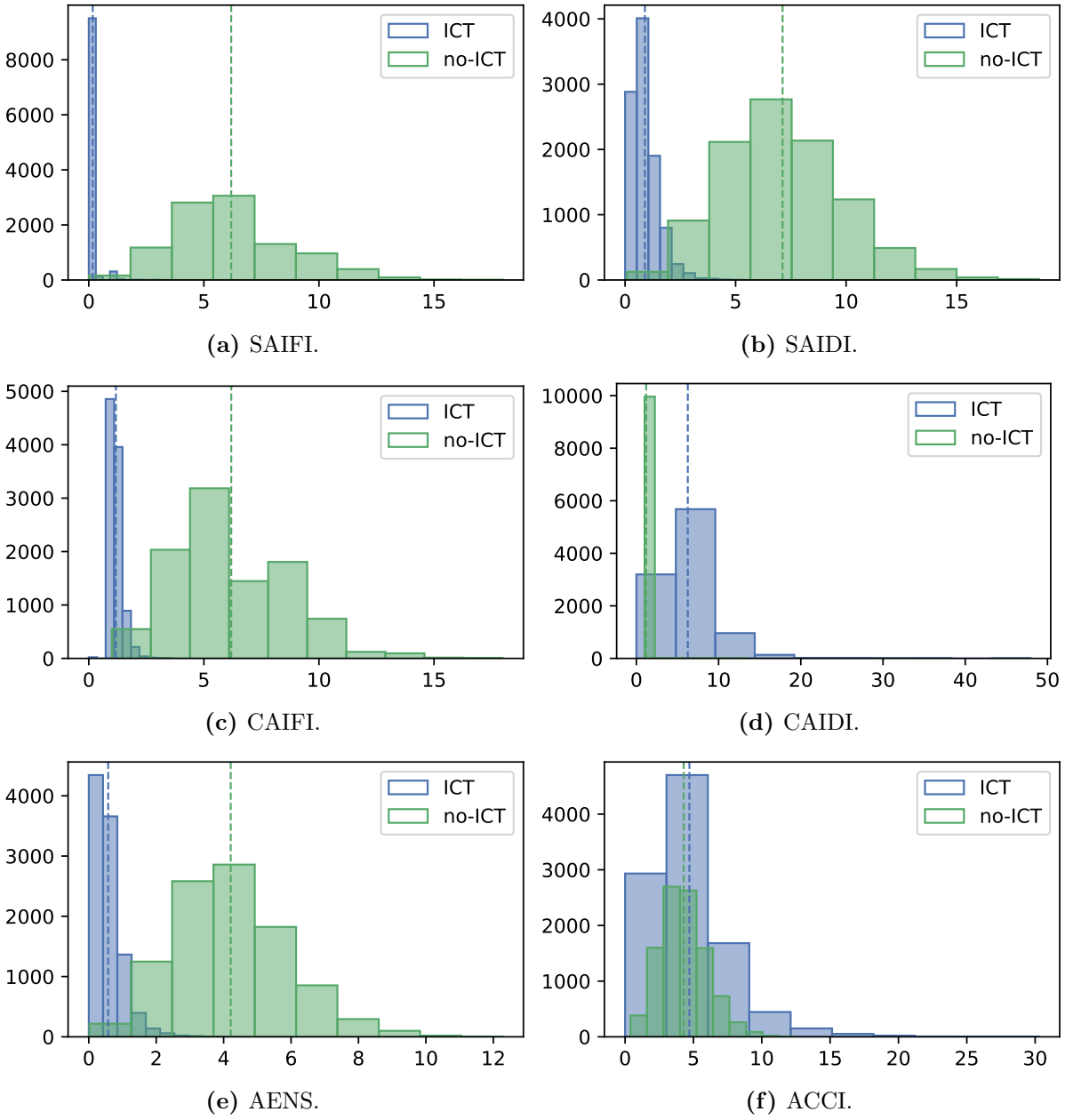

(a) SAIFI.

(b) SAIDI.

(c) CAIFI.

(d) CAIDI.

(e) AENS.

(f) ACCI.

Figure 4.4: Histogram of all indices for Case 0 (see subsection 2.7 for explanation of the indices). The y-axis is the count of years inside the width of the bar. The dashed lines are the index‘s mean per case. Simulation for 10000 years.

argumentation can be used when comparing the CAIDI and the ACCI (Figure 4.4d and 4.4f, respectively), but with a lower correlation. The CAIDI and the ACCI index both have a few years that experience a much higher value than the average. This limits the visual distribution property of the histograms.

In the SAIDI histogram, Figure 4.4b, the mean value, i.e. the mean fault duration, is around 5–7 hours for the scenario without ICT. These values indicate that the typical faults in the system causing interruptions are faults on a line and at a node, as lines have a $ttr = 6\,\text{h}$ and nodes have a $ttr = 8\,\text{h}$ (or $6\,\text{h}$). This will give a mean fault duration of 6–8 hours. However, when the faults are combined with the sectioning time, which is set to be one hour, the mean fault duration will decrease. It is therefore plausible that the mean is around 5–7 hours with this explanation.

Looking at the SAIFI, SAIDI, CAIFI, and AENS indices, the ICT scenario index value (blue) is clearly much lower than the scenario without ICT (green). This is the desired behaviour when introducing ICT parts to the system, where there are less interruptions and they last for a shorter time period, resulting in higher overall reliability. Although systems with ICT perform better in comparison to those without, both systems have relatively high reliability compared to distribution systems without backup lines (a case further explored later in this thesis). This leads to the SAIDI index, which indeed, shows that the ICT scenario has higher availability than the scenario without.

The opposite trend is observed for the CAIDI index, where the scenario with ICT has a histogram with a higher mean than the scenario without. This is because only interruptions of at least one hour are counted as an interruption at a node, and for the scenario without ICT this happens for all line and disconnector faults. From the simulation output it is found that there were most line faults, with 28.5% less node faults and 95.7% less disconnector faults in the system annually compared to line faults. For the scenario with ICT, it is assumed that the sectioning-time is much less than an hour, as compared to the scenario without ICT, thus not all nodes experience an “interruption”. The interruptions remaining after the sectioning time are often longer than one hour. Figure 4.5 illustrates some of the same tendencies as the CAIDI index in Figure 4.4d. The difference between the two figures is that Figure 4.5 is divided into the Average failure duration r for each individual node. For the scenario without ICT, represented by the green bars, nodes with higher values correspond to nodes that have no backup line connection, with a higher value longer out on the radials and away from the root node. In the scenario with ICT, represented by the blue bars, the same nodes have higher than average r values, but here other nodes also have sporadically high r. It must be noted that the index value of r, for each individual node, does not necessarily converge as well as the same index for the whole system. The system experiences faults much more frequently than just looking at an individual node.

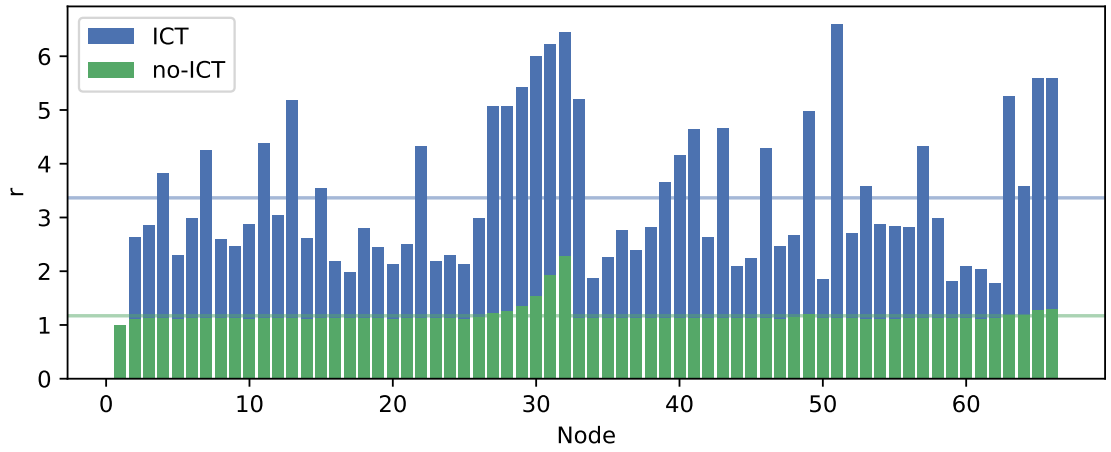

Figure 4.5: Average failure duration r bar plot. The horizontal lines are the mean of the value of the nodes. The bars are not stacked. Simulation for 10000 years.

In conclusion, the CAIDI index in these two cases *could* give an excellent view of the duration of the faults experienced by the customers. However, for the scenario without ICT, short faults overwhelm the longer failings to such a degree that the longer faults become invisible. This hides the often greater consequence of longer faults, as mentioned in section 2.4. One should, in such cases, combine the CAIDI index with the cost function based on the interruption length to better represent the impact these interruptions have on society.

For the ACCI index, i.e. the average energy interrupted per interrupted customer that year, the mean of the two cases are somewhat similar, as seen in 4.4f. Although the means are almost equal, the standard deviations σ_X are quite different; $\sigma_{X,ICT} = 2.84$ and $\sigma_{X,no-ICT} = 1.70$. One reason could be that the scenario without ICT, for many faults, has a sectioning time that interrupts power in the whole system, affecting all customers. The scenario with ICT has a much lower frequency of times where all customers are interrupted, since the sectioning time is neglected for this case. The total energy interrupted is therefore divided on fewer customers for more years, leading to higher variation in the ACCI index.

4.3 Unchanged topology — Case 1

In this case, Case 1, there is no change in topology, i.e. no backup lines are used, as described in section 3.3. The advantage of lower frequency of interruptions when using ICT is expected to be less pronounced, as customers downstream of a fault now have no alternative path of power connection that ensured uninterrupted power as in Case 0.

The convergence is fast for all indices. In the appendix, Table C.2 present the values for all indices for this case and histogram of all indices are presented in Figure C.4. Figure 4.6 shows the changes compared to Case 0, base case, presented in the previous section.

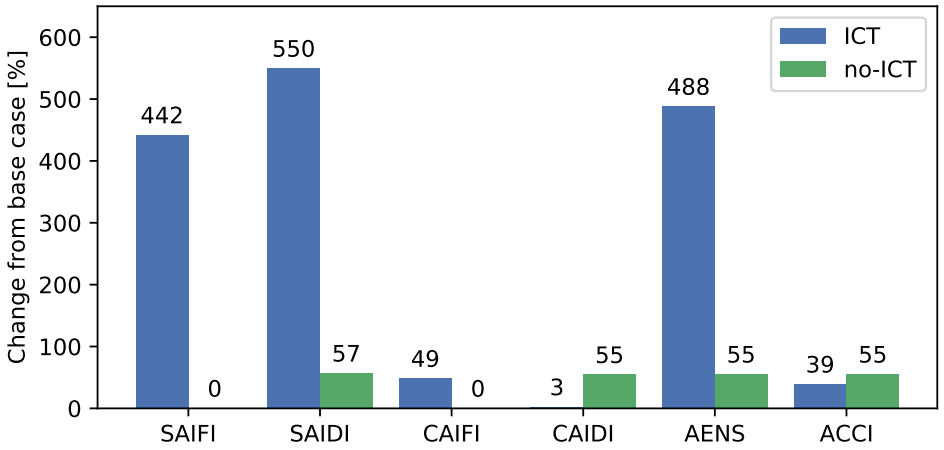

(a) Change in %.

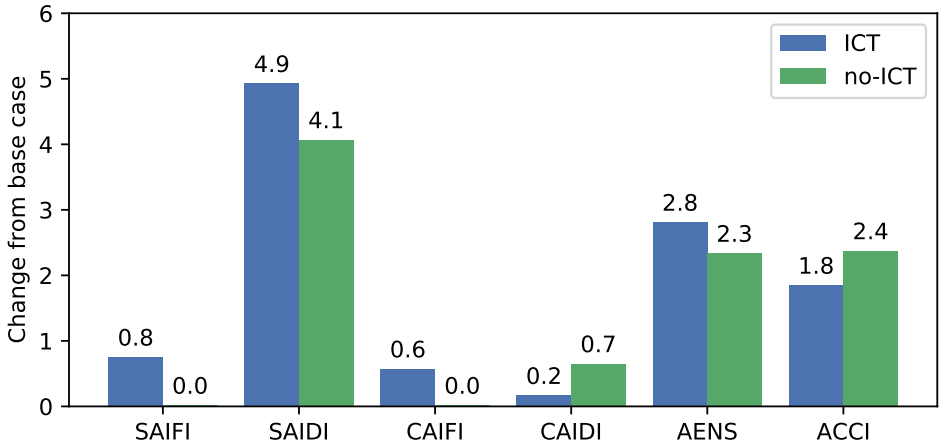

(b) Numerical change.

Figure 4.6: Change from Case 0 to Case 1 for all indices. Simulation for 10000 years.

A general trend for almost all indices in Figure 4.6 is that the values worsen to some degree compared to Case 0. The exception is that the SAIFI and the CAIFI indices without ICT have not changed. This is expected, as this part of the MCS is indirectly measured, and the frequency of failures has not changed. In addition, the CAIDI index shows only small changes for the scenario with ICT, as the interruption duration on all nodes downstream is the same when backup lines are not used. When backup lines are used, the ICT parts manage to keep the power on the nodes downstream uninterrupted. Thus the average interruption time for customers that experience a fault that year, which CAIDI represents, is mostly unchanged. The small change could originate from another fault happening in the system before the first fault is repaired, which affects some of the same nodes. Two failures close in time, affecting the same customer(s), are more likely to happen when the backup lines cannot be used since after the second fault, a backup line could again redirect the flow of power to customers.

For the indices that do change significantly in the scenario without ICT in Figure 4.6a,

they all have a mean change of 55–57%; thus, all those indices are strongly correlated for the change in system operation as presented in Case 1. This is expected as SAIDI and CAIDI measure interruptions in hours and AENS measures interruptions in energy (kWh). That is not the case for the scenario with ICT. With ICT the change of indices is much more pronounced, and for some indices the change is over 400% larger compared to Case 0. An explanation could be that Case 0 with ICT had such low indices that the percentage of change became high for SAIFI, SAIDI, and AENS, even for a moderate change.

Moving away from percentages and over to Figure 4.6b, which presents the absolute changes for each index. The absolute changes in the indices are much more equal between the two cases, with and without ICT, in comparison to the percentage change in Figure 4.6a. The similarity could indicate that the impact of having backup lines versus not having backup lines in the system is mainly independent of the ICT parts for the duration and energy indices.

Table 4.2 presents a 99.9% confidence interval for both Case 0 and Case 1, calculated using equation 2.21. One can be 99.9% certain that the true value lies within these intervals. Comparing the confidence intervals of the scenario without ICT in the Case 0 (top right) with the ICT scenario in Case 1 (bottom left), reveals that there are no indices with overlapping confidence intervals. This may indicate that the reliability in the system increases more with the introduction of ICT parts with quick sectioning time than having backup lines that can be connected and restore some of the supply after the section time in the power system.

The SAIDI index has confidence intervals that are close for the compared cases (top right versus bottom left), where upper limit for line change without ICT is 7.04 hours per customer year and lower limit for no line change with ICT is 5.96 hours per customer year. These values are coloured in blue in Table 4.2. A similar observation can be made for the AENS index, as the SAIDI index measures the interruption duration for each customer, the AENS index multiplies by the customer load, giving an energy value. The AENS index‘s upper limit for line change with ICT is 3.47 hours per customer year and lower limit for no line change without ICT is 4.16 hours per customer year.

Comparing the confidence intervals between the two cases with ICT, all the changes are significant, except for CAIDI where the confidence intervals overlap. When doing the same comparison for the scenario without ICT, it is evident that the confidence intervals of SAIFI and CAIFI overlap, and the changes are therefor not significant. In Table 4.2, all these values are coloured in green.The confidence intervals of the other indices without ICT do not overlap, indicating considerable changes of the indices. These results are as expected, since Figure 4.6a shows a 55–57% change for the SAIDI, CAIDI, AENS, and ACCI indices.

Figure 4.7 presents the unavailability U for each node in the system. In Case 0, all nodes

Table 4.2: 99.9% confidence interval for all indices. 10000 years of simulation.

Index	ICT		No ICT	
	Lower	Upper	Lower	Upper
	Case 0 — Base case			
SAIFI	0.1637	0.1769	6.1068	6.2704
SAIDI	0.8767	0.9156	7.0372	7.2139
CAIFI	1.1710	1.1873	6.1092	6.2725
CAIDI	6.1573	6.3533	1.1779	1.2038
AENS	0.5617	0.5896	4.1554	4.2661
ACCI	4.6107	4.7975	4.2289	4.3409
	Case 1 — Unchanged topology			
SAIFI	0.9066	0.9400	6.1253	6.2883
SAIDI	5.6873	5.9607	11.0177	11.3738
CAIFI	1.7338	1.7701	6.1277	6.2904
CAIDI	6.3242	6.5214	1.8185	1.8670
AENS	3.3048	3.4694	6.4390	6.6561
ACCI	6.4268	6.6812	6.5510	6.7709

with an alternative path for the power have more or less the same U. As seen in the figure of the power system, Figure 3.6, the nodes 25–32 have no backup line, and thus have a much lower absorptive capacity compared to the other nodes. This is easily seen in Figure 4.7a, where these nodes have higher values than the other nodes, both for the cases with and without ICT. On the other hand, looking at Case 1 in Figure 4.7b, it reveals that the shorter path to the root node for nodes 25–32 give them a lower U than some of the other nodes, especially on the long radial 2–24, which now includes the nodes with the highest U. As expected, without the use of backup lines, the unavailability increases with a high correspondence to the number of nodes to the root node.

From Figure 4.7 it is clear that the sectioning time has some impact on the unavailability U. In the resilience perspective, the sectioning time and topology change are part of the restorative capacity giving a shorter time to recovery. Change of topology is also, in a system with ICT, a resistant capacity, as the interruption is so short that it does not (in this thesis) count as an interruption. This can be seen, in Figure 4.7b, as the gap between the scenario with ICT and the scenario without ICT, based on the unavailability value. At nodes with relatively low U, the contribution of the sectioning time gives a much higher U compared to the scenario without ICT, causing a big gap between the two cases. However, at a relatively high U the contribution of the sectioning time is less of the total, leaving a smaller gap.

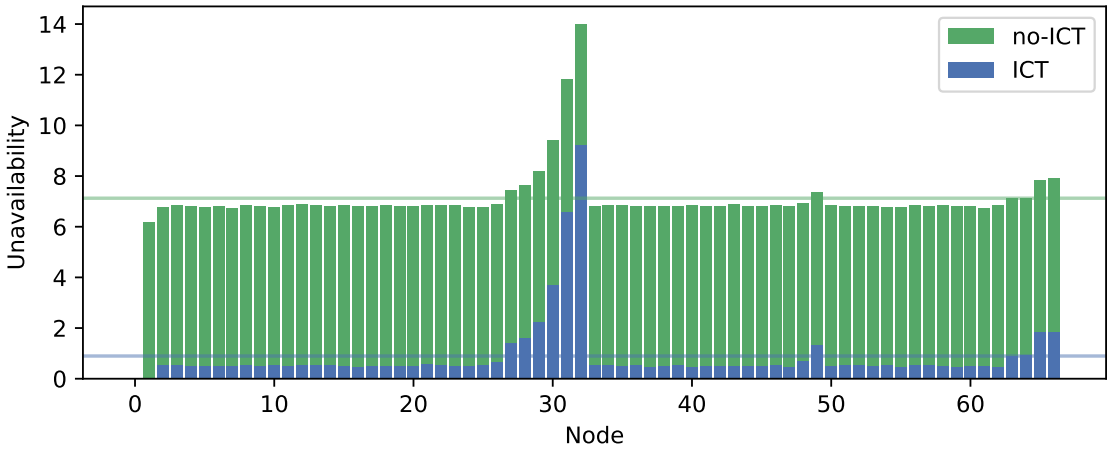

(a) Case 0 — base case.

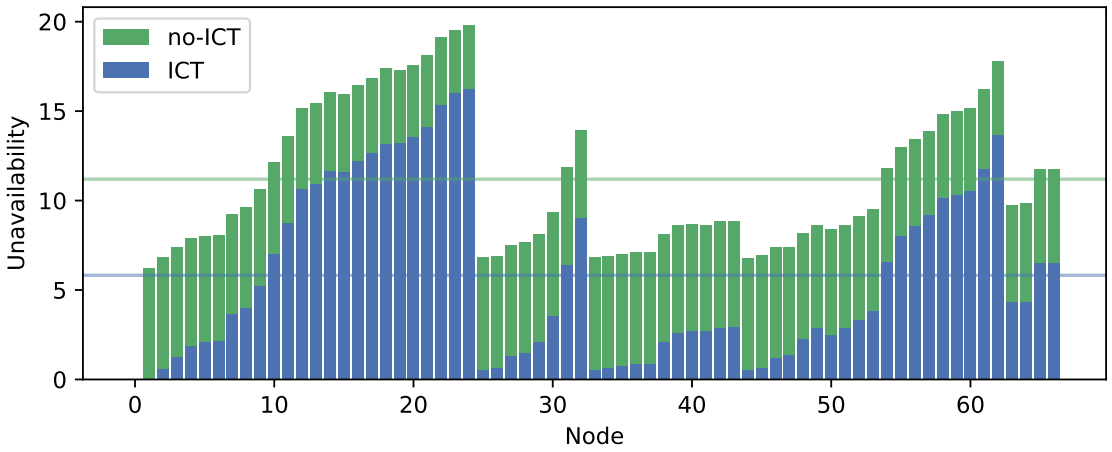

(b) Case 1 — unchanged topology.

Figure 4.7: Unavailability U for all nodes for both Case 0 and Case 1. The bars are not stacked. The horizontal lines are the mean of the value of the nodes. Simulation for 10000 years.

The effect is similar for the average failure duration r, presented in Figure 4.8. The nodes furthest from the root node have longer r relative to the nodes close to the root node in the scenario with ICT compared to the scenario without ICT. The nodes without backup lines, nodes 25–32, have the same r and U for both cases, as one should expect. The median r number for the scenario with ICT is close to 6 hours per fault, which fits well with the line-MTTF of 6 hours.

As explained for Figure 4.5 and in section 3.3, when just looking at a specific node one cannot assume the same level of convergence, and this is probably the cause of the one spike of node 33 for the scenario with ICT in Figure 4.8. Node 33 is connected directly to the root node and only experience interruptions in power when the root node fails, it fails by itself, or the communication system has failed due to another line or disconnector fail. As a consequence, if a node experiences a few particular lengthy faults, the average will increase dramatically. This hypothesis is strengthened when using another seed, 10336.

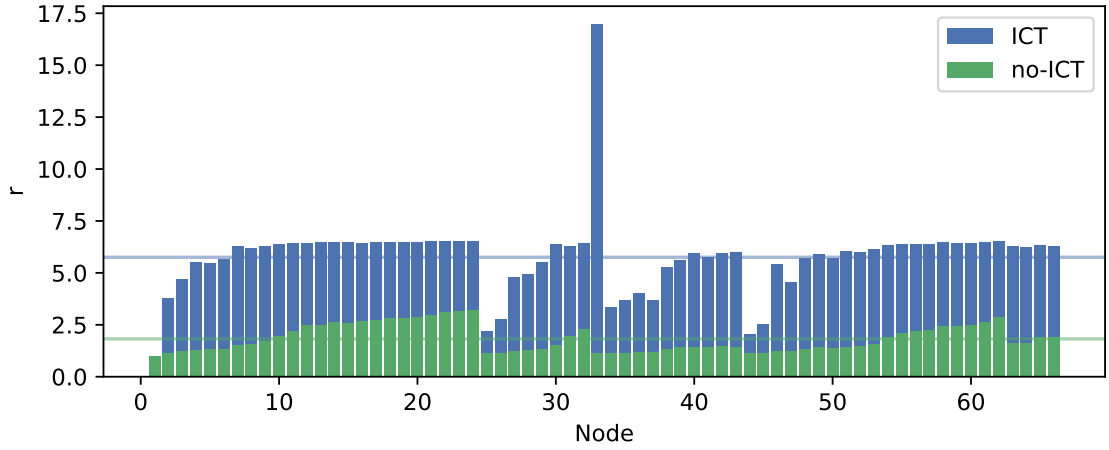

Figure 4.8: Average failure duration r bar plot for Case 1. The horizontal lines are the mean of the value of the nodes. The bars are not stacked. Simulation for 10000 years.

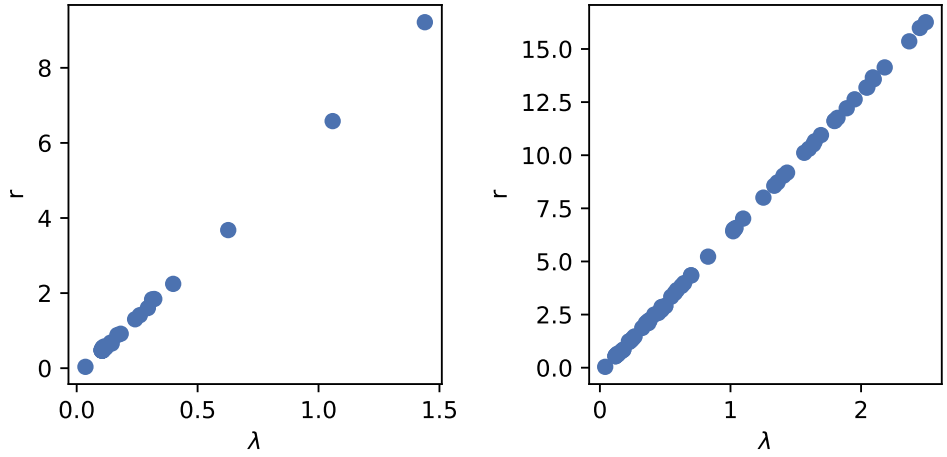

(a) Case 0, base case.

(b) Case 1, unchanged topology.

Figure 4.9: Failure rate λ versus average failure duration r for all nodes, unlabelled. Run with ICT for 10000 years.

With the new seed, Node 33 has an r value close to the other nodes in proximity to the root node, seen in Figure C.3 in the appendix. Other explanations, like a programming error or other logical errors, are also possible as the other nodes directly connected to the root nodes do not have an increased r value, rather they have a smaller r value than the average.

The failure rate λ and the average failure duration r have a linear relationship in the system, as seen in Figure 4.9. This indicates that the nodes with more interruptions per year also have the longest interruptions. In comparison with Figure 4.5 and Figure 4.8 it is evident that, from the nodes without a backup line (nodes 25–32), the proximity to the root node is important.

4.4 Factorial experiment — Case 2

The case descriptions for the cases are found in section 3.3. In short, for each sub-case in this section, there is an increase or decrease of a component's MTTF or MTTR. The resulting changes for SAIFI and SAIDI are presented in Figure 4.10, CAIFI and CAIDI are presented in Figure 4.11, and AENS and ACCI indices are presented in Figure C.5 in appendix. The factorial experiment method is explained in the theory subsection 2.5.7.

For both indices shown in Figure 4.10, an increase (incF) or decrease (decF) of the failure rate for a line (L), gives respectively a strong increase or decrease of the indices. The change is almost twice as big for the scenario without ICT, as it is for the scenario with ICT. This means that without ICT, the average frequency of faults is more sensitive towards a change in the failure rate of the lines, compared to with ICT. The change after Case 2 increase and Case 2 decrease of the transformer (bus, B) failure rates for the scenario with ICT is around the same as for the line failure rate change. This could just be a coincidence, but the resulting impact of the change is nevertheless almost equal. This would not be the scenario without the backup lines, then the system would be much more sensitive to line failures.

When looking at the transformer failure changes in the cases without ICT, the frequency of faults, i.e. SAIFI (Figure 4.10a), is not significantly changed, while the duration of faults, i.e SAIDI (Figure 4.10b), changes a bit, but around ten times less than for changes in line failures. Such a small change of the indices could mean that the failure of a node is better than the failure of a line for the system reliability. However, the failure rate for the lines are higher than the failure rate for the transformers, leading to a decrease in the significance of the result. Thus an increase in the failure rate of lines gives a higher increase in failures in the system compared to the same increase in failure rate for transformers.

The ACCI index, presented in Figure C.5, shows quite similar changes as the SAIDI index, except for the change in failure rate for the transformer (incF -1.9% and decF 3.5%). Thus the effect of increasing the failure rate for transformers may increase the number of different customers that experience interruptions, but a second interruption to a customer due to a transformer fault in a year is unlikely.

Changes in the failure rate and repair time (incR and decR) for disconnectors (D), communication hubs (CH), and communication lines (CL) are only possible in the scenario with ICT. The mentioned components have a lot less impact on the reliability than a change in failures in transformers and lines. Of the three, the communication hub has the greatest impact on the increase of SAIFI, as can be seen from the 15.1% increase in Figure 4.10a, while it is also the component with the most failures originally. However, it does not directly impact the interruption of power. The impact is through the obstruction of communication, which leads to the system needing one hour of sectioning time to find a fault, interrupting the power on all nodes in the meantime. This increases the SAIFI

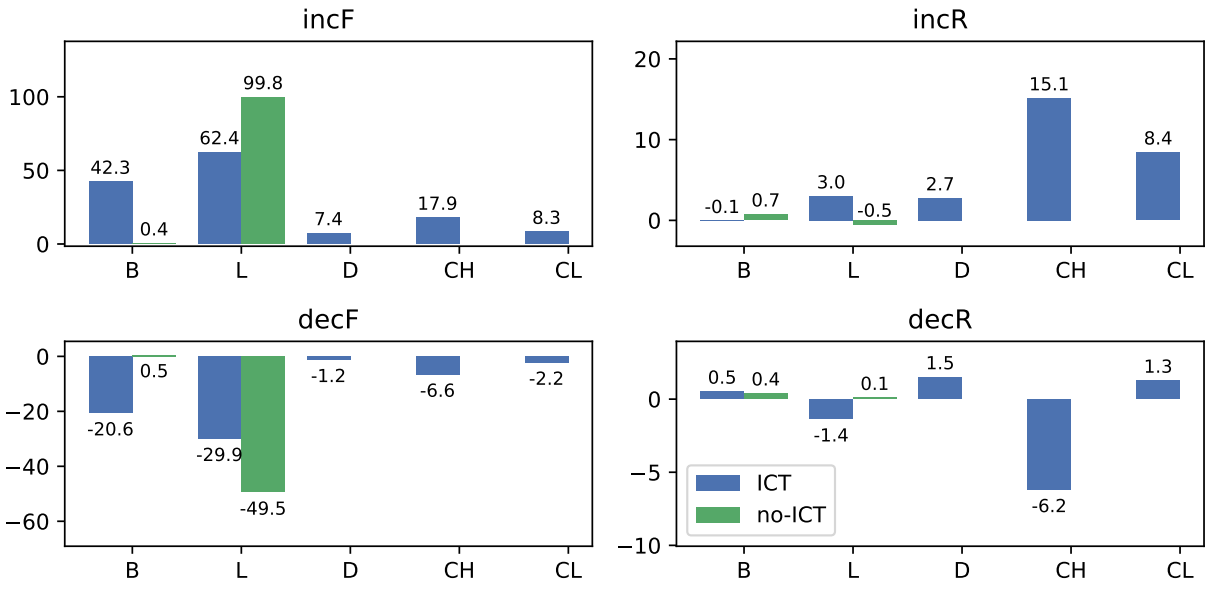

(a) SAIFI.

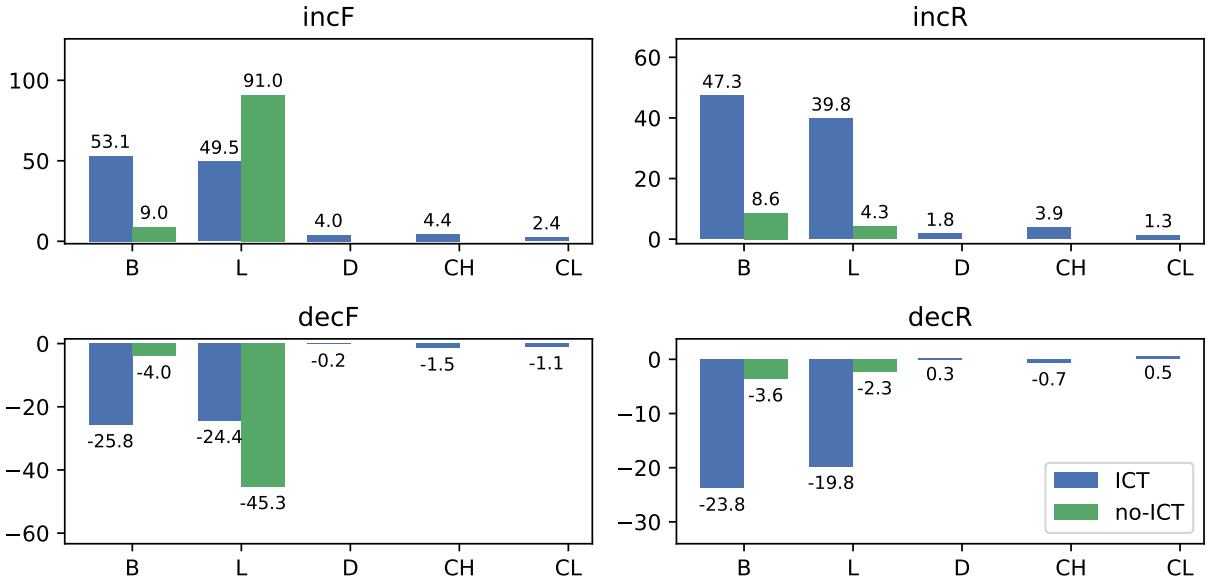

(b) SAIDI.

Figure 4.10: Factorial experiment change from Case 0 in percent for the SAIFI and SAIDI indices. Simulation for 10000 years. Bus (B), Line (L), Disconnector (D), Communication Hub (CH), and Communication Line (CL). Increase in failures (incF), decrease in failures (decF), increase in repair time (incR), and decrease in repair time (decR).

index, and in turn the total failure time, represented by SAIDI. The increase or decrease of the repair time has almost exactly the same effect on the disconnectors (incR 1.8%), communication hubs (incR 3.9% and decR -0.7%), and communication lines (incR 1.3%) in Figure 4.10a, for the same reasons as mentioned above. Exceptions are observed for the decreased repair time of disconnectors (decR 0.3%) and communication lines (decR 0.5%). The deviating ones could stem from an unlucky draw of random numbers, as discussed in the previous section about the r value of node 33.

The changes in SAIFI from changes in transformer and line repair time are minimal, while the changes in SAIDI are much higher. In addition, for the SAIDI index in the scenario with ICT, the changes are only slightly lower with a change in repair time compared to a change in failure rate. For a DSO this could mean that they could have old or cheaper components if they decrease the repair time approximately the same, and the resulting outage duration would be unchanged. Also in a system without ICT, the effect of changed repair time on SAIDI for transformers is only slightly lower than the failure rate. For lines, on the other hand, the SAIDI index only shows a minimal change for repair time compared to failure rate, as can be seen from Figure 4.10a. This comes down to the sectioning time adding the bulk of the outage duration, and the actual repair of the line only giving a slight increase. The modelling choice of having a disconnector at each end of every line has an effect here. Without disconnectors on every line it would be necessary to interrupt the power to several nodes for a longer time, giving a stronger increase in the SAIDI index than shown here. This may be more realistic for most distribution systems, and is a weak spot of the model ICT topology.

The CAIFI index in Figure 4.11a shows that only a line change in failure rate (incF, ICT 20.9% and no-ICT 99.7%, and decF, ICT -9.4% and no-ICT -48.8%) gives a significant percentage change above 3%. For the scenario without ICT this change is close to the change of SAIFI, indicating that most customers, in that case, already experience an interruption, and few extra customers experience an interruption when there are more line failures. In comparison, the scenario with ICT shows approximately 1/3 of the change of CAIFI as compared to SAIFI. This may indicate that, per year, there are more customers that experience interruptions.

The CAIDI index, i.e. the average failure duration, in Figure 4.11b shows much of the same trends as SAIDI for a change in repair time (incR and decR). For failure rates (incF and decF) however, many component changes have a negative correlation with SAIDI. Changes of failure rate in ICT components still give small index changes, but the index changes have the opposite sign. As expected, an increase in the failure rate of transformers gives a higher CAIDI, and vice versa, since the failure type has the longest MTTR, as seen in Table 3.1. The opposite is the case for changes in the line failure rate, as fewer line failures compared to transformer failure causes the average to increase. This apparently shows the limitations of the CAIDI index, an overall large reduction of interruption durations does

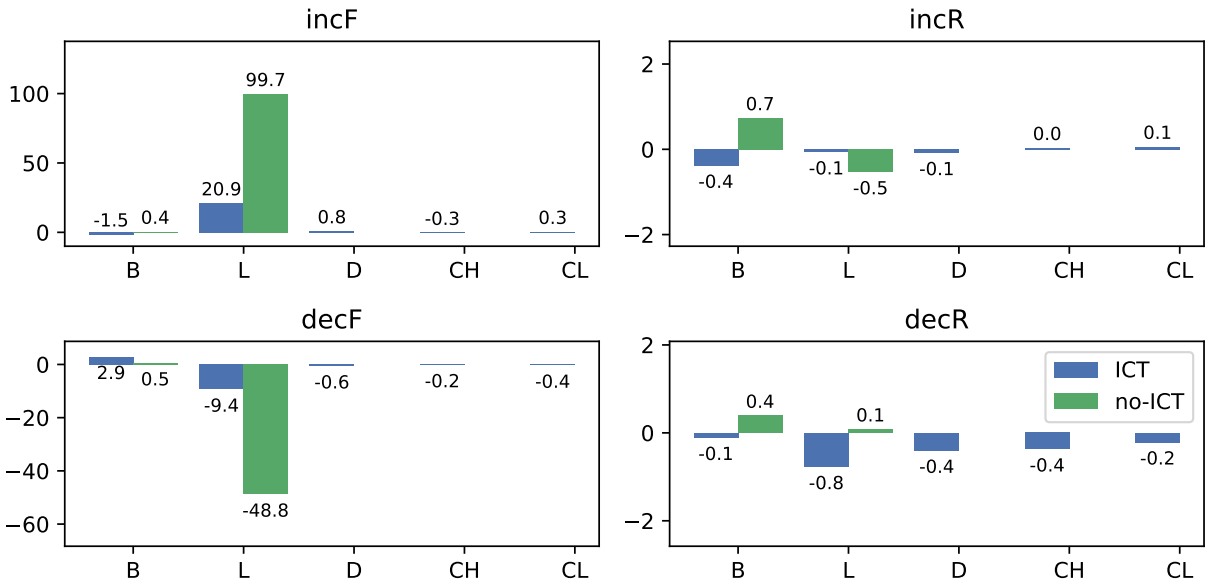

(a) CAIFI.

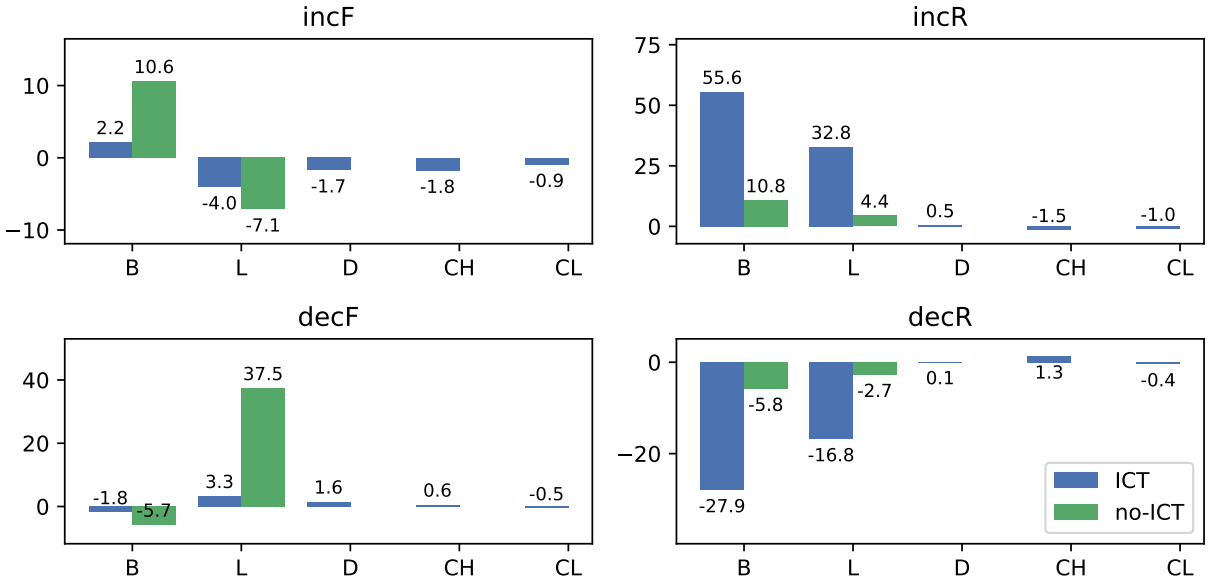

(b) CAIDI.

Figure 4.11: Factorial experiment change from Case 0 in percent for the CAIFI and the CAIDI indices. Simulation for 10000 years. Bus (B), Line (L), Disconnector (D), Communication Hub (CH), and Communication Line (CL). Increase in failures (incF), decrease in failures (decF), increase in repair time (incR), and decrease in repair time (decR).

not necessarily reflect on the index. However, in combination with the SAIDI index one can see that the failures remaining are not evenly spread out, proving the advantage of the CAIDI index.

In summary, both cases with and without ICT are sensitive to a change in line failure rate. In addition, the scenario with ICT is sensitive toward line repair time, and transformer failure rate and repair time, and the ICT components (i.e. D, CH, and CL) show some impact on the model indices, but generally less than the effect of lines and transformers on failure rate. However, the ICT components, communication hub and communication line, show a higher sensitivity than other components in the model for the SAIFI index when changing the repair time. A note to the figure and discussion; all increases doubles and decreases half the MTTF and MTTR. This could be an unrealistic high change for many of the parameters, but the high value change decreases the potential for errors because of random number variations.

5 Discussion of the model and indices

This chapter discusses what the model does, what information the indices can give, and which limitations the model and indices have, how accurate they are, and what they can be used for.

5.1 Indices

Cost is always an important metric in business, and for reliability, it is also an aspect of what upgrades and targets are chosen for the increase of reliability. A cost function dependent on interruption time could be added to reflect the customer value of reliability. The cost function needs to not only address the revenue lost by the customer or the DSO, but in order to estimate the impact, it should include indirect costs as an effect of the interruption. Examples of indirectly affected parts are the customer, society in general, the natural environment, and others. The cost of an increase in reliability is seldom the same for the different levels of reliability, see Figure 5.1. At low values the cost of a 1% increase is low, at higher values this could cost much more, and it could be too expensive to get a 100% reliable system. Hence, the goal of the DSO is often to get a "good enough" reliability relative to the buying power of the customers.

In the case discussion, the shape of the histograms does not necessarily reflect the underlying numbers exactly. The histograms are created by placing all 10000 index samples into 10 bins of equal length on the value axis. Combining this with rounding errors in the floating point numbers could give a slightly distorted shape for numbers at the limit between two bins/bars.

There are many factor outside the power system that influence the reliability of the

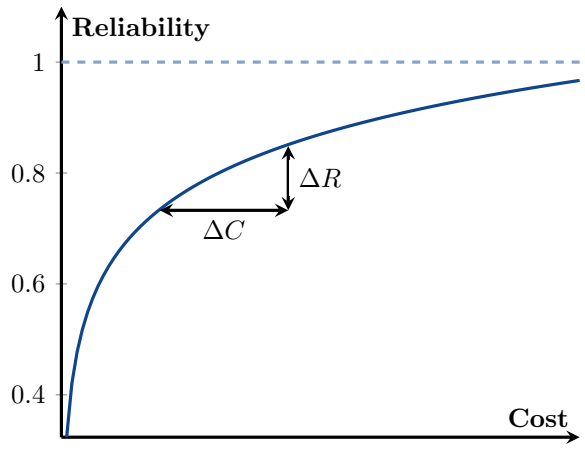

Figure 5.1: A typical cost versus reliability function where ΔC is a change in the cost and ΔR is a change in the reliability.

system, causing the indices calculated from real world power systems to differ widely. Geographical characteristics and typical weather phenomena such as steep terrain, forests, and wind-swept areas (coastal regions with damp and salty wind are especially challenging) could decrease reliability performance dramatically. Hence, each analysis of a power system needs to be tailored to the specific conditions that system experiences. By doing so, the effect of ICT and other reliability questions could be answered.

As the electrical power system is a critical infrastructure, reliable operation is essential. The indices used in this thesis are well fitted for the purpose of indicating the likely performance of the system, based on previous research [20], use in the industry [35], and the results in this thesis. Designing systems from just these indicators of performance lead to reliable systems but they could also increase the consequences of unlikely faults, making the systems more vulnerable [3]. A too strong focus on the likely faults could then have devastating consequences for the realisation of impact by the unlikely faults.

Typically, indices for reliable performance are averaged in some way to the system as a whole. A reduction of one of these indices does not necessarily mean a reduction of the value at each node. Thus the minority of the nodes could, without intention, suffer significantly in exchange for a bit more reliable service to the majority of the nodes in a large system.

5.2 Interdependencies

In the modern power system the important interdependencies with the ICT systems are; Physical, Cyber and Geographic, potentially causing Cascading, Escalating, and Common cause failures (definitions can be found in section 2.1). Examples of this are; A fault in the ICT system gives an increase in the sectioning time from minutes to one hour, repair of ICT components are delayed by a power outage, and a functioning ICT system reduces the repair time of transformers. The model thus implements the physical and the cyber interdependency, with cascading failures. To get a more complete picture of the behaviour, geographic interdependencies should be modelled such that the common cause failures are implemented. Escalating failures are harder to implement in an adequacy assessment, since the failure type dynamically change with time and the model in this thesis is calculated for a steady state. Thus the model can only show parts of the bigger picture of the interdependencies between the two systems.

This thesis has been focusing more on the power system, and so the ICT system modelling should get more attention in the future. As a start, a distinction between active and passive faults would be valuable to model more closely to see the different impacts the two types of faults can have. ICT systems could be used to find failures doomed to happen shortly in the power system, increasing the resistant capacity of the combined system. A possible method to model this is to use a set probability for the ICT components to

eliminate the future failure a few hours before the event. It would not necessarily need to eliminate the fault to increase the reliability; eliminating the sectioning time for failures will be sufficient.

5.3 Model validity

The modelling choice of having a disconnector at each end of every line has an effect on the model accuracy compared to a real power system. Without disconnectors on every line, one would have to interrupt the power to several nodes for a longer time during the reparation of a failure, causing a stronger increase in the SAIDI index than shown in this thesis. This may be more realistic for most distribution systems, and is a less robust part of the model ICT topology.

An exponential distribution of failures fits well with existing data, while for repair times it does not necessarily fit as well [21]. In general, no distribution function does fit all types of repair times, this is a weakness of the MCS. Other possible distributions are log-normal, gamma and normal distributions. The time independence of the exponential distribution is a strong advantage, and is the reason why many models, including the one in this thesis, use it.

Potential pitfalls of all MCS are High Impact Low Probability (HILP) events. They impact the average unavailability to a large degree when the number of samples are low. This is seen in Figure 4.2, where the simulation for 100 years has two HILP events for the seed 67505, but none for the seed 10336, which results in an underestimation of the variation of the mean for the seed 10336. However, the MCS is able to cover HILP events on all seeds for 10000 simulation years. Johansson draws the same conclusion [3]; the MCS covers HILP events if it runs for enough years.

There is a potential for systematic errors in the MCS implementation in this thesis, both in the code and in the data used. The results should be examined further by comparing the reliability indices to other methods of implementation and evaluate the precision of the estimates.

6 Conclusions and further work

6.1 Conclusions

A Monte Carlo Simulation (MCS) tool was developed and thoroughly explained, and the model assumptions and limitations are pointed out and discussed. The focus is the implementation of interdependencies. Where both the the physical and the cyber interdependency is modelled, with cascading failures. Further, several cases were simulated using the MCS on a standardised test system, the IEEE 69 bus test system. Each case changes one or more essential factors in the simulation. The factors changed were;

- the use of ICT components in the system,
- the use of backup lines as a remedial action after a failure, and
- a change in the component‘s MTTF or MTTR.

All cases were discussed by using both basic and aggregated reliability indices.

Three simulations of Case 0 (base case) with three different starting seeds for the pseudo-random number generator showed that with 10000 years of simulation the indices did converge to a satisfactory level. However, one case of weakness was found for the average failure duration r of node 33 in the test system, seen in Figure 4.8. The value was over 250% higher than all other r values in the simulation with the seed 67505, but with the seed 10336, the r value was in line with the other r values. If investigating the system‘s vulnerability through analysis of chosen hours with lots of interrupted power, the assortment of years can be improved by increasing the number of simulation years further. No seasonal changes of interest were found, but adding more differences between the seasons could lead to results of interest. Increasing the failure rate in the high-load season and decreasing it in the low-load season is one method to increase the seasonal differences.

In general, the power system with ICT was more reliable than the power system without ICT. In comparison to a system without backup lines, both systems have relatively high reliability. The sectioning time in a system plays a crucial role in the reliability of a system. However, it is less critical if the system does not have backup lines. Still, the results may indicate that the reliability increases more with the introduction of ICT to have a quick sectioning time compared to having backup lines that can be connected during the duration of the failure in this power system.

The CAIDI index, the average interruption duration, was shown to reflect the typical interruption duration, but not necessarily the reliability of the system. This index was, for all cases, higher in the system with ICT than the system without, as a contrast to the generally lower indices for the system with ICT. A frequent one-hour section time for the system without ICT is assumed to be the cause of the difference. A combination of the

CAIDI index and a cost function could increase the quality of the information output.

It was found that in Case 1 (unchanged topology) without ICT, the duration indices (SAIDI, CAIDI, AENS, and ACCI) are strongly correlated with the change in system operation. With ICT, the change of the same indices is much more pronounced, and for some indices the change is over 400% larger compared to Case 0. However, the results show that in absolute terms, the change in each index, comparing with and without ICT, were surprisingly similar. Indicating that the impact on the system reliability of having backup lines is mostly independent of the use of ICT components.

As expected, without the use of backup lines, the unavailability increases with a high correspondence to the number of nodes to the root node. With the use of backup lines, the unavailability for all nodes with a backup line was similar.

In the resilience perspective, the sectioning time and topology change are part of the restorative capacity giving a shorter time to recovery. Change of topology is also, in a system with ICT, a resistant capacity, as the interruption is so short that it does not (in this thesis) count as an interruption.

The factorial experiment (Case 2) indicates that;

- The scenario with ICT is sensitive toward line repair time, and transformer failure rate and repair time. In addition, the ICT components (i.e. Disconnector, Communication Hub, and Communication Line) show some impact on the model indices, but generally much less than the effect of lines and transformers on failure rate.
- In a system without ICT, the average frequency of faults is more sensitive towards a change in the failure rate of the lines, compared to a system with ICT. Such a small change of the indices could indicate that a node failure has a lower impact than a line failure for the system‘s reliability.
- Of the three ICT components, the communication hub has the greatest impact on the increase of SAIFI (15.1%), while it is also the component with the most failures originally.

Without disconnectors on every line, one would have to interrupt the power to several nodes for a longer time, giving a stronger increase in the SAIDI index than shown in this thesis. This may be more realistic for some distribution systems, and is a weak spot of the modelled ICT topology.

The factorial experiment indicates that the power system model corresponds well with the predicted behaviour of a real-world power system. It is more difficult to conclude if the ICT system behaviour is realistic, as there is a shallow foundation on the topic. Nevertheless, one could predict that the general increase in reliability seen in the cases from the use of an ICT system could occur. This is still an uncertain prediction, as the

MTTF for the ICT components is questionable. It was discovered, however, that an increase in the MTTF for communication hubs did decrease the overall reliability.

6.2 Further Work

The models proposed in this thesis should be implemented and validated in several other scenarios. It would be valuable to model and simulate a historical power system failure. This may be used to calibrate the model according to realistic operation. The validation of a model is particularly important to the usefulness and the limitations of the results from further simulations.

The factorial experiment included in this thesis merely scratches the surface of which factor-combinations could be changed between the different cases. Examples of factors that could be changed, but not covered in this thesis, are;

- the assumption of a negligible amount of mechanical faults in disconnectors,
- dividing the system into four sectors (one for each line connected to the root-node),
- what requirements the system needs to have a low sectioning time, or
- differentiated sectioning time based on the partial working of the communication system.

In addition, in this thesis only two levels are used for the factor changes. This could be extended to investigate how the indices will develop with smaller and bigger changes in the factors, as it might not be a linear relationship. The model only counts interruptions larger than one hour. Shorter interruptions could be analysed and the indices get more granular with a shorter time increments.

Modelling of regular (or irregular) maintenance could shift the reliability in either direction. This would further extend the opportunities of a DSO when comparing alternative changes in the system to increase the reliability.

Changing the MTTF and MTTR through the year, for special events or extreme weather scenarios could highlight what impact such increased failure scenarios have on the reliability. Even though it was not implemented in the presented model, places with strong seasonal changes in the climate could experience that the weather variations have a big impact on the reliability.

Other aspects that could potentially be optimised is how many ICT parts that are available to be changed, and the communication hubs and lines could get a more optimal placement regarding both faults and economics. Also, experimentation with backup lines and their opportunities benefit can be examined.

Further, the model could be extended to include distributed generation throughout the

system. In such an extension a microgrid could be formed when some nodes (with distributed generation) are isolated from the main feeder. This could further enhance the reliability of the system, and could pose as an alternative to backup lines.

Topological analysis methods use network and graph theory to describe the topology of the systems. This is a part of the vulnerability analysis of a system. These methods have been used to model complex systems such as critical infrastructures. Such methods are useful for evaluating the importance of real and modelled geographic interdependencies of the infrastructures [5]. The basic topological model needs only limited amounts of data to analyse the system, and it also has short simulation times compared to the MCS. It could pose as an interesting second view of the system vulnerability to compliment the reliability analysis in the MCS.

References

[1] Work group from Energi Norge and Telenor, spring 2013, "Sikkerhet og beredskap mot ekstremvær i telesektoren," 2013.

[2] S. Henriksen, "Samfunnsmessige konsekvenser av bortfall av elektrisk kraft-hva skjer med oss når strømmen blir borte?" 2001.

[3] J. Johansson, H. Hassel, and E. Zio, "Reliability and vulnerability analyses of critical infrastructures: Comparing two approaches in the context of power systems," *Reliability Engineering and System Safety*, vol. 120, pp. 27–38, dec 2013.

[4] R. Billinton and R. N. Allan, *Reliability of Electric Power Systems: An Overview*. London: Springer London, 2003, pp. 511–528. [Online]. Available: https://doi.org/10.1007/1-85233-841-5_28

[5] I. A. Tøndel, J. Foros, S. S. Kilskar, P. Hokstad, and M. G. Jaatun, "Interdependencies and reliability in the combined ICT and power system: An overview of current research," *Applied Computing and Informatics*, vol. 14, no. 1, pp. 17–27, sep 2018. [Online]. Available: http://www.sciencedirect.com/science/article/pii/S2210832716300552

[6] E. H. Allen, R. B. Stuart, and T. E. Wiedman, "No Light in August: Power System Restoration Following the 2003 North American Blackout," *IEEE Power and Energy Magazine*, vol. 12, no. 1, pp. 24–33, 2014. [Online]. Available: https://ieeexplore.ieee.org/document/6684692

[7] M. Amin, "Toward self-healing energy infrastructure systems," *IEEE Computer Applications in Power*, vol. 14, no. 1, pp. 20–28, 2001. [Online]. Available: https://ieeexplore.ieee.org/abstract/document/893351/similar#similar

[8] T. Amare, B. E. Helvik, and P. E. Heegaard, "A modeling approach for dependability analysis of smart distribution grids," in *21st Conference on Innovation in Clouds, Internet and Networks, ICIN 2018*. Institute of Electrical and Electronics Engineers Inc., jun 2018, pp. 1–8.

[9] W. Wangdee and R. Billinton, "Considering load-carrying capability and wind speed correlation of wecs in generation adequacy assessment," *IEEE Transactions on Energy Conversion*, vol. 21, 2006.

[10] I. N. L. (INL), "Critical Infrastructure Interdependency Modeling: A Survey of U.S. and International Research," Idaho National Laboratory (INL), Tech. Rep., 2006. [Online]. Available: http://cip.management.dal.ca/publications/CriticalInfrastructureInterdependencyModeling.pdf

[11] T. O'Rourke and T. Briggs, "Critical Infrastructure, Interdependencies, and Resilience," *The Bridge*, vol. 37, 2007.

[12] S. M. Rinaldi, J. P. Peerenboom, and T. K. Kelly, "Identifying, understanding, and analyzing critical infrastructure interdependencies," *IEEE Control Systems Magazine*, vol. 21, no. 6, pp. 11–25, 2001. [Online]. Available: https://ieeexplore.ieee.org/document/969131

[13] M. Ouyang, "Review on modeling and simulation of interdependent critical infrastructure systems," *Reliability Engineering and System Safety*, vol. 121, pp. 43–60, 2014. [Online]. Available: http://www.sciencedirect.com/science/article/pii/S0951832013002056

[14] D. J. Snowden and M. E. Boone, "A leader's framework for decision making," *Harvard business review*, vol. 85, no. 11, p. 68, 2007.

[15] I. B. Sperstad, G. H. Kjølle, and O. Gjerde, "A comprehensive framework for vulnerability analysis of extraordinary events in power systems," *Reliability Engineering and System Safety*, vol. 196, p. 106788, 2020. [Online]. Available: https://linkinghub.elsevier.com/retrieve/pii/S0951832019307008

[16] M. Bruneau, S. Chang, R. Eguchi, G. Lee, T. O'Rourke, A. Reinhorn, M. Shinozuka, K. Tierney, W. Wallace, and D. Winterfeldt, "A Framework to Quantitatively Assess and Enhance the Seismic Resilience of Communities," *Earthquake Spectra - EARTHQ SPECTRA*, vol. 19, 2003.

[17] G. P. Cimellaro, A. M. Reinhorn, and M. Bruneau, "Framework for analytical quantification of disaster resilience," *Engineering Structures*, vol. 32, no. 11, pp. 3639–3649, 2010. [Online]. Available: http://www.sciencedirect.com/science/article/pii/S014102961000297X

[18] P. Kundur, J. Paserba, V. Ajjarapu, G. Andersson, A. Bose, C. Canizares, N. Hatziargyriou, D. Hill, A. Stankovic, C. Taylor, T. V. Cutsem, and V. Vittal, "Definition and classification of power system stability IEEE/CIGRE joint task force on stability terms and definitions," *IEEE Transactions on Power Systems*, vol. 19, no. 3, pp. 1387–1401, 2004. [Online]. Available: https://ieeexplore.ieee.org/abstract/document/1318675

[19] S. M. Amin and B. F. Wollenberg, "Toward a smart grid: power delivery for the 21st century," *IEEE Power and Energy Magazine*, vol. 3, no. 5, pp. 34–41, 2005. [Online]. Available: https://ieeexplore.ieee.org/document/1507024?arnumber=1507024&contentType=Journals%26Magazines

[20] R. Billinton and R. N. Allan, *Reliability Evaluation of Power Systems*. Springer US, 1996.

[21] R. Billinton and W. Li, *Reliability Assessment of Electric Power Systems Using Monte Carlo Methods*. Springer US, 1994.

[22] G. Kjolle and K. Sane, "Relrad - an analytical approach for distribution system reliability assessment," *IEEE Transactions on Power Delivery*, vol. 7, 1992.

[23] R. Allan and R. Billinton, "Probabilistic assessment of power systems," *Proceedings of the IEEE*, vol. 88, no. 2, pp. 140–162, 2000. [Online]. Available: https://ieeexplore.ieee.org/document/823995

[24] T. O'Rourke, T. Briggs, B. Tornqvist, M. Fontela, P. Mellstrand, R. Gustavsson, C. Andrieu, J. Machowski, J. W. Bialek, and J. Bumby, "Power System Dynamics: Stability and Control," *IEEE Transactions on Power Systems*, vol. 37, sep 2020. [Online]. Available: https://ieeexplore.ieee.org/document/7995099

[25] D. Kirschen and F. Bouffard, "Keeping the lights on and the information flowing," *IEEE Power and Energy Magazine*, vol. 7, no. 1, pp. 50–60, 2009. [Online]. Available: https://ieeexplore.ieee.org/abstract/document/4723866

[26] J. Wäfler, P. E. Heegaard, D. Hutchison, T. Kanade, J. Kittler, J. M. Kleinberg, F. Mattern, J. C. Mitchell, M. Naor, O. Nierstrasz, C. Pandu Rangan, B. Steffen, M. Sudan, D. Terzopoulos, D. Tygar, M. Y. Vardi, and G. Weikum, "Interdependency Modeling in Smart Grid and the Influence of ICT on Dependability," in *Advances in Communication Networking*, T. Bauschert, Ed. Berlin, Heidelberg: Springer Berlin Heidelberg, 2013, vol. 8115, pp. 185–196. [Online]. Available: http://link.springer.com/10.1007/978-3-642-40552-5_17

[27] J.-C. Laprie, K. Kanoun, and M. Kaâniche, "Modelling Interdependencies Between the Electricity and Information Infrastructures," *Lecture Notes in Computer Science*, pp. 54–67, 2007. [Online]. Available: https://link.springer.com/content/pdf/10.1007%2F978-3-540-75101-4_5.pdf

[28] Statnett, "Feil under testing av nordlink," Webpage, 2020. [Online]. Available: https://www.statnett.no/om-statnett/nyheter-og-pressemeldinger/nyhetsarkiv-2020/feil-under-testing-av-nordlink/

[29] H. Farhangi, "The path of the smart grid," *IEEE Power and Energy Magazine*, vol. 8, no. 1, pp. 18–28, 2010. [Online]. Available: https://ieeexplore.ieee.org/document/5357331

[30] R. H. Lasseter, "MicroGrids," in *2002 IEEE Power Engineering Society Winter Meeting. Conference Proceedings (Cat. No.02CH37309)*, vol. 1, 2002, pp. 305–308 vol.1. [Online]. Available: https://ieeexplore.ieee.org/document/985003

[31] O. Fosso, "PyDSAL - Python Distribution System Analysis Library," *IEEE International Conference on Power System Technology*, 2020. [Online]. Available: https://www.researchgate.net/publication/34367

[32] M. Amin, "National Infrastructures as Complex Interactive Networks," in *Automation, Control, and Complexity: An Integrated Approach*. John Wiley and Sons, 2000, pp. 263–286.

[33] R. E. Walpole, R. H. Myers, K. Ye, and S. L. Myers, *Probability and Statistics for Engineers and Scientists*, 9th ed. Person, 2016.

[34] Walmes, "Walmes GitHub page," 2021. [Online]. Available: https://github.com/walmes/Tikz

[35] Statnett SF, "Årsstatistikk 2018," 2018. [Online]. Available: https://www.statnett.no/contentassets/5fb5605039314f498ed16f8561695a0c/arsstatistikk-2018-1-22-kv.pdf

[36] E. Bompard, E. Carpaneto, G. Chicco, and R. Napoli, "Convergence of the backward/forward sweep method for the load-flow analysis of radial distribution systems," *International Journal of Electrical Power and Energy Systems*, vol. 22, no. 7, pp. 521–530, 2000. [Online]. Available: http://www.sciencedirect.com/science/article/pii/S0142061500000090

[37] M. H. Haque, "Load flow solution of distribution systems with voltage dependent load models," *Electric Power Systems Research*, vol. 36, no. 3, pp. 151–156, mar 1996.

[38] Subcommittee, Gold Book Working Group of the Power Systems Reliability, "IEEE 493-2007 - IEEE Recommended Practice for the Design of Reliable Industrial and Commercial Power Systems," Institute of Electrical and Electronics Engineers, Inc., Tech. Rep., 2007. [Online]. Available: https://standards.ieee.org/standard/493-2007.html

[39] "Python Random," 2021. [Online]. Available: https://docs.python.org/3/library/random.html

[40] M. Matsumoto and T. Nishimura, "Mersenne Twister: A 623-Dimensionally Equidistributed Uniform Pseudo-Random Number Generator," in *ACM Transactions on Modeling and Computer Simulation*, vol. 8, no. 1. ACM PUB27 New York, NY, USA, jan 1998, pp. 3–30. [Online]. Available: https://dl.acm.org/doi/abs/10.1145/272991.272995

[41] M. E. Baran and F. F. Wu, "Optimal capacitor placement on radial distribution systems," *IEEE Transactions on Power Delivery*, vol. 4, no. 1, pp. 725–734, 1989. [Online]. Available: https://ieeexplore.ieee.org/document/19265?arnumber=19265&abstr

Appendix

A Python code

The Python code written is attached as `monte_carlo.zip`. All data and plots for the test system shown in this thesis are acquired by running the file `main.py`. The code is written and run with the following version of Python with libraries:

- Python 3.9.0
- Numpy 1.19.3
- Pandas 1.1.4
- Matplotlib 3.3.3
- Openpyxl 3.0.7
- Seaborn 0.11.1

B IEEE 69bus power system

Table B.1: Definition of nodes in the IEEE 69 bus test power system. The bus number (bus num.) is followed by the active and reactive load at that node, for both high load (P_{high} and Q_{high}) and low load (P_{low} and Q_{low}).

Bus num.	P_{high} (pu)	Q_{high} (pu)	P_{low} (pu)	Q_{low} (pu)
1	0	0	0	0
2	0.673805952	0.471664166	0.297746685	0.208422679
3	0.935399639	0.654779747	0.37807147	0.264650029
4	0.630189612	0.441132728	0.275381036	0.192766725
5	0.863267278	0.604287094	0.511646522	0.358152565
6	0.806589992	0.564612994	0.348647452	0.244053217
7	0.637238708	0.446067096	0.378236594	0.264765616
8	1.091008997	0.763706298	0.596163701	0.41731459
9	0.813938871	0.56975721	0.33157229	0.232100603
10	0.902290069	0.631603049	0.466203869	0.326342709
11	0.85117965	0.595825755	0.445600897	0.311920628
12	0.961733427	0.673213399	0.385360777	0.269752544
13	0.569816451	0.398871516	0.234423434	0.164096404
14	0.937590931	0.656313652	0.432742757	0.30291993
15	0.778857508	0.545200256	0.410004263	0.287002984
16	0.746703638	0.522692547	0.364733158	0.255313211
17	0.970930188	0.679651131	0.430997496	0.301698247
18	0.689933238	0.482953267	0.332395443	0.23267681
19	0.677925811	0.474548067	0.313128949	0.219190264
20	0.611177101	0.427823971	0.346247723	0.242373406
21	1.050356801	0.735249761	0.493065751	0.345146025
22	0.995353547	0.696747483	0.566394525	0.396476167
23	0.532690786	0.37288355	0.215060131	0.150542092
24	0.982772261	0.687940583	0.484548952	0.339184266
25	0.984552787	0.689186951	0.458414258	0.32088998
26	0.560670971	0.39246968	0.26777564	0.187442948
27	1.061198714	0.7428391	0.635674471	0.444972129
28	1.091067381	0.763747167	0.500272553	0.350190787
29	0.607818549	0.425472984	0.361892017	0.253324412
30	0.971426126	0.679998288	0.475018998	0.332513299
31	1.098274756	0.768792329	0.654014785	0.457810349
32	0.94134778	0.658943446	0.418541062	0.292978743
33	0.818453261	0.572917283	0.338130139	0.236691098
34	0.535616685	0.374931679	0.301344443	0.21094111

Table B.1: Definition of nodes in the IEEE 69 bus test power system.

Bus num.	P_{high} (pu)	Q_{high} (pu)	P_{low} (pu)	Q_{low} (pu)
35	0.819114602	0.573380222	0.438313685	0.30681958
36	1.031404635	0.721983245	0.57550445	0.402853115
37	1.040986908	0.728690835	0.515277104	0.360693973
38	1.093395814	0.76537707	0.648135405	0.453694784
39	0.715889271	0.50112249	0.314431809	0.220102266
40	0.600529131	0.420370392	0.291001965	0.203701375
41	0.923819695	0.646673786	0.37332866	0.261330062
42	0.763290129	0.53430309	0.360893344	0.252625341
43	0.708169794	0.495718856	0.366049034	0.256234324
44	1.054420042	0.73809403	0.594108438	0.415875906
45	0.834279425	0.583995598	0.46652803	0.326569621
46	0.837783136	0.586448195	0.467499797	0.327249858
47	0.641344919	0.448941443	0.300140309	0.210098216
48	1.038736876	0.727115813	0.436949312	0.305864519
49	0.937571662	0.656300163	0.560431937	0.392302356
50	0.51815741	0.362710187	0.239547558	0.16768329
51	0.549764189	0.384834932	0.280836068	0.196585248
52	0.567587503	0.397311252	0.303272092	0.212290465
53	0.8033979	0.56237853	0.479536476	0.335675533
54	0.557195754	0.390037028	0.312853925	0.218997747
55	0.664385626	0.465069939	0.384497541	0.269148279
56	1.006740461	0.704718323	0.402810099	0.281967069
57	0.517011276	0.361907893	0.215588975	0.150912282
58	0.515071492	0.360550044	0.25635959	0.179451713
59	0.613504871	0.429453409	0.259243983	0.181470788
60	0.660514265	0.462359986	0.39401761	0.275812327
61	0.524847995	0.367393596	0.242372753	0.169660927
62	1.098128857	0.7686902	0.5253755	0.36776285
63	0.943897728	0.66072841	0.450401727	0.315281209
64	0.528513941	0.369959759	0.284274156	0.198991909
65	0.557959486	0.39057164	0.24057148	0.168400036
66	0.621529959	0.435070972	0.260222119	0.182155483
Total	51.67012222	36.16908555	25.68982717	17.98287902

Table B.2: Definition of the lines in the IEEE 69 bus test power system. $state = 0$ is enabled and $state = 3$ is disabled. From [41].

From	To	Resistance, R (pu)	Reactance, X (pu)	state
1	2	1.72203E-05	2.2087E-05	0
2	3	0.000228357	0.0001163	0
3	4	0.000237778	0.000121104	0
4	5	5.75259E-05	2.93245E-05	0
5	6	3.07595E-05	1.56605E-05	0
6	7	0.000510995	0.000168897	0
7	8	0.000116799	4.31132E-05	0
8	9	0.00044386	0.000146685	0
9	10	0.000642643	0.000212135	0
10	11	0.000651378	0.000215254	0
11	12	0.000660113	0.000218124	0
12	13	0.000122664	4.05551E-05	0
13	14	0.000233598	7.7242E-05	0
14	15	2.93245E-06	9.9828E-07	0
15	16	0.000204398	6.75711E-05	0
16	17	0.000131399	4.30508E-05	0
17	18	0.000213133	7.04412E-05	0
18	19	8.73495E-06	2.87006E-06	0
19	20	9.92665E-05	3.28185E-05	0
20	21	0.000216065	7.14394E-05	0
21	22	0.000467195	0.000171267	0
22	23	0.000192731	6.37028E-05	0
23	24	0.000108064	3.56885E-05	0
1	25	2.74527E-06	6.73839E-06	0
25	26	3.99312E-05	9.76443E-05	0
26	27	0.000248197	8.20462E-05	0
27	28	4.37996E-05	1.44751E-05	0
28	29	0.000218998	7.23753E-05	0
29	30	0.000523473	0.000175697	0
30	31	0.001065664	0.000352268	0
31	32	0.000919666	0.00029156	0
1	33	2.74527E-06	6.73839E-06	0
33	34	3.99312E-05	9.76443E-05	0
34	35	6.56993E-05	7.67428E-05	0
35	36	1.89673E-05	2.21493E-05	0
36	37	1.12307E-06	1.31024E-06	0

Table B.2: Definition of the lines in the IEEE 69 bus test power system.

From	To	Resistance, R (pu)	Reactance, X (pu)	state
37	38	0.000454405	0.000530898	0
38	39	0.000193417	0.000226048	0
39	40	2.55809E-05	2.98236E-05	0
40	41	5.74011E-06	7.23753E-06	0
41	42	6.79455E-05	8.56649E-05	0
42	43	5.61533E-07	7.4871E-07	0
1	44	2.12135E-06	5.24097E-06	0
44	45	5.3096E-05	0.000129964	0
45	46	0.000180814	0.000442425	0
46	47	5.12867E-05	0.000125471	0
5	48	5.79003E-05	2.95117E-05	0
48	49	0.000207081	6.95053E-05	0
6	50	0.000108563	5.52798E-05	0
50	51	0.000126657	6.45139E-05	0
51	52	0.00017732	9.0282E-05	0
52	53	0.00017551	8.94085E-05	0
53	54	0.000992041	0.000332989	0
54	55	0.00048897	0.000164092	0
55	56	0.000189798	6.27669E-05	0
56	57	0.000240898	7.3124E-05	0
57	58	0.000316642	0.000161285	0
58	59	6.07703E-05	3.09467E-05	0
59	60	9.04692E-05	4.60457E-05	0
60	61	0.000443299	0.000225799	0
61	62	0.000649506	0.000330805	0
8	63	0.000125534	3.81218E-05	0
63	64	2.93245E-06	8.73495E-07	0
9	65	0.00046133	0.000152487	0
65	66	2.93245E-06	9.9828E-07	0
8	40	0.0001	0.00005	3
10	18	0.0001	0.00005	3
12	43	0.0001	0.00005	3
47	56	0.0001	0.00005	3
24	62	0.0001	0.00005	3

C Indices from the different cases

Table C.1: Indices mean $\overline{X}$, standard deviation σ_X and the convergence parameter α for Case 0, base case. 10000 years of simulation.

Index	ICT			No ICT		
	$\overline{X}$	σ_X	α	$\overline{X}$	σ_X	α
Seed 67505						
SAIFI	0.170289	0.201804	0.011851	6.188600	2.487509	0.004020
SAIDI	0.896147	0.590221	0.006586	7.125577	2.684784	0.003768
CAIFI	1.179172	0.246897	0.002094	6.190830	2.482456	0.004010
CAIDI	6.255315	2.979253	0.004763	1.190859	0.393692	0.003306
ASAI	0.999898	0.000067	0.000001	0.999187	0.000306	0.000003
AENS	0.575678	0.424585	0.007375	4.210712	1.682630	0.003996
ACCI	4.704086	2.839620	0.006036	4.284893	1.700816	0.003969
Seed 10336						
SAIFI	0.175753	0.212603	0.012097	6.218100	2.466566	0.003967
SAIDI	0.904452	0.592727	0.006553	7.134888	2.659178	0.003727
CAIFI	1.178895	0.246943	0.002095	6.221100	2.459658	0.003954
CAIDI	6.228022	2.901420	0.004659	1.196219	0.581905	0.004865
ASAI	0.999897	0.000068	0.000001	0.999186	0.000304	0.000003
AENS	0.579127	0.419085	0.007236	4.226545	1.666662	0.003943
ACCI	4.676287	2.781124	0.005947	4.310453	1.697019	0.003937
Seed 33620						
SAIFI	0.173488	0.207920	0.011985	6.214700	2.489423	0.004006
SAIDI	0.906273	0.597693	0.006595	7.142685	2.687730	0.003763
CAIFI	1.178458	0.250294	0.002124	6.216584	2.485144	0.003998
CAIDI	6.286438	2.936352	0.004671	1.182593	0.321327	0.002717
ASAI	0.999897	0.000068	0.000001	0.999185	0.000307	0.000003
AENS	0.578578	0.423827	0.007325	4.230165	1.684620	0.003982
ACCI	4.702530	2.831789	0.006022	4.302163	1.703812	0.003960

Table C.2: Indices mean $\overline{X}$, standard deviation σ_X and the convergence parameter α for Case 1, unchanged topology. 10000 years of simulation.

Index	ICT			No ICT		
	$\overline{X}$	σ_X	α	$\overline{X}$	σ_X	α
SAIFI	0.923318	0.507412	0.005496	6.206800	2.478249	0.003993
SAIDI	5.824000	4.155082	0.007134	11.195736	5.411421	0.004833
CAIFI	1.751919	0.551634	0.003149	6.209069	2.473074	0.003983
CAIDI	6.422802	2.995973	0.004665	1.842747	0.738327	0.004007
ASAI	0.999335	0.000474	0.000005	0.998722	0.000618	0.000006
AENS	3.387132	2.501861	0.007386	6.547585	3.299175	0.005039
ACCI	6.554009	3.866390	0.005899	6.660904	3.341975	0.005017

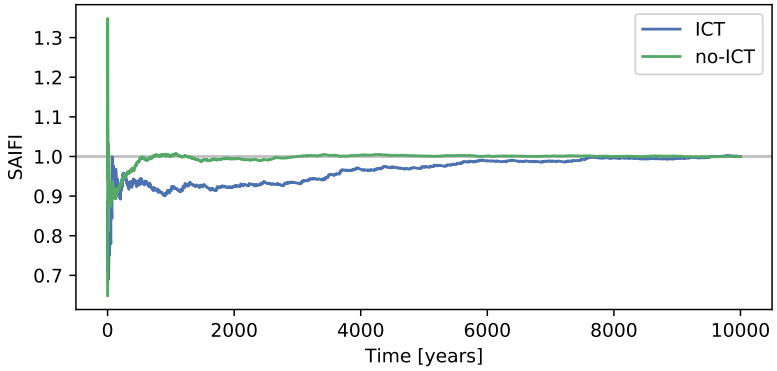

(a) SAIFI

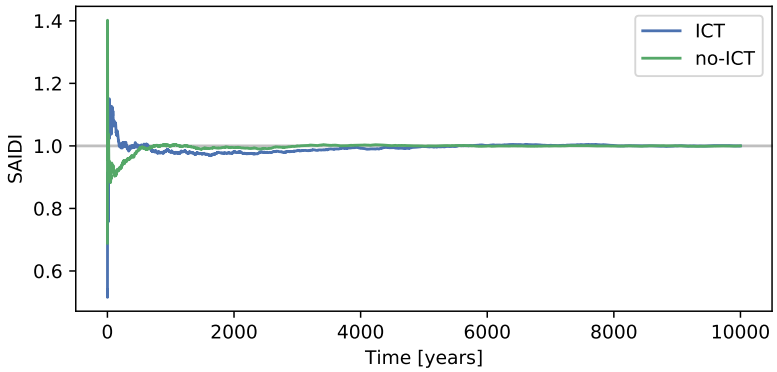

(b) SAIDI

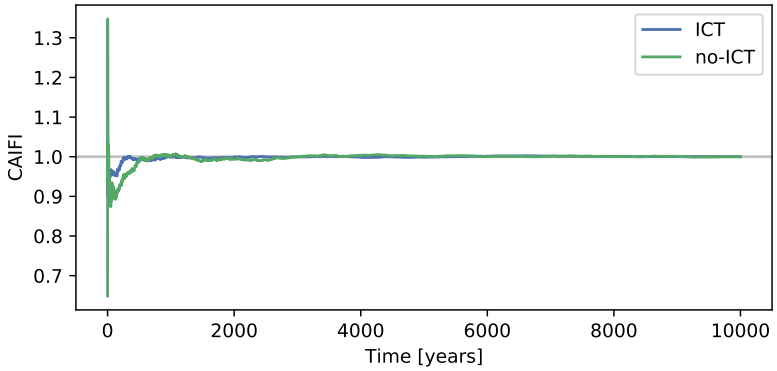

(c) CAIFI

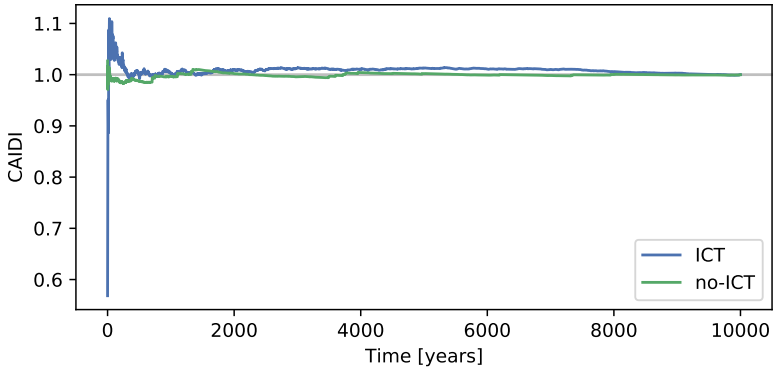

(d) CAIFI

Figure C.1: Indices divided by the mean of the index. Simulation for 10000 years.

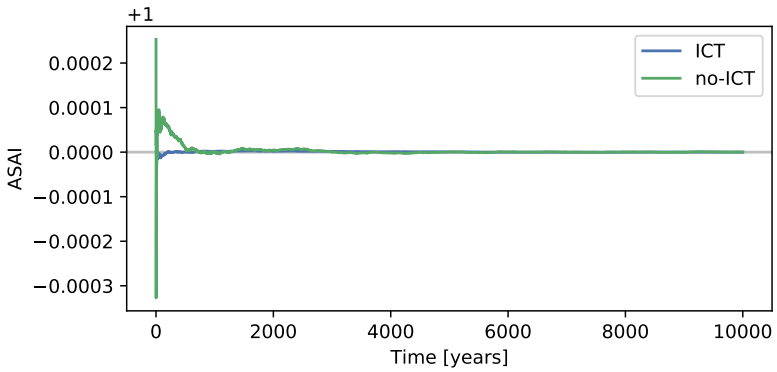

(e) ASAI

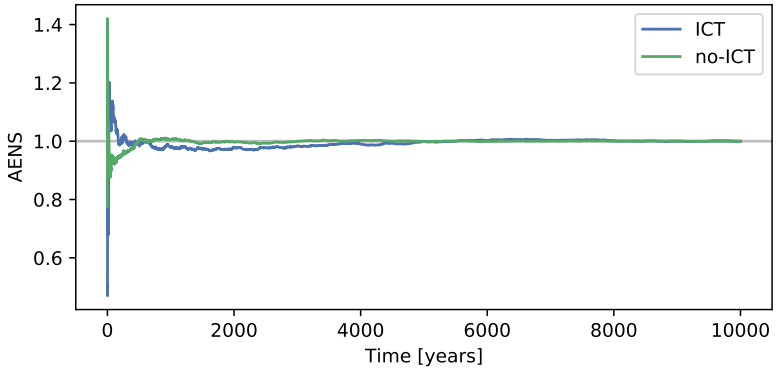

(f) AENS

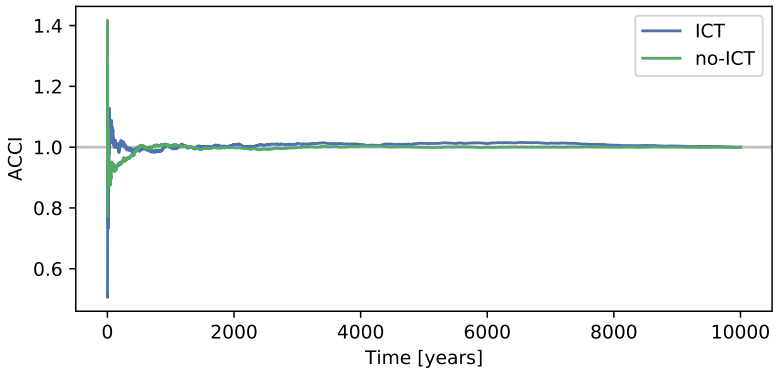

(g) ACCI

Figure C.1: Indices divided by the mean of the index. Simulation for 10000 years.

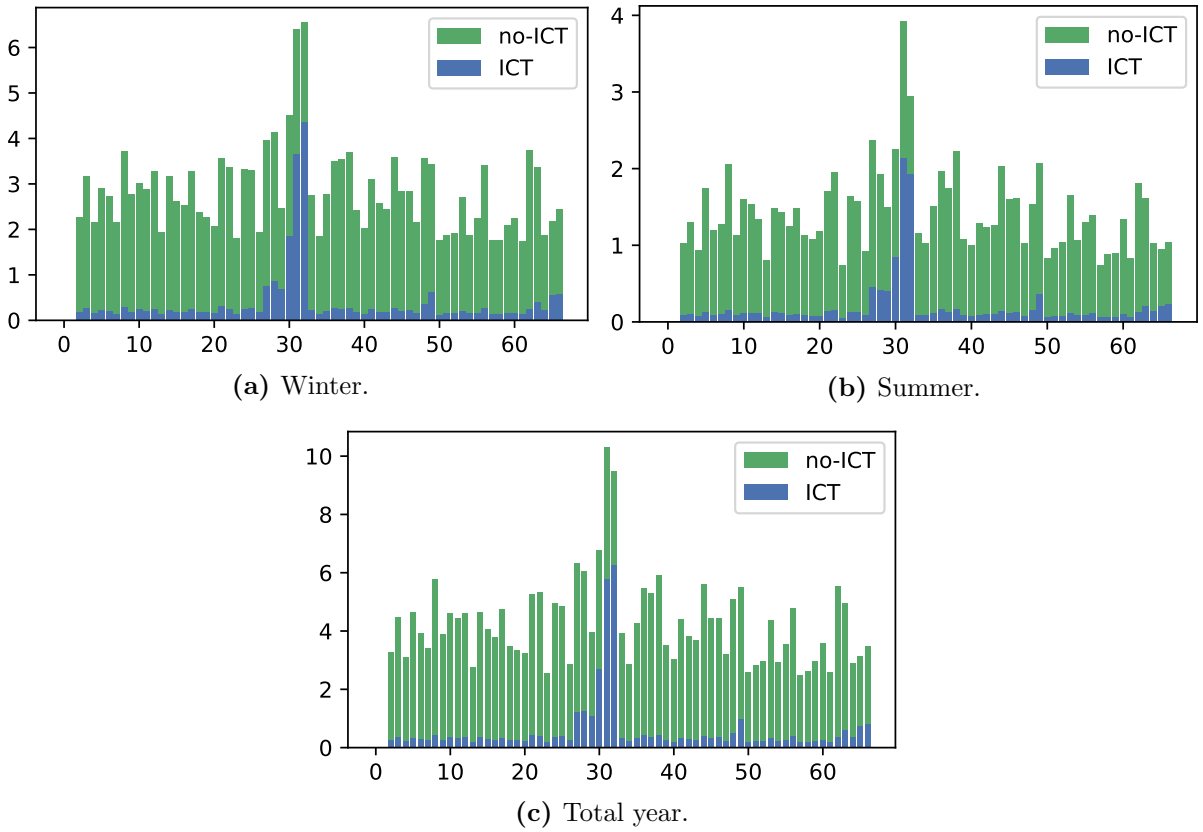

(a) Winter.

(b) Summer.

(c) Total year.

Figure C.2: Bar plot of the ENS index from Case 0. Divided into the seasons, winter and summer, and the total year. Simulation for 10000 years.

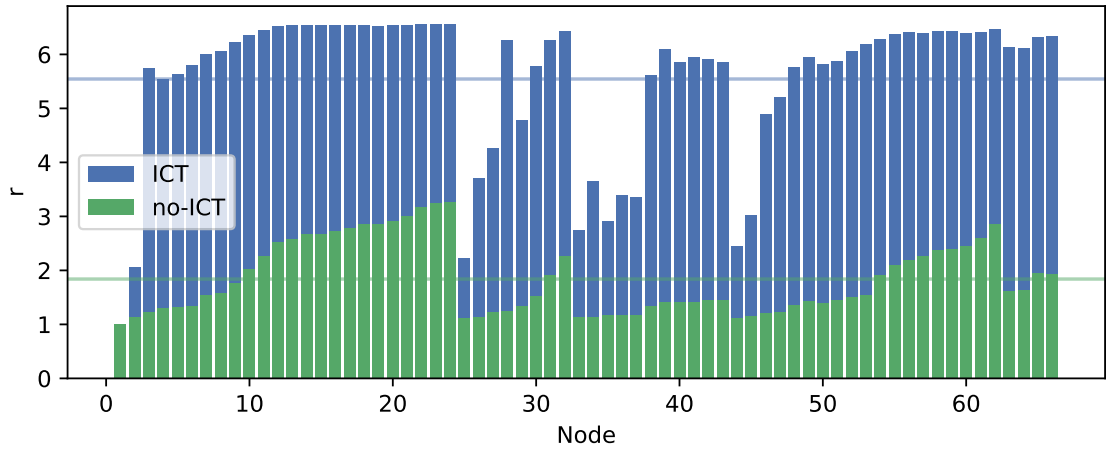

Figure C.3: Average failure duration r bar plot for Case 1 using seed 10336. The horizontal lines are the mean of the value of the nodes. Simulation for 10000 years.

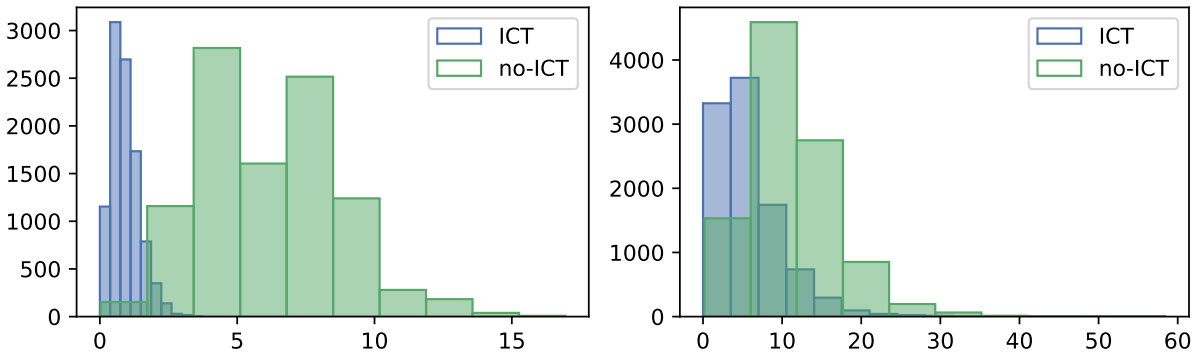

(a) SAIFI.

(b) SAIDI.

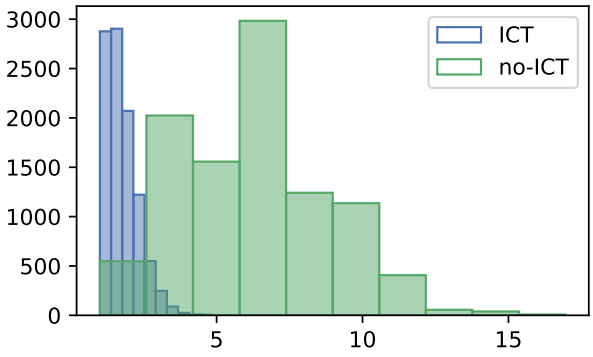

(c) CAIFI.

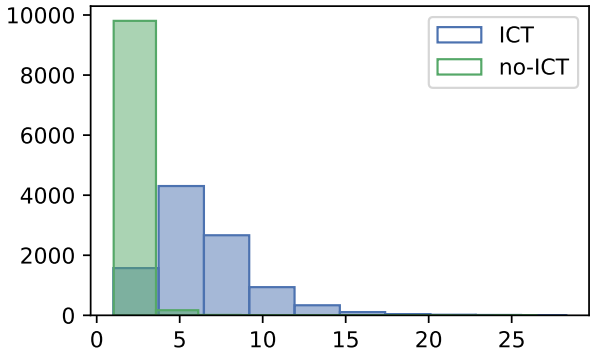

(d) CAIDI.

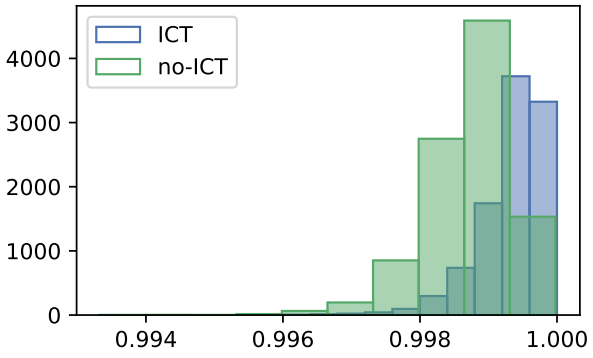

(e) ASAI.

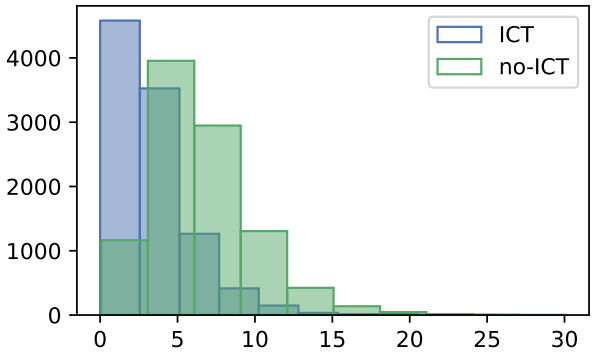

(f) AENS.

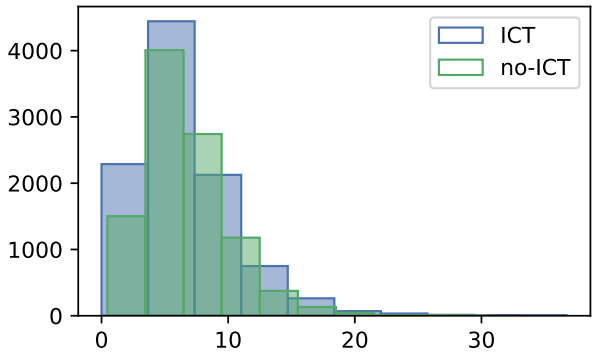

(g) ACCI.

Figure C.4: Histogram of the indices from Case 1 (see subsection 2.7 for explanation of the indices). The y-axis is the count of years inside the width of the bar. Simulation for 10000 years.

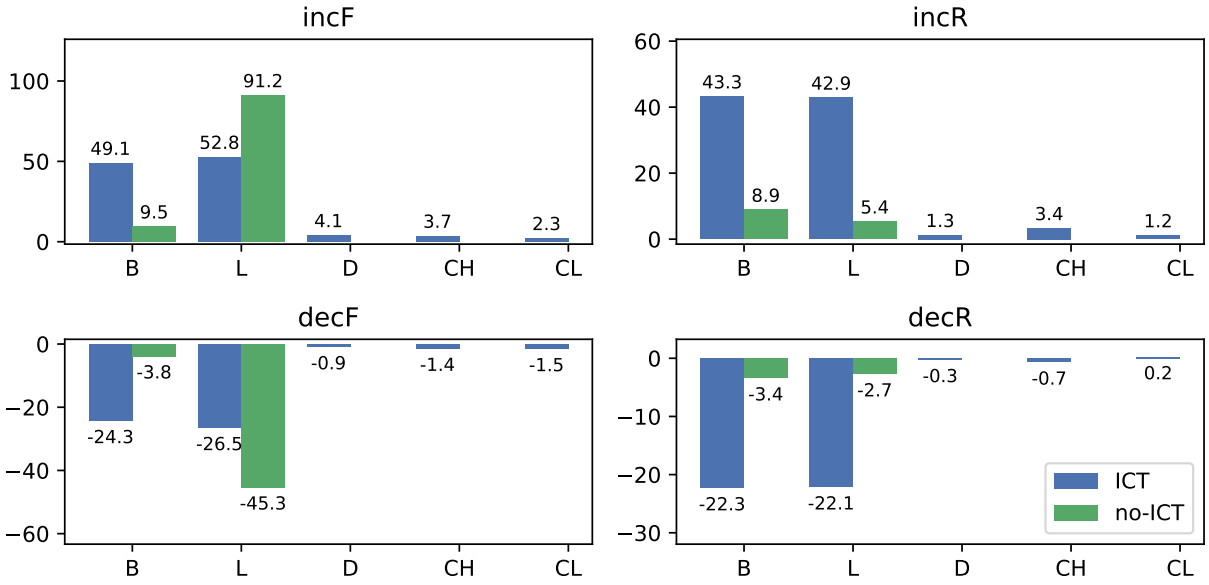

(a) AENS.

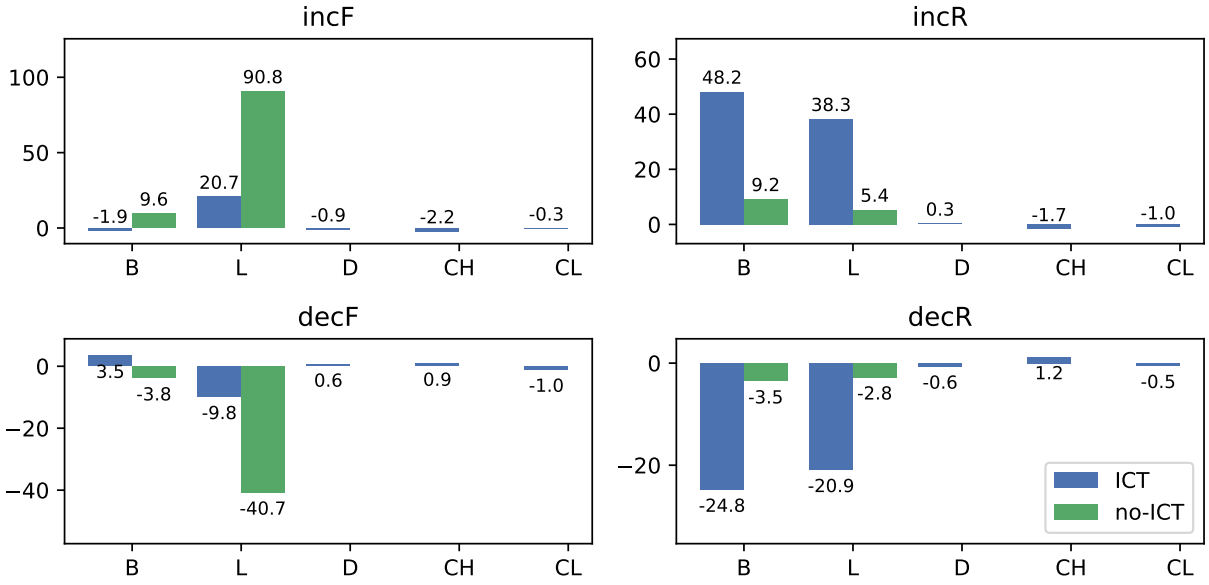

(b) ACCI.

Figure C.5: Factorial experiment change from Case 0 in percent for the AENS and ACCI indices (see subsection 2.7 for explanation of the indices). Simulation for 10000 years. Bus (B), Line (L), Disconnector (D), Communication Hub (CH), and Communication Line (CL). Increase in failures (incF), decrease in failures (decF), increase in repair time (incR), and decrease in repair time (decR).

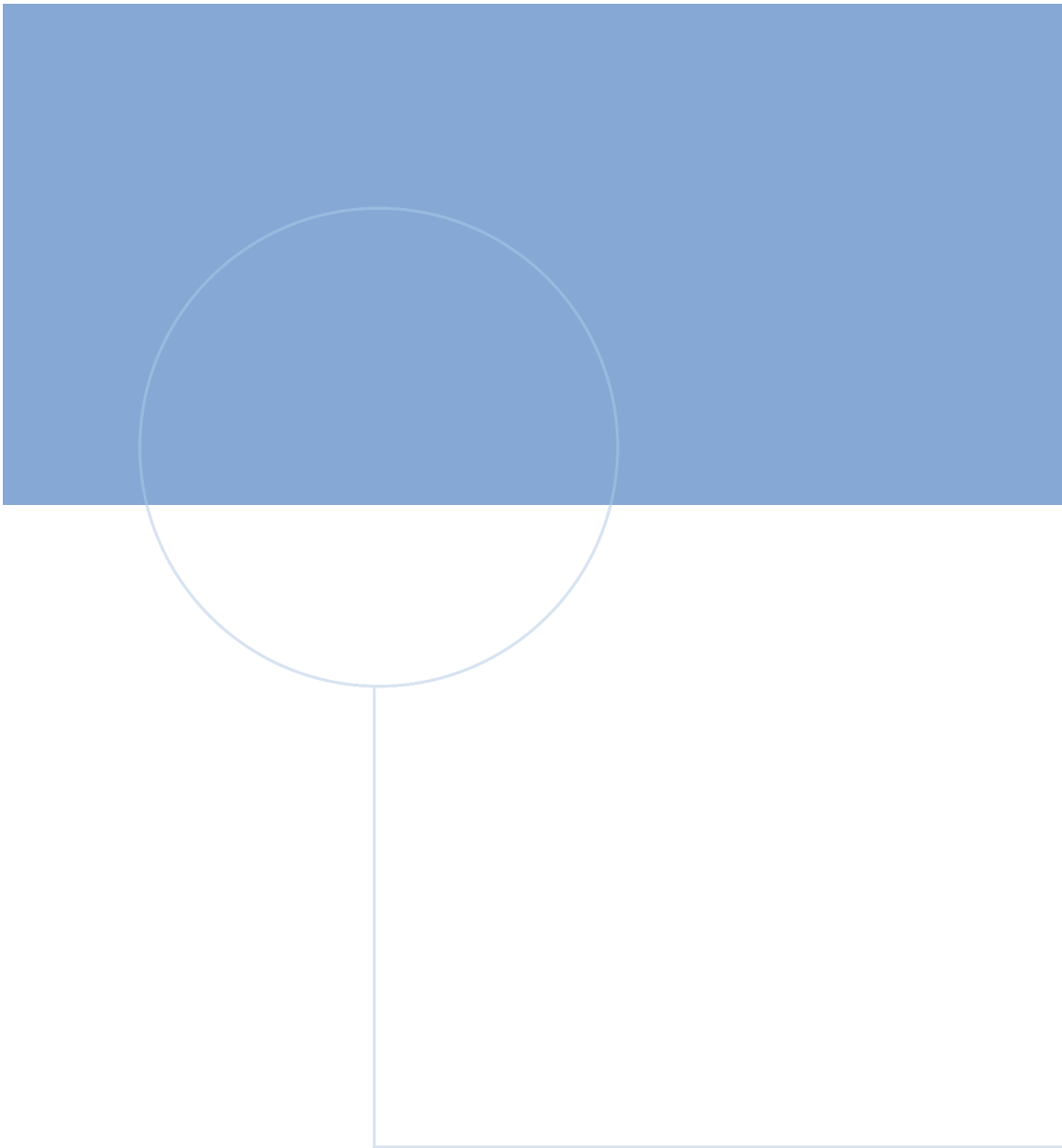

NTNU

Norwegian University of
Science and Technology